

Aus dem Bereich Klinische Medizin
der Medizinischen Fakultät
der Universität des Saarlandes, Homburg/Saar

Influence of Vitamin D on Genome-Wide Expression in Natural Killer Cells

Dissertation zur Erlangung des Grades eines Doktors der Medizin

der Medizinischen Fakultät

der UNIVERSITÄT DES SAARLANDES

2021

vorgelegt von: Konstantinos Christofyllakis

geb. am.: 06.05.1988 in Athen, Griechenland

Tag der Promotion: 19. April 2021

Dekan: Univ.-Prof. Dr. med- Michael D. Menger

Berichterstatter: PD Dr. Frank Neumann

Prof. Dr. Markus Hoth

The experiments for the present doctoral thesis were conducted at the Clinic for Internal Medicine I - Oncology, Hematology, Clinical Immunology and Rheumatology, as well as at the José Carreras Institute of Saarland University in Homburg (Saar).

Konstantinos Christofyllakis

Saarland University Medical Center – IMED (bldg. 41)

Department of Internal Medicine I

Oncology, Hematology, Rheumatology and clinical Immunology

Director: Prof. Dr. Stephan Stilgenbauer

Kirrberger Strasse 100

66421 Homburg/Saar, Germany

Mail: konstantinos.christofyllakis@uks.eu

TABLE OF CONTENTS

Table of Contents	i
List of Figures	iv
List of Tables	v
1 Summary	1
2 Introduction.....	2
2.1 Natural Killer Cells	2
2.1.1 Subsets of NK Cells.....	2
2.1.2 NK-Cell-mediated Cytotoxicity	3
2.1.3 Regulation of NK-Cell Activity – NK-Cell Receptors	5
2.1.4 Toll-Like Receptors.....	7
2.1.5 Antibody-Dependent Cytotoxicity	8
2.2 Vitamin D.....	9
2.2.1 Synthesis and Metabolism of Vitamin D.....	10
2.2.2 Role of Vitamin D in Humans.....	10
2.2.3 Vitamin D Deficiency	11
2.2.4 Skeletal Effects of Vitamin D Supplementation	11
2.2.5 Non-Skeletal Effects of Vitamin D Supplementation	11
2.2.6 Vitamin D and Cancer.....	12
2.2.7 Vitamin D and the Immune System.....	12
2.2.8 Vitamin D and Natural Killer Cells	13
2.3 Aims of this Thesis	14
3 Materials and Methods	15
3.1 Study Design	15
3.1.1 Inclusion and Exclusion Criteria.....	15
3.1.2 Data Handling and Ethical Aspects.....	15
3.1.3 Vitamin D Supplementation	15
3.1.4 Sample Labeling.....	16
3.1.5 Participant Characteristics and Vitamin D Levels.....	16

3.2	Materials.....	17
3.2.1	Chemicals, Reagents, Buffers, Mediums and Solutions.....	17
3.2.2	Antibodies, Enzymes, Primers.....	19
3.2.3	Consumables.....	19
3.2.4	Equipment.....	20
3.3	Methods.....	21
3.3.1	Cell Counting.....	21
3.3.2	Isolation of PBMC.....	22
3.3.3	NK-Cell Enrichment by Magnetic Cell Sorting.....	22
3.3.4	Flow Cytometry.....	23
3.3.5	RNA Extraction.....	24
3.3.6	Spectrophotometry.....	24
3.3.7	RNA Electrophoresis.....	25
3.3.8	Microarray Assay.....	25
3.3.9	Microarray Quality Control.....	26
3.3.10	Quantitative Real Time Polymerase Chain Reaction Validation.....	33
3.4	Statistical Analysis.....	35
3.4.1	Data Analysis Strategy.....	35
3.4.2	Comparisons.....	35
3.4.3	Differentially Expressed Genes.....	36
3.4.4	Pathway Analysis.....	37
4	Results.....	39
4.1	Quantitative Real Time Polymerase Chain Reaction Validation.....	39
4.2	Comparison I: Deficiency – Substitution.....	41
4.2.1	Overview of Differentially Expressed Genes.....	41
4.2.2	Differentially Expressed Genes.....	47
4.3	Comparisons Based on Vitamin D Status und Sex.....	59
4.3.1	Comparison II: Male – Female.....	59
4.3.2	Comparison III: Differentially Expressed Genes – Female Subjects.....	61
4.3.3	Comparison IV: Differentially Expressed Genes – Male Subjects.....	64

4.3.4	Comparison V: Female vs. Male in the Vitamin D Deficient State	66
4.3.5	Comparison IV: Female vs. Male after Vitamin D Supplementation	69
4.4	Pathway Analysis	70
4.4.1	NK-Cell Cytotoxicity Pathway	72
4.4.2	Immune System-Related Pathways – Upregulated.....	74
4.4.3	Immune System-Related Pathways – Downregulated	76
4.4.4	Unsupervised Pathway Analysis.....	81
5	Discussion	83
5.1	Role of Pathway Analysis in Genomic Research	83
5.2	Altered Cytokine - mRNA Profile After Vitamin D Supplementation.....	84
5.3	Altered Pathways After Vitamin D Supplementation	86
5.4	Indirect Influence of Vitamin D on NK Cells	89
5.5	Role of Sexual Dimorphism	89
5.6	Vitamin D in the Context of Autoimmunity and Chronic Inflammation.....	91
5.7	Critical View and Outlook.....	92
5.8	Conclusion.....	93
6	References	94
7	Publications	110
8	Acknowledgements.....	111
9	Curriculum Vitae	112

LIST OF FIGURES

Figure 1: Distribution of signal strengths	27
Figure 2: Log probe cell intensity	27
Figure 3: Relative log probe cell intensity.....	28
Figure 4: Log expression signal	28
Figure 5: Relative log expression signal.....	29
Figure 6: Pearson's correlation (signal).....	30
Figure 7: Spearman rank correlation (signal)	30
Figure 8: $\Delta\Delta Ct$ (a-b) values for the AIF1 and CLEC7A genes per qRT-PCR.....	40
Figure 9: Fold change values for the AIF1 and CLEC7A genes per microarray	41
Figure 10. Normal Q-Q plot of average log ₂ signal before supplementation	41
Figure 11. Normal Q-Q plot of average log ₂ signal after supplementation	42
Figure 12: Volcano plot of log ₂ p-values versus log ₂ fold change.....	43
Figure 13: Scatter plot	44
Figure 14: Hierarchical clustering.....	45
Figure 15: Principal component analysis – 1	46
Figure 16: Principal component analysis – 2.....	46
Figure 17: Summarized ANOVA results for comparisons II-VI	59
Figure 18: Venn diagram of comparisons II, V and VI	67
Figure 19: Heat map of the 50 most significant transcripts for each phenotype as per GSEA ranked list	71
Figure 20: Enrichment Plot: “NK cell cytotoxicity” pathway.....	72
Figure 21: Enrichment plot: “Regulation of type I interferon mediated signaling” pathway....	75
Figure 22: Enrichment plot: “Response to type I interferon” pathway	75
Figure 23: Leading edge analysis of the upregulated pathways involved in the immune response.....	76
Figure 24: Leading edge analysis of the downregulated pathways involved in the immune response	77
Figure 25: Common gene distribution among the downregulated pathways.....	78
Figure 26: TLR gene expression in all subjects.....	80
Figure 27: TLR gene expression in females.....	80
Figure 28: Proposed model of effect of vitamin D deficiency and supplementation on NK cells	88

LIST OF TABLES

Table 1: Human NK cell receptors	9
Table 2: Sample labeling	16
Table 3: Participant characteristics and 25(OH)D serum levels.....	16
Table 4: Chemicals, reagents, buffers, mediums and solutions used in the study.....	17
Table 5: Antibodies, enzymes, primers used in the study.....	19
Table 6: Consumables used in the study	19
Table 7: Equipment used in the study	20
Table 8: Technical Information about the Human Gene 2.1 ST Array Plate	26
Table 9: Quality control metrics 1.....	31
Table 10: Quality control metrics 2.....	32
Table 11: Oligonucleotide primers used for qRT-PCR	33
Table 12: Parameters for PCR.....	34
Table 13: Annealing temperature of the different primers.....	34
Table 14: qRT-PCR results.....	39
Table 15: Fold change microarray signal values after vitamin D substitution.....	40
Table 16: qRT-PCR $\Delta\Delta C_t$ (a-b) values after vitamin substitution	40
Table 17: Upregulated transcripts after supplementation of vitamin D3 scoring $p < 0.01$	47
Table 18: Downregulated transcripts after supplementation of vitamin D3 scoring $p < 0.01$.	51
Table 19: Selected genes associated with the immune system or vitamin D signaling	55
Table 20: Comparison II – Significantly differentially expressed genes	60
Table 21: Comparison III – Differentially expressed genes in females	62
Table 22: Comparison IV – Differentially expressed genes in males.....	65
Table 23: Comparison V – Differentially expressed genes – Female vs. male in the vitamin D deficient state	68
Table 24: Comparison VI – Differentially expressed genes – Female vs. male after vitamin D supplementation	69
Table 25: NK cell cytotoxicity pathway – Metrics.....	72
Table 26: NK-cell cytotoxicity pathway - Genes contributing to the enrichment score	73
Table 27: Upregulated pathways involved in the immune response.....	74
Table 28: Downregulated pathways involved in the immune response	77
Table 29: Pathways influenced by vitamin D supplementation – Unsupervised analysis.....	81
Table 30: Downregulated genes involved in the ubiquitin ligase complex	82

1 SUMMARY

Introduction: Vitamin D deficiency has been associated with decreased overall survival in patients with diffuse large B-cell lymphoma treated with rituximab. Natural killer cell-mediated antibody-dependent cytotoxicity is one of the main mechanisms of action of rituximab, and it has been shown to be enhanced after in vivo vitamin D supplementation. This effect was more pronounced in females. We aimed to explore molecular mechanisms behind these findings using whole transcriptome analysis of natural killer cells after vitamin D supplementation.

Methods: Natural killer cells were isolated by magnetic depletion from eight otherwise healthy subjects (four females and four males) with vitamin D deficiency, before and after vitamin D supplementation to a target serum level of 65 ng/ml. RNA was extracted followed by whole transcriptome microarray analysis. Results were verified by quantitative polymerase chain reaction. For differential expression analysis, the paired t-test and two-way ANOVA were used. Comparisons were made with regard to both vitamin D status and sex. In addition, pathway analysis using gene set enrichment analysis was performed.

Results: After correction for multiple testing no genes showed statistically significant differential expression in the sex-independent comparison. For hypothesis generation, genes with an unadjusted p-value < 0.01 are reported (n = 505). An impact on known vitamin D-dependent genes was demonstrated. Genes involved in cytokine signaling like *IFNL3* and *IL-2RB* were found to be upregulated, while others like *IFNG* and *TLR* genes were downregulated. In the sex-dependent analysis 28 transcripts with statistically significant sex- and vitamin D-dependent expression after adjustment were identified, like the *JPX* gene which was upregulated in females. Pathway analysis highlighted the role of interferon- α genes (*IFNA2*, -*A4*, -*A6*, -*A8*, -*A10*) in statistically significantly upregulated pathways. Other pathways involved in the immune response were found to be significantly downregulated, mainly by downregulation of the *TLR2*, -*5*, -*7* and -*8* genes. Finally, the ubiquitin ligase pathway was found to be downregulated.

Conclusion: Vitamin D supplementation has only a slight effect on the natural killer cell transcriptome and the small sample size used in this study limits detection of such subtle changes. Our results implicate a role for vitamin D in gene expression involving the toll-like receptor and type I/III interferon axis and its regulation through the ubiquitin ligase system. IFN- γ downregulation may well be consistent with the observation of increased lymphoma killing of natural killer cells. *JPX*-dependent epigenetic regulation of X-chromosome deactivation in females could explain the downregulation of genes like *TLR7* and -*8* which are located on the X-chromosome. It is also possible, that vitamin D exerts its effects on natural killer cells indirectly through other, regulatory cells such as dendritic cells or macrophages.

2 INTRODUCTION

2.1 NATURAL KILLER CELLS

Natural killer (NK) cells are large granulated lymphocytes playing a key role in the innate immune response. Their name implies their ability to kill virally infected cells and tumor cells without prior sensitization [51]. Their functions include secretion of cytokines and direct cytotoxic effects [145] as well as a key role in homeostasis through elimination of degenerate or malignant cells. They make up 2-18 % of lymphocytes in the peripheral blood [129]. NK cells lack a highly variable antigen-specific surface receptor resulting from rearrangement of immunoglobulin-like genes as known from B cells (B cell receptor) or T cells (T cell receptor) [26]. In lieu thereof, they express CD16 and CD56 as well as other inhibitory and stimulatory receptors, which working closely with toll-like receptors and other pattern recognition receptors to regulate NK-cell activity. The resulting equilibrium between activating and inhibitory signals mandates NK cell activation and target cell lysis [149].

2.1.1 Subsets of NK Cells

Human NK cells can be divided into two categories due to the expression of the two surface molecules CD16 (low-affinity Fc γ receptor III, Fc γ RIII) and CD56. It is possible, that these two populations represent different stages of differentiation [124].

2.1.1.1 Cytotoxic CD56^{dim}, CD16^{high} NK Cells

These NK cells circulate in the peripheral blood, accounting for up to 90 % of the NK cells in the peripheral blood and spleen [150]. Their cytotoxic activity is mediated by perforin and granzymes in a similar mechanism as in cytotoxic CD8⁺ T lymphocytes. After contacting the target cell, perforin induces pore formation in the membrane of the target cell upon polymerization, enabling the entrance of granzymes and granulysin into the interior [26,51,124,145,150] of the target cell. NK-cell-mediated cytotoxicity is described in detail in the next chapter. Another mechanism of cytotoxicity is the induction of apoptosis via the TRAIL or Fas pathway [26]. CD16 allows NK cells specifically to identify antigens marked with corresponding antibodies. Via this CD16/antibody binding, the NK cell can directly contact cells expressing a corresponding antigen on their surface, thus inducing the so-called antibody-dependent cell-mediated cytotoxicity (ADCC). Furthermore, CD56^{dim}/ CD16^{high} NK cells are able to produce different cytokines such as IFN- γ , TNF- β , and GM-CSF which activates macrophages at sites of infection [5]. This interaction between NK cells and macrophages allows an initial control over days or even weeks of an infection with intracellular bacteria until

T-cell-mediated adaptive immunity develops and ultimately takes over the eradication of the pathogens.

2.1.1.2 Immunomodulatory CD56^{bright}, CD16^{dim} NK Cells

They are primarily located in the lymph nodes. Their primary function is the modification of type 1 T-helper cell (Th1) immune responses, the activation of macrophage-driven killing of obligate intracellular pathogens and to induce anti-proliferative effects on viral- and malignant-transformed cells through IFN- γ secretion [26,47,96]. Other effects of IFN- γ -secreting NK cells include the activation of antigen-presenting cells (APC) especially by enhancing MHC I expression [26]. IFN- γ is secreted in response to stimulation with the interleukins (IL) IL-12, IL-15, and IL-18. CD56^{bright}/CD16^{dim} NK cells also secrete other cytokines like tumor necrosis factor (TNF)- α , TNF- β , GM-CSF, or IL-10. Under activation by cytokines like IL-2 and IL-15 they can furthermore induce cytotoxicity comparable to CD56^{dim}/CD16^{high} NK cells. Lastly, these NK cells can also differentiate to CD56^{dim}/CD16^{high} NK cells, leaving the lymph node to circulate in the peripheral blood [26].

2.1.1.3 Natural Killer T Cells

Natural killer T (NKT) cells represent a very small subset of human lymphocytes (< 1 %) which exhibit T cell as well as NK cell phenotype and function. They express both NK cell markers such as CD161 and CD94, as well as a T-cell receptor (TCR) alpha/beta. This TCR however does not recognize antigens presented MHC-I- or -II-molecules. It is a semi-invariant TCR that only interacts with glycolipids presented by CD1d, a non-classical antigen-presenting molecule [17]. Upon stimulation they produce a variety of cytokines which include IFN- γ , TNFs, IL-2, IL-4, IL-10, IL-13, IL-17, and transforming growth factor (TGF)- β [159].

2.1.2 NK-Cell-mediated Cytotoxicity

Cytotoxic cells employ various agents for lysing their target cells.

2.1.2.1 Perforin

Perforin is a cytolytic protein found in granules of cytotoxic CD8⁺ T lymphocytes and NK cells. During degranulation, it perforates the cell membrane of the target cell by forming a pore. It has been shown to play a role in antiviral immune response, elimination of tumor cells as well as allograft rejection [66,103]. The structural similarity of perforin with the bacterial cholesterol-dependent cytolysins has allowed a better understanding of its mechanism of action. After Ca²⁺-dependent binding to the target cell membrane, cholesterol-dependent cytolysins and most probably perforin also polymerize, forming initially a pre-pore construct. Then two α -

helices (named TMH1 and TMH2) unwind and insert as amphipathic β -strands into the target membrane, thus forming the full pore [82].

Recent advances have shed light to the transcriptional regulation of the perforin gene (*PRF1*). Ten DNase I hypersensitivity sites have been identified in its locus control region [117], including binding sites for runt-related transcription factor 3 (*RUNX3*) and eomesodermin (*eomes*) [151].

2.1.2.2 Granzymes

Granzymes are serine proteases, which are stored in intercellular granules of cytotoxic T lymphocytes and NK cells. There are eleven different granzymes (A, B, C, D, E, F, G, H, K, M, and N), but only five of these have been shown to be expressed in humans (A, B, H, K and M) [131]. Granzymes do not act by untargeted protein digestion. Their general mechanism of function is the coordinated activation of caspases, triggering specific cell death pathways, such as apoptosis. Although many in vitro experiments have demonstrated cytolytic activity, their exact pathophysiological role remains unclear, as granzyme deficiency does not lead to any known human disease [139]. Knock out studies in mice have demonstrated that loss of perforin negates granzyme-induced apoptosis, whereas single granzyme gene disruption results in a defect but not in loss of the cytotoxic NK cell activity.

2.1.2.3 Granulysin

Granulysin is another cytotoxic agent found in the granules of NK cells and cytotoxic T lymphocytes. It is a member of the saposin-like protein family including NK lysin and amoebapores. Positively charged residues of the molecule interact with the negatively charged target cell membrane or the bacterial cell wall, respectively, leading to increased permeability and cell lysis [34,69]. In tumor cells, granulysin induces sphingomyelinase-dependent apoptosis [35]. Granulysin gene (*gnly*) expression is dependent on the transcription factors AP-1 and C/EBP β . Furthermore, its expression is upregulated under stimulation with IL-2 or bacterial antigen [81].

2.1.2.4 Granule Exocytosis

A shift of the balance of inhibitory and activating signals toward NK-cell activation results primarily in a considerable increase in cytosolic Ca²⁺ concentration. The next step is the intracellular polarisation of the microtubule-organizing center toward the target cell. The cytotoxic granules move along this structure until they fuse with the cell membrane of the NK cell, thus releasing their content into the synaptic cleft. Disorders of the cytoskeleton result in varying degrees of impairment of NK cell cytotoxicity. A disturbed F-actin remodelling as in the

Wiskott-Aldrich syndrome results in such a NK-cell defect. Similarly, mutations of adhesion molecules as in the leukocyte adhesion deficiency syndromes 1 and 3 [76,140], or in case of the autosomal recessive hyper-IgE-recurrent infection syndrome (AR-HIES) with a defect of the gene encoding the dedicator of cytokinesis 8 (DOCK8) leading to impaired defense against viral and bacterial infections. It is assumed that the NK cell protects itself from the content of its granules by secretion of serpin B9.

2.1.3 Regulation of NK-Cell Activity – NK-Cell Receptors

Activation of NK cells is induced by the interleukins IL-2, IL-12, IL-15, IL-18, and interferon- α/β [153],[79]. These cytokines along with interactions with cells in the microenvironment like dendritic cells (DC), macrophages and T cells determine the extent of the cytolytic activity of NK cells [95]. Finally, the cytotoxic activity depends on the balance of inhibitory and promoting interactions with the microenvironment but also with the target cells. Binding of inhibitory receptors to MHC class I molecules block NK-cell effector function, although some non-MHC class I inhibitory ligands can be recognized too.

There are two types of inhibitory receptor families in humans: killer cell Ig-like receptors (KIR) and the CD94/NKG2A lectin-like receptors.

NK cells express several activating receptors simultaneously. These include natural-killer group 2 member D (NKG2D), activating KIRs, NKp80, NKp30, NKp44, NKp46, CD94/NKG2C, DNAX accessory molecule (DNAM)-1 and 2B4 [73].

NK cells derived from humans and mice express different receptors, and this has complicated research in this area. In this thesis, only NK-cell receptors expressed in humans are described.

Table 1 provides an overview.

2.1.3.1 *Killer Inhibitory Receptors (KIR)*

Located superficially on the NK cell, KIRs represent a family of inhibitory as well as activating receptors binding specifically to MHC class I molecules [21,39,79]. MHC-I-molecules are expressed constitutively on every nucleated healthy cell indicating the affiliation to the host's immune system. In contrast, the lack of expression or even a complete missing on the cell surface indicates a "missing self" status and is always associated to profound changes in the cell function/phenotype, such as a viral infection or a malignant transformation. The type and number of extracellular immunoglobulin domains define the specificity of KIRs, whereas their function as activating or inhibitory receptors is mediated through their intracellular domains: short "S" = activating or long "L" = inhibitory [79]. These characteristics are reflected in the nomenclature, for example, KIR2DS1, KIR3DL1, or KIR3DS1. Activating KIR signals using the short intracellular domain are initiated by the adapter protein DAP12, while inhibitory KIR are carrying one or two immunoreceptor tyrosine-based inhibitory motifs (ITIM) in their intracellular

long domain. Various KIRs bind to HLA-A (e.g. KIR3DL2 to HLA-A3 und HLA-A1), to HLA-B (e.g. KIR3DL1 to HLA-Bw4) or HLA-C (e.g. KIR2DL1 to HLA-C2). Each NK cell is equipped with an individual KIR repertoire, and it undergoes a selection process to ensure that it expresses one KIR for each HLA class I molecule. Furthermore, there are significant polymorphisms in KIR haplotypes in each individual. The KIR haplotype “A” is associated with few or no activating KIRs, whereas haplotype “B” contains a number of activating KIRs. NK cells which lack KIR inhibitory receptors express the inhibitory receptor CD94/NKG2A whose function is HLA-E dependent, as explained below (2.1.3.36) [122].

2.1.3.2 *Natural Cytotoxicity Receptors (NCR):*

The NCRs (NKp30, NKp44, NKp46 and NKp80) belong to the immunoglobulin superfamily and recognize various stress signals and viral as well as tumor cell ligands.

NKp30 associates with immunoreceptor tyrosine-based activation motif (ITAM) to initiate signal transduction. Three isoforms of NKp30 exist: NKp30a, NKp30b, and NKp30c, with NKp30a and NKp30b being stimulatory, whereas NKp30c is immunosuppressive. NKp30 recognizes tumor antigens and binds several viral ligands including the protein pp65 of the cytomegaly virus (CMV).

NKp44 is coupled to a dimer of the ITAM-containing adaptor DNAX-activation protein 12 (DAP12) for downstream signal transduction. Ligands include cellular proteoglycans, influenza virus hemagglutinin and other viral hemagglutinins–neuraminidase proteins as well as elements of the bacterial cell wall.

NKp46 is the most specific marker of NK cells. For signaling, NKp46 associates with CD3 ζ and with the γ -chain of Fc γ RI. Activating ligands include viral hemagglutinins-neuraminidase proteins, expressed on pancreatic β -cells (which can lead to type I diabetes upon activation) as well as not yet completely characterized ligands on normal and on tumor cells [73].

2.1.3.3 *The NKG2-receptor family*

The NKG2-receptors are C-Type lectin-receptors which dimerize with a CD94 molecule before binding to atypical MHC-I molecules expressed on target cells.

NKG2A/C/E: They are expressed as heterodimers with CD94 on the cell surface and bind on HLA-E. CD94–NKG2C and CD94–NKG2E have been shown to associate also with DAP-12 and therefore playing an activating role. The CD94–NKG2A receptors are important inhibitors of NK cell function which also bind to HLA-E. Their inhibitory activity is associated with the ITIM-motif of their cytoplasmatic domain[84].

NKG2D: Contrary to the other NKG2-receptor family members, does not bind to CD94. Instead, it is expressed as a homodimer. Its downstream signaling involves association with DAP-10 molecules to induce a cytotoxic response. It recognizes several ligands including MHC class I chain-related protein MIC-A, MIC-B, and UL16-binding proteins (ULBP1-4). Expression of MIC-A and MIC-B has been reported to be induced upon malignant transformation or cellular stress as a result of the DNA damage response pathway and/or the heat shock response pathway. Its activation enables NK cells to recognize “stressed cells”[114].

2.1.3.4 NKRP1 receptor family

NKp80 is a C-type-lectin-like receptor similar to the NKG2-receptor family discussed above. It binds an activation-induced C-type lectin (AICL) receptor, which is often expressed by monocytes, operating as a bridge for mutual crosstalk between NK and myeloid cells [79].

NKp65 induces cytotoxicity and secretion of IFN- γ when it encounters its ligand keratinocyte-associated C-type lectin (KACL). Both NKp65 and NKp80 contain a hemITAM cytoplasmic domain which is used in Syk-dependent downstream signaling [14].

NKRP1A has an inhibitory function. It inhibits IFN- γ production and NK cell activation when it encounters activated leukocytes expressing lectin-like transcript 1 (LLT1). Intracellular signaling is mediated through a cytoplasmic ITIM domain which recruits Src homology 2-containing protein tyrosine phosphatase-1 (SHP-1) [14].

2.1.4 Toll-Like Receptors

The immune system of the vertebrates must be able to respond to bacterial, viral, and fungal infections. This function depends on molecular patterns unique to each pathogen class known as pathogen-associated molecules (PAMP). Cells of the innate immune system express pattern recognition receptors (PRR) which are responsible for the recognition of PAMPs as a sign of infection and consequent initiation of the innate immune response. The toll-like receptors (TLR) are the most studied class of such PRRs in mammals. TLRs are not only expressed differently by different cells of the innate immune system, but also by the different cell types themselves in terms of where they are expressed: either on the cell surface (TLR1, 2, 4-6, 10, 11), within endosomes (TLR3, 7-9, 12, 13), or intracellular (TLR2 and TLR4 in endothelial, dendritic and epithelial cells) [1]. The TLR1, 2, 4, 5 and 6 are mainly responsible for the recognition of bacterial-derived patterns. There is no risk of cross-reaction with the host, since bacterial PAMPs are very specific. In contrast, the recognition of viral-derived PAMPs, mostly nucleic acid fragments, takes place via TLR3, 7, 8 and 9. However, since these nucleic acid sequences are not always virus-specific, their TLRs are not expressed on the surface but in intracellular compartments to exclude cross-reactivity with sequences also present in host

DNA leading to autoimmunity [60]. In pooled human NK cells (CD3⁺/CD56⁺) as well as in NK-T-like cells (CD3⁺/CD56⁺) mRNA of TLRs 1-9 has been detected [133,134]. Upon TLR activation, NK cells produce cytokines like IFN- α , granulocyte macrophage colony-stimulating factor, which are necessary to fight infection but also can cause deleterious inflammation if excreted in excessive amounts [1].

2.1.5 Antibody-Dependent Cytotoxicity

Antibody-dependent cytotoxicity (ADCC) is a separate way of NK cells to mediate cytotoxicity that combines elements from the innate and the adaptive/humoral immune system. CD16 (low-affinity Fc- γ receptor III, Fc γ RIIIa) on the NK-cell surface bind to the Fc part of an antibody. Through their Fab part, antibodies also bind cell-bound antigens and thus antibodies can build a bridge between the NK cell with its CD16 receptor on one side and a target cell with a specific surface antigen on the other side. Like "normal" cytotoxic activity, NK cell-mediated ADCC is under control of the ratio of activating and inhibiting receptors stimulated by their respective ligands on the target cell. In addition, cytokines also influence NK cell activity. Thus, IL-2, IL-12 or IL-21 enhance ADCC [123]. ADCC is being widely exploited therapeutically by the use of monoclonal antibodies (mAb), for example in breast cancer by anti-HER2-mAb (Trastuzumab), in head and neck cancer by anti-HER1-mAb (Cetuximab) and lymphoma by anti-CD20-mAb (Rituximab and Obinutuzumab) [8,77,156].

2.1.5.1 CD16, Low Affinity Receptor for IgG (Fc γ RIIIa)

The most studied membrane receptor on NK cells is the CD16 molecule or Fc- γ receptor III (Fc γ RIIIa), a member of the immunoglobulin superfamily. The receptor is also present on monocytes and some T-cell subsets. Some NK cells also express Fc γ RIIc (CD32c), which is similarly involved in ADCC. Fc γ RIIIa is associated with the γ -subunit of the high-affinity IgE receptor (Fc γ RI- ϵ) and the ζ -subunit of T-cell receptor (TCR), or CD3 ζ . Downstream signaling after contact with CD16 ligands is mediated through activation of immunoreceptor tyrosine-based activation motifs (ITAM) and leads to stimulation of the phosphatidylinositol 3-kinase (PI3K), mitogen-activated protein kinase (MAPK), ZAP70-phosphorylation, activation of phospholipase C γ 1 C γ 2, activation of p21 ras and nuclear translocation and activation of NFATp and NFATc (NFAT: nuclear factor of activated T cells). This results in cytokine release, NK-cell degranulation and signaling through TNF family death receptors leading finally to target cell lysis. Furthermore, secreted IFN- γ activates nearby immune cells and promotes antigen presentation and adaptive immune responses [79],[155]. CD16 is only associated in ADCC and is not involved in other forms of NK cell-mediated cytotoxicity [79]. The efficacy of rituximab has been shown to depend on single-nucleotide polymorphisms of the Fc γ RIIIa gene.

Specifically, the 158-valine and 158-phenylalanine variants have predictive value in the outcome of patients with diffuse large B-cell lymphoma (DLBCL) treated with rituximab [2].

Table 1: Human NK cell receptors

Receptor families	Role	Name	Ligands	Signaling molecules
NCR	Activating	NKp46	HSPG, heparin, vimentin	FcR γ and CD3 ζ , ZAP70/Syk
		NKp44	NKp44L	DAP12, ZAP70/Syk
		NKp30a, b	B7-H6, BAG-6, CMV pp65 antigen	CD3 ζ , ZAP70/Syk
	Inhibitory	NKp44	PCNA	ITIM, SHP1, 2
		NKp30c	unknown	unknown
NKG2	Activating	NKG2D	MICA/B, ULBP1-6	DAP10, Grb2, Vav, SOS
		CD94/NKG2C	HLA-E	DAP12, ZAP70/Syk
	Inhibitory	CD94/NKG2A	HLA-E	ITIM, SHP1, 2
		CD94/NKG2E		
		CD94/NKG2F		
KIR	Activating	2DS1/S2/S4	HLA-C/ unknown	DAP12, ZAP70/Syk
		3DS1	unknown	
	Inhibitory	2DL1/L2/L3	HLA-C	ITIM, SHP1, 2
		3DL1/L2/L3	HLA- A, -B	
		3DL1/L2/L3	HLA- A, -B	
FcγR11a	Activating	CD16	Fc IgG	FcR γ and CD3 ζ , ZAP70/Syk
NKRP1	Activating	NKp80	AICL	hemITAM/Syk
	Activating	NKp65	KACL	hemITAM/Syk
	Inhibitory	NKRP1A	LLT1	ITIM, SHP1

Adapted from Konjević et al [74].

2.2 VITAMIN D

Vitamin D is a member of the secosteroid hormones and essentially regulates calcium, phosphate, and bone metabolism. In addition, many non-skeletal, sometimes systemic effects have been described in recent years. New vitamin D effects have been hypothesized by experimental, genetic, clinical and epidemiological studies as well as a number of meta-analyses, but their practical significance is still unclear. It is both supplied through the diet and formed by humans themselves through solar light exposure, specifically ultraviolet B radiation

(UVB). The dietary intake of usual foods is not sufficient to reach the estimated value for an adequate intake in the absence of endogenous synthesis [55].

2.2.1 Synthesis and Metabolism of Vitamin D

Humans synthesize vitamin D in their skin after exposure to sunlight. Steroids are composed of four combined ring structures named A to D. Solar UVB radiation (wavelength 290 to 315 nm) opens the B-ring of provitamin D₃ (7-dehydrocholesterol) and converts it non-enzymatically to previtamin D₃. This spontaneously isomerises under the effect of heat and it is further converted to vitamin D₃ (cholecalciferol). Excessive exposure to sunlight causes degradation of the provitamin D₃ and vitamin D₃ to inactive photoproducts, so an accumulation to toxic levels through sun exposure is not possible. Another source of vitamin D is dietary uptake, either as vitamin D₃ mainly from fish oil, or in form of vitamin D₂ (ergocalciferol) [125]. Vitamin D (D₃ or D₂) is transported in chylomicrons through the lymphatics to the circulation. There it is either stored in fat cells or binds to the vitamin-D-binding protein and is delivered to the liver, where it undergoes conversion from the vitamin-D-25-hydroxylase to 25-hydroxyvitamin D [25(OH)D]. Several cytochrome P450 (CYP) isoforms have been proposed to perform this hydroxylation step (CYP27A1, CYP2R1, CYP3A4 and CYP2J3). Finally, the 25-hydroxyvitamin D-1 α -hydroxylase (CYP27B1) in the kidneys converts it to its biologically active form 1,25-dihydroxyvitamin D [1,25(OH)₂D or 1 α ,25(OH)₂-Cholecalciferol or Calcitriol] [12].

2.2.2 Role of Vitamin D in Humans

Vitamin D plays a central role to calcium and phosphorus homeostasis. Its active form, 1,25-dihydroxyvitamin D, increases the absorption of renal and intestinal calcium and phosphorus absorption. Production of 1,25(OH)₂D is stimulated by low serum phosphate levels and by parathyroid hormone, which in turn is secreted in response to low serum calcium levels. Fibroblast growth factor 23 (FGF-23) suppresses 1,25(OH)₂D synthesis. Also, the active 1,25(OH)₂D form affects the parathyroid glands directly as a negative feedback mechanism, reducing parathyroid hormone synthesis itself [89].

Active vitamin D enters the cell and forms a heterodimer with the vitamin D receptor, which in turn binds to the retinoid receptor. This complex activates vitamin D responsive genes leading to transcription and translation, such as that of osteocalcin or calcium binding protein in the intestinal mucosa. Calcium binding protein in turn regulates the active transport of calcium through the intestinal cells [89]. By activation of the vitamin D receptor, 1,25(OH)₂D causes in osteoblasts an increase of the receptor activator of nuclear factor- κ B ligand (RANKL). This ligand interacts with RANK expressed on preosteoclasts and thus induces their maturation to

osteoclasts. Mature osteoclasts remove calcium and phosphorus from the bone, causing an increase of calcium and phosphorus serum levels.

2.2.3 Vitamin D Deficiency

There is no consensus on the optimal vitamin D levels in serum. A widely accepted cut off for “vitamin D deficiency” is 20 ng per milliliter. Serum 25-hydroxyvitamin D concentrations are related inversely to parathyroid hormone concentrations, which begin to rise when 25-(OH)D concentration falls below 30-40 ng/ml[31]. Intestinal calcium transport also increases by 20 % when 25-(OH)D levels rise from 20 ng/ml to 32 ng/ml. This has led to the introduction of the term “vitamin D insufficiency” referring to serum vitamin D levels of 21-29 ng/ml. Above 150 ng/ml, on the other hand, vitamin D intoxication may occur. Consequently, 25-(OH)D serum levels between 30 and 100 ng/ml are considered as normal.

Low concentrations of vitamin D lead to an impaired calcium absorption. Low calcium levels induce a compensatory rise in parathyroid hormone (PTH), which results in excessive bone resorption and osteoporosis.

2.2.4 Skeletal Effects of Vitamin D Supplementation

While the data has been inconsistent, meta-analyses of randomized-controlled trials of vitamin D and calcium supplementation have shown a reduction in fracture risk and a modest increase in bone density, especially in patient subgroups with good compliance to the treatment [19,67]. A relationship between 25-(OH)D serum levels and fracture risk has been established for levels below 20 ng/ml. A prospective trial with older women has shown the highest benefit at levels of about 25 ng/ml [125].

2.2.5 Non-Skeletal Effects of Vitamin D Supplementation

In observational studies low levels of 25-(OH)D have repeatedly been associated with increased risk of diabetes mellitus, cancer, autoimmune as well as cardiovascular disease [125]. Prospective trials and meta-analyses, however, have failed so far to provide solid data of a reversal of these risks under vitamin D supplementation.

Specifically, vitamin D supplementation has not been associated with a lower risk of cardiovascular events or all-cause mortality [67]. Concerning muscle strength, a benefit in supplementation has been shown in systematic reviews of randomized trials in older individuals with low vitamin D levels [158].

2.2.6 Vitamin D and Cancer

Data on cancer incidence has been contradictory. Whereas some suggest an association between vitamin D deficiency and an increase in cancer incidence, in other trials higher vitamin D levels (≥ 40 versus 20-30 ng/ml) were associated with an elevated cancer risk [135,136].

In colon cancer, higher vitamin D levels were associated with an improvement in overall survival (OS) and progression-free survival (PFS) in a prospective trial [165]. A double-blind phase 2 randomized clinical trial of 139 patients with advanced or metastatic colorectal cancer receiving mFOLFOX6 plus bevacizumab and either high- or standard-dose vitamin D was able to demonstrate a non-significant increase in PFS with high dose vitamin D [106]. A Japanese single center, double-blind, placebo-controlled trial randomized 417 patients with digestive tract cancer to receive vitamin D (2000 IU/d) or placebo. Supplementation did not result in significant improvement in relapse-free survival at five years [147].

A recent post hoc analysis of the RICOVER trial of the German High Grade Lymphoma Study Group (DSHNHL) led to the important finding, that a sufficient supply of vitamin D positively influenced the prognosis of patients with DLBCL treated with chemotherapy combined with rituximab, but not of patients treated with chemotherapy alone. This effect is more pronounced in female compared to male patients [20]. Since ADCC is one of the major effector mechanisms of rituximab, a further study was conducted analyzing (among others) rituximab-mediated cellular cytotoxicity against a lymphoma cell line before and after vitamin D substitution. It could be shown that healthy subjects who achieved 25(OH)D serum levels of > 30 ng/mL had a significantly stronger ADCC. Again, ADCC enhancement was more pronounced in NK cells derived from female patients [105].

2.2.7 Vitamin D and the Immune System

Several epidemiological studies have linked vitamin D levels with the incidence of autoimmune diseases like diabetes mellitus type I, systemic lupus erythematosus, multiple sclerosis, inflammatory bowel disease and rheumatoid arthritis. Vitamin D receptor (VDR) is expressed in almost all immune cells, including activated CD4⁺ and CD8⁺ T cells, B cells, NK cells, neutrophils, and antigen-presenting cells such as macrophages and DCs [12][162]. Furthermore, most immune cells express CYP27B1 including macrophages, B-, T-lymphocytes and DCs which also express CYP2R1. It has been subsequently suggested that these cells can convert 25(OH)D₃ into bioactive 1,25(OH)₂D₃.

2.2.7.1 Innate Immunity

1,25(OH)₂D has been shown to enhance the antimicrobial properties of immune cells such as **monocytes** and **macrophages**. Vitamin D particularly affects the differentiation of monocytes into macrophages and enhances their chemotactic and phagocytic properties. In addition, the

cell-typical surface molecules MHC-II, CD40, CD80, and CD86 are less well expressed under $1,25(\text{OH})_2\text{D}$ and production of IL-1, IL-6, TNF- α , IL-8, and IL-12 is reduced [12].

Vitamin D dependent antimicrobial activity via cathelicidin antimicrobial peptide (CAMP) has been confirmed in monocytes/macrophages against *Mycobacterium tuberculosis* in a TLR-dependent manner [90]. More recently, macrophage activity against high-grade B cell lymphoma cells has also been shown to be vitamin D dependent [24]. The mechanism underlying this pathway seems to be the upregulation of the genes of cathelicidin hCAP-18, defensin b2 and NOD2 in monocytes, macrophages as well as in **neutrophils and other myeloid cells**. Exposure to vitamin D also induces downregulation of TLR2 and TLR4 on monocytes, which has been suggested to be a negative feedback mechanism to prevent excessive TLR activation and inflammation [12].

2.2.7.2 Adaptive Immunity

Within the acquired immune system, $1,25(\text{OH})_2\text{D}$ inhibits **dendritic cell** maturation and thus reduces the potential of these cells for activation of and antigen presentation to their corresponding target cells. DCs treated with $1,25(\text{OH})_2\text{D}$ have a reduced capacity to trigger T-cell proliferation and alter T-cell responses. Typical surface markers of DCs, such as MHC-class II and co-stimulatory molecules like CD40, CD80 and CD86 have been shown to be downregulated after activation of the vitamin D receptor. Furthermore, vitamin D regulates cytokine production, inhibiting the production of IL-12 and IL-23 while stimulated the IL-10 and CCL22 excretion.

VDR expression is increased in **T cells** in their activated state. $1,25(\text{OH})_2\text{D}$ exerts a direct effect on the cytokine profiles of T cells. It causes reduced secretion of both inflammatory Th1-cytokines such as IL-2 and IFN- γ as well as Th17-derived cytokines IL-17 and IL-21.

B cells are also directly affected by vitamin D. $1,25(\text{OH})_2\text{D}$ inhibits B cell proliferation, differentiation to plasma-cells, immunoglobulin secretion, memory B cell generation and induces B cell apoptosis [12].

2.2.8 Vitamin D and Natural Killer Cells

In healthy elderly subjects, the NK-cell number and/or cytolytic activity has been positively associated with serum levels of vitamin D [98]. Recently, 25-OH-D_3 substitution in deficient individuals has been shown to increase rituximab- as well as obinutuzumab-mediated NK-cell cytotoxicity in vitro. Maximum NK-cell activity was observed at 65 ng/ml 25-OH-D_3 , which means that supplementation to lower levels would result in the failure of interventions with vitamin D [105]. Other studies have also shown increased NK-cell cytotoxicity with calcitriol supplementation in patients on hemodialysis with vitamin D₃ deficiency [120]. However, it has

not yet been possible to show a molecular relationship between vitamin D supply and NK-cell mediated ADCC.

2.3 AIMS OF THIS THESIS

So far we have seen that vitamin D deficiency correlates with worse survival in patients with DLBCL treated with rituximab-chemotherapy [20] and that NK-mediated ADCC in the presence of rituximab is enhanced after in vivo vitamin D supplementation against lymphoma cell lines [105]. Furthermore, these effects are more pronounced in female subjects. This implies a direct effect of vitamin D on NK cells and suggests that this may be, at least to some extent, a sex-specific effect. This study aims primarily to unveil the molecular mechanisms through which vitamin D supplementation enhances NK-cell mediated ADCC. Secondary analyses will explore possible sex-specific interactions.

3 MATERIALS AND METHODS

3.1 STUDY DESIGN

3.1.1 Inclusion and Exclusion Criteria

We recruited eight otherwise healthy volunteers with 25(OH)D serum levels below 20 ng/ml. Other inclusion criteria were a minimum age of 30 years and a written informed consent to the planned procedure including possible side effects that may result from taking vitamin D supplementation. Exclusion criteria were lack of consent, the presence of hematological diseases and ongoing therapy with immune-modulating or -suppressive drugs. In particular, the intake of glucocorticoids, chemotherapeutics or biologicals was not compatible with inclusion in the study.

3.1.2 Data Handling and Ethical Aspects

The data of the volunteers were encrypted. Each participant was assigned an internal identification number, which could be used to send pseudonymised blood samples to the Institute of Clinical Chemistry and Laboratory Medicine at the Saarland University Medical Center without risking invasion of privacy. The study was approved by the Ethics Commission of the Saarland Medical Association (identification number 178/17) and carried out in accordance with the Declaration of Helsinki.

3.1.3 Vitamin D Supplementation

Each individual received vitamin D supplementation a target 25(OH)D serum level of 65 ng/ml. For this a modified formula according the one proposed by van Groningen et al. was used [148]. Cholecalciferol (I.U.) = Δ 25-OH-D3 (ng/ml) \times body weight (kg) \times 200 (with “ Δ 25-OH-D3” meaning the difference between the current and the target 25-OH-D3 serum level). Applying this formula, the pre-defined serum level was achieved within a narrow margin in nearly all individuals. The cholecalciferol product Dekristol® 20.000 I. U. (*mibe GmbH Arzneimittel, Brehna, Germany*) was used.

After vitamin D supplementation, serum levels of calcium and phosphate were determined in order to avoid vitamin D intoxication and take appropriate countermeasures if necessary. In all subjects, however, the calcium and phosphate levels remained within the normal range.

3.1.4 Sample Labeling

Samples obtained at the stage of vitamin D deficiency were assigned the suffix “a”. Samples obtained after vitamin D supplementation received the suffix “b”. **Table 2** provides the participant list and the label of each sample.

Table 2: Sample labeling

Test subject identification number	Vitamin D deficient status	After vitamin D supplementation
70	70a	70b
71	71a	71b
72	72a	72b
73	73a	73b
74	74a	74b
75	75a	75b
92	92a	92b
99	99a	99b

3.1.5 Participant Characteristics and Vitamin D Levels

A previous study done by our group had shown that NK cell cytotoxicity was highest at approximately 65 ng/ml vitamin D [105]. We collected the samples from these same eight healthy volunteers at the at vitamin D deficient state and after vitamin D supplementation to approximately 65 ng/ml. Their characteristics and vitamin D levels are presented in **Table 3**.

Table 3: Participant characteristics and 25(OH)D serum levels

Test subject identification number	Sex	Age (years)	Vitamin D levels in deficient status (ng/ml)	Vitamin D levels after supplementation (ng/ml)
70	male	78	5.9	64.3
71	female	71	23	68.2
72	male	57	15.7	62.6
73	female	78	4.6	68.8
74	male	79	6.1	72.8
75	female	79	9.7	68.5
92	male	86	10.3	58.2
99	female	42	8.8	61.5
Mean	-	71.3	10.5	65.6

3.2 MATERIALS

3.2.1 Chemicals, Reagents, Buffers, Mediums and Solutions

Table 4: Chemicals, reagents, buffers, mediums and solutions used in the study

Name	Manufacturer, Article number
Dekristol® 20.000 I. U.	mibe GmbH Arzneimittel Brehna, Germany
Phosphate-buffered saline (PBS)	Sigma-Aldrich Chemie GmbH Munich, Germany Article number: D8537-1L
Ethylenediaminetetraacetic acid (EDTA, 0,5 M)	Life Technologies Europe BV Bleiswijk, Niederlande Article number:15575020
Fetal calf serum (FCS)	Sigma Aldrich Chemie GmbH Munich, Germany Article number: F0804-500ML
L-Glutamin (200 mM)	Sigma-Aldrich Chemie GmbH Munich, Germany Article number: G7513-100ML
Penicillin-Streptomycin (10.000 U/ml Penicillin, 10 mg/ml Streptomycin)	Sigma Aldrich Chemie GmbH Munich, Germany Article number: P0781-100ML
Pancoll human, Density: 1.077 g/ml	PAN Biotech GmbH Aidenbach, Germany Article number: P04-60500
Deionised water (Aqua)	Braun GmbH Kronberg im Taunus, Deutschland Article number: 113328002
Ethanol, absolute for analysis EMSURE® ACS, ISO, Reag. Ph Eur	Merck KGeA Darmstadt, Germany Article number: K49631383743
Agarose NEEO Ultra-quality	Carl Roth GmbH + Co. KG Karlsruhe, Germany Article number: 2267.4
Sodium-Acetate (C₂H₃NaO₂)	Merck KGeA Darmstadt, Germany Article number: TA555568 920 / 1062681000

Sodium Hydroxide (NaOH)	Merck KGeA Darmstadt, Germany Article number: 1064691000
3-(N-morpholino)propanesulfonic acid (MOPS) Buffer	Calbiochem San Diego, USA Article number: B32914
Diethyl Pyrocarbonate (DEPC)	SERVA Electrophoresis GmbH Heidelberg, Germany Article number: 23020
Ethidium Bromide Solution 1%	Carl Roth GmbH + Co. KG Karlsruhe, Germany Article number: 2218.1
Cell wash	BD GmbH (Becton, Dickinson and Company) Heidelberg, Germany Article number:349524
MACS[®]-Buffer	0,5 % FCS 2 mM EDTA ad 15 ml PBS
MACS[®] NK Cell Isolation Kit, human	Miltenyi Biotec GmbH Bergisch-Gladbach, Germany Article number:130-092-657
miRNeasy[®]Mini Kit	Qiagen N.V. Venlo, Netherlands Article number: 217004
SuperScript[™] III Reverse Transcriptase kit	Thermo Fisher Scientific, Waltham, Massachusetts, USA Article number: 18080093
LightCycler[®] FastStart DNA Master SYBR Green I	Hoffmann-La Roche AG Basel, Switzerland Article number: 12239264001
RNA Gel Loading Dye (2X)	Thermo Fisher Scientific, Waltham, Massachusetts, USA Article number: R0641
RiboRuler High Range RNA Ladder	Thermo Fisher Scientific, Waltham, Massachusetts, USA Article number: SM1821
AffymetriGeneChip WT PLUS Reagent Kit	Affymetrix, Inc., Santa Clara, USA Article number: 902281

GeneChip™ Human Gene 2.1 ST Array Plate	Thermo Fisher Scientific, Waltham, Massachusetts, USA Article number: 902136
--	--

The article number is only given if the item in question is not part of a laboratory's standard equipment.

3.2.2 Antibodies, Enzymes, Primers

Table 5: Antibodies, enzymes, primers used in the study

Name	Manufacturer, Article number
Anti CD16-FITC	BD GmbH (Becton, Dickinson and Company) Heidelberg, Germany Article number: 656146
Anti CD56-PE	BD GmbH (Becton, Dickinson and Company) Heidelberg, Germany Article number: 345812
Primer for cDNA Synthesis (oligo-p(dt)15)	Hoffmann-La Roche AG Basel, Switzerland Article number: 10814270001
Primer "random"	Hoffmann-La Roche AG Basel, Switzerland Article number: 11034731001
CleanAmp™ dNTP	Merck KGeA Darmstadt, Germany Article number: DNTPCA10-1KT

3.2.3 Consumables

Table 6: Consumables used in the study

Name	Manufacturer, Article number
Centrifuge tube 15 ml	Sarstedt AG & Co KG Nümbrecht, Germany
Centrifuge tube 50 ml	
Reaction tube 0,5 ml	
Reaction tube 1,5 ml	
Reaction tube 2 ml	
Various pipette tips	
Serological pipettes 5ml	
Serological pipettes 25ml	

Serological pipettes 10ml	Corning GmbH Kaiserslautern, Germany
RNase-free Microfuge Tubes, 2.0 ml	Thermo Fisher Scientific, Waltham, Massachusetts, USA Article number: AM12425
RNase-free Microfuge Tubes, 1.5 mL	Thermo Fisher Scientific, Waltham, Massachusetts, USA Article number: AM12400
RNase-free Microfuge Tubes, 0.5 mL	Thermo Fisher Scientific, Waltham, Massachusetts, USA Article number: AM12300
MACS[®] LS-Column	Miltenyi Biotec GmbH Bergisch-Gladbach, Germany Article number: 130-042-401
QIAshredder[®] Column	Qiagen N.V. Venlo, Netherlands Article number: 79654
Microseal 'B' PCR Plate Sealing Film, adhesive, optical	Bio-Rad Laboratories, Inc. California, USA Article number: MSB1001
Hard-Shell[®] 96-Well PCR Plates, low profile, thin wall, skirted, white/clear	Bio-Rad Laboratories, Inc. California, USA Article number: HSP9601

The article number is only given if the item in question is not part of a laboratory's standard equipment.

3.2.4 Equipment

Table 7: Equipment used in the study

Name	Manufacturer, Article number
Centrifuge 5810 R	Eppendorf AG Hamburg, Germany
Centrifuge 5415 D	
Pipette Research[®] 1-10 µl	
Pipette Research[®] 10-100 µl	
Pipette Research[®] 100-1.000 µl	
Handdispenser Multipipette[®] M4	
Biological Safety Cabinet HERAsafe[™] HSP 18	Life Technologies GmbH / Thermo Fisher Scientific Darmstadt, Germany

MACS® MidiMACS™ Separator	Miltenyi Biotec GmbH Bergisch-Gladbach, Germany Article number: 130-042-302
Flow cytometer FACSCalibur™	BD Biosciences GmbH Heidelberg, Germany Article number: 342975
Vortex mixer Heidolph REAX top	Heidolph Instruments GmbH & Co.KG Schwabach, Germany
Mini-Sub DNA cell™ Electrophoresis Cell	Bio-Rad Laboratories, Inc. California, USA
UVP High-Performance UV Transilluminator TFS-20, 25 Watt, 254 nm UV	Thermo Fisher Scientific, Waltham, Massachusetts, USA Article number: P/N 95-0319-02
NanoDrop 1000 Spectrophotometer	Thermo Fisher Scientific, Waltham, Massachusetts, USA
Biotron Biometra TRIO Thermoblock Heat Cycler	Biometra GmbH Göttingen, Germany
IKA® KS250 basic Shaker	IKA-Werke Staufen im Breisgau, Germany Article number: 93-139-20
CFX Connect™ Real-Time PCR Detection System	Bio-Rad Laboratories, Inc. California, USA Article number: 788BR03770

The article number is only given if the item in question is not part of a laboratory's standard equipment.

3.3 METHODS

3.3.1 Cell Counting

The experimental setup required precise knowledge of the number of cells in a suspension. Since the exact volume of the cell suspension must be known in order to calculate the cell number, it was first determined using a suitable graduated pipette. 5 µl were taken from the cell suspension and diluted with PBS to a total volume of 50 µl. This diluted suspension was mixed with trypan blue in a ratio of 1:1. Trypan blue is a staining agent commonly used in cell biology to identify dead cells, since it is exclusively absorbed by apoptotic and necrotic cells, while vital cells do not stain [137]. Therefore, it was easy to count selectively the vital unstained cells. The proportion of dead cells was always below 10 %. Counting itself was done according to the Neubauer method using a chamber slide with the same name.

3.3.2 Isolation of PBMC

To isolate the NK cells, approx. 50 ml of whole blood were taken from the respective volunteer on the day of the ADCC test in commercial blood collection tubes with the anticoagulant EDTA. To isolate the NK-cell fraction, the peripheral blood mononuclear cells (PBMC) were first separated by density gradient centrifugation. PBMC are a mixture of T- and B-lymphocytes, monocytes, DCs, and NK cells. The relative proportion of individual leukocyte populations varies inter- and intraindividually. Granulocytes (also: polymorphonuclear cells; PMN) do not belong to the PBMC.

Pancoll™, a synthetic sucrose-epichlorohydrin copolymer, was used to build up the density gradient required to isolate the PBMC. With a density of 1.077 g/ml, Pancoll™ separates the PBMC fraction during centrifugation from the erythrocytes and granulocytes, the two remaining cell populations of the peripheral blood, due to their higher density towards the centripetal. Due to its slightly cytotoxic effect, Pancoll™ has to be rinsed out immediately after isolation of the PBMC[23].

For density gradient centrifugation, 4 ml Pancoll™ were placed in a 15 ml centrifuge tube. The approximately 50 ml of EDTA whole blood were diluted with about 16 ml PBS to be distributed to six centrifuge tubes. To this end, the 4 ml Pancoll™ were carefully coated with 11 ml of the EDTA whole blood/PBS suspension and centrifuged for 30 minutes at room temperature and 500 g.

After centrifugation, the phase containing the PBMC was harvested from all tubes and collected in a 50 ml centrifuge tube. Then the PBMC were washed twice with cold PBS and centrifuged in each case (10 min, 4 °C, 300 g). After centrifugation the supernatant was discarded, and the pellet was resuspended in fresh PBS. After the second washing, the pellet was resuspended in 7 ml PBS and the vital PBMC were counted.

3.3.3 NK-Cell Enrichment by Magnetic Cell Sorting

The second step, after the isolation of the PBMC, was the enrichment of the NK cells from the PBMC. This was done by means of magnetically activated cell sorting (MACS™). In this process, the cell types which ought to be enriched or eliminated, were magnetically marked with cell-type-specific markers (mostly CD molecules). This was done with marker-specific antibodies, which are bead-coupled. In this case the non-NK cells were depleted from the PBMC. The different cell populations of the PBMC that are not NK cells, i.e. T cells, B cells and monocytes, as well as post-Pancoll cell type residues (granulocytes, erythroid cells, etc.) were labelled with an appropriate antibody cocktail. The bound antibodies were then coupled with magnetic beads via a biotin/anti-biotin bridge. This bead/antibody-cell suspension then was applied to an LS separation column that was positioned in a magnetic field. In the magnetic field, the labelled non-NK cells remained stuck, while the unlabeled NK cells passed through

the column unhindered. The NK cells then were centrifuged, and the pellet was resuspended in medium. From this NK-cell suspension, both the sample to determine the cell count according to Neubauer and the sample for flow cytometric analysis of CD16/CD56 purity were taken.

The NK Cell Isolation Kit, human from Miltenyi Biotec GmbH, was used for this purpose. The kit was used according to the protocol of the provider. Calculating the number of PBMC used, the capacity of the MACS™ column and the isolation strategy were considered. Due to the binding capacity of the LS-separation column of a maximum of 10^8 marked (non-NK) cells and the depletion strategy described above, a maximum of only 10^8 PBMC were used from each subject. These were centrifuged once more (10 minutes, 300 G, 4 °C), the liquid supernatant discarded and the PBMC pellet resuspended in 40 µl MACS™ buffer per 10^7 cells. Now 10 µl of the biotin antibody mixture per 10^7 cells were added to label the non-NK cells. This suspension was thoroughly mixed and incubated at 4 °C for 5 minutes. Then 30 µl MACS™ buffer and 20 µl MicroBeads were added to label the bound antibodies for MACS separation, again per 10^7 cells. After subsequent mixing and 10 minutes incubation at 4 °C, the PBMCs could be sorted. The cell suspension was placed in the MACS™-LS column, which had meanwhile been equilibrated with 3 ml MACS™ buffer. After passing through this suspension, the column was rinsed twice with 3 ml MACS™ buffer.

The LS column with the bound non-NK cells was discarded. The NK cells isolated in the run were centrifuged after sampling for flow cytometric quality control to remove the MACS™ buffer (300 G, 10 minutes, 4 °C). The cell pellet was incorporated in 500 µl ADCC medium (NK-cell stock suspension). The cells were then quantified.

3.3.4 Flow Cytometry

Approximately 90 % of the NK cells are to be assigned to subtype CD56^{dim}/CD16^{high}, which has pronounced cytotoxicity. CD16 refers to FcγRIIIa, which is an antibody receptor essential for ADCC. Instead, other subpopulations such as CD56^{bright}/CD16^{dim} show increased immunoregulatory functions such as the production of cytokines. They may also be precursors of CD16+ NK cells. However, since the aim of this work was to investigate the ability of NK cells to ADCC, the proportion of CD16+ cells, regardless of CD56 expression, was determined by fluorescence-activated flow cytometry.

After MACS™ isolation, 80 µl of the NK cell stock suspension was removed and centrifuged in a reaction vessel (2 minutes, 400 G). The supernatant was discarded, and the cell pellet was resuspended in 50 µl PBS. This NK suspension was incubated for 15 minutes with 2.5 µl each of the two fluorescence-labeled antibodies CD16 FITC (CD16 fluorescein isothiocyanate) and CD56 PE (CD56 phycoerythrin). After renewed centrifugation (same parameters) to remove unbound antibodies, the CD16- and CD56-labelled NK cells were dissolved in 120 µl Cell

Wash™. The number of vital lymphocytes was counted according to Neubauer and the proportion of CD 16+ cells was determined by flow cytometry. With these two parameters the exact number of enriched NK cells was calculated.

3.3.5 RNA Extraction

After the ADCC assay, the remaining NK cells were stored in pellets at - 80 °C. The stored cell suspensions contained from 5×10^6 to 1×10^7 NK cells. Prior to storage cells culture medium was removed after centrifugation of the cell suspension for five minutes at 300 G. At the time of RNA extraction, the cell pellets were removed from storage and immediately processed. For RNA isolation, the miRNeasy Mini Kit™ (Qiagen, Velno, Holland) was used, according to the included protocol. To perform cell disruption, after loosening the cell pellets by manual flicking of the tubes, 700 µl QIAzol Lysis Reagent™ was added and the mixture was mixed by pipeting and vortexing for a few seconds. The tubes were then left for five minutes on the benchtop at room temperature. Homogenization was achieved with a QIAshredder spin column™ (Qiagen) to avoid cross-contamination of samples. 700 µl of each lysate were added on the individual spin columns, which were each placed in 2 ml collection tubes. The tubes were centrifuged for two minutes at maximum speed. The spin columns were then disposed. After adding 140 µl of chloroform to the collection tubes, the mixture was vortexed for 15 s and the homogenates were left at room temperature for two minutes. Another centrifugation followed at 12,000 G at 4°C for 15 minutes. Subsequently the upper aqueous phases were transferred to new collection tubes. 525 µl of 100 % ethanol were added to each sample followed by thorough mixing with the pipette. 700 µl of this sample were transferred into an RNeasy™ spin column in a 2 ml collection tube. A short centrifugation of 15 s at 8,000 G followed. The process was repeated with the rest of the sample, the flow-through was discarded. 700 µl of buffer RWT™ was added to the spin column and after centrifugation for 15 s at 8,000 G the flow-through was discarded. The same centrifugation und discarding of flow-through was repeated after adding 500 µl of RPE buffer™. Thereafter, the spin column again was transferred into a new 2 ml collection and centrifuged at full speed for one minute, to avoid carry over of flow-through remains into the RNA elution phase. For the final step, the spin columns were transferred one last time to new 1.5 ml collection tubes. 30 µl of RNase-free water were pipetted onto each sample, followed by centrifugation at 8,000 G for 1 minute. A relatively small sample volume (30µl) was chosen on purpose in favour of a higher sample RNA concentration.

3.3.6 Spectrophotometry

For spectrometry, the NanoDrop 1000 Spectrophotometer was used. Prior to each measurement 2 µl RNase-free water aliquots were loaded to clean measurement surfaces. For each sample 2 µl were loaded onto the measurement pedestal.

3.3.7 RNA Electrophoresis

RNA is particularly susceptible to degradation. Therefore, all used solutions were prepared with RNase free, deionized water, which was prepared using DEPC. For this 2 ml DEPC was added to one liter deionized water. After mild shaking, the solution was shaken at 37 °C overnight. The remaining DEPC was removed by autoclaving.

To create the gel for RNA electrophoresis, an appropriate 3-(N-morpholino) propanesulfonic acid (MOPS) 20x buffer solution was prepared. For this purpose, 83.72 g of MOPS and 8.23 g of sodium acetate were added to 700ml of DEPC-treated water, followed by stirring until complete dissolution. 7.4 g EDTA were added to the mixture as well as NaOH until a pH of 7 was achieved. Finally, DEPC-treated water was added up to 1000 ml and the flask was covered with aluminum foil.

For the purpose of our experiment, a 150 ml agarose gel was cast. Initially 1,5 g of the agarose powder was mixed with 142.5 ml of DEPC-treated water and was left to boil in the microwave for three minutes. The solution was cooled down on a shaker for ten minutes, after which 75 µl of ethidium bromide and 7.5 ml 20x MOPS buffer were added. The gel was casted under the hood in sterile conditions and subsequently stored at 4 °C.

As running buffer for the electrophoresis 1x MOPS solution was used. To create 250 ml of 1x MOPS solution 12.5 ml of the 20x MOPS solution were diluted with 237.5 ml DEPC-treated water.

The sample preparation was done in a prompt matter and RNA samples were kept in ice. In a new, 0.5 ml RNase-free tube, 5 µl of RNA loading dye and 5 µl of RNA-free water as well as 100 ng of sample RNA were added. The tubes were heated up to 65 °C for five minutes and loaded onto the gel. The mixture was run with 80 Watt for approximately 30 minutes. Finally, gels were read out on an UV transilluminator.

3.3.8 Microarray Assay

For RNA expression analysis the GeneChip™ Human Gene 2.1 ST Array Plate was chosen. RNA coverage and technical information of the chosen microarray are demonstrated in **Table 8**. Because of the broad coverage of the microarray, we refrained from testing for expression of receptors on the NK cell surface or measuring cytokine levels. We assumed that an increase/decrease in protein production must be reflected in the produced mRNA levels.

Table 8: Technical Information about the Human Gene 2.1 ST Array Plate

Transcript Category	Number covered
Total RefSeq transcripts covered	40,716
NM – RefSeq coding transcript, well-established annotation	30,654
NR – RefSeq non-coding transcript, well established annotation	5,638
XM – RefSeq coding transcript, provisional annotation	996
XR – RefSeq non-coding transcript, provisional annotation	3,428
lncRNA transcripts	11,086
RefSeq (Entrez) gene count	24,838

The microarray contained both non-coding and coding transcripts. Furthermore, of the coding transcripts, not all have well established annotations. Referring to microarray results, we use the term “transcript” to include all the above. By using the term “gene”, we refer to probes containing DNA sequences encodings proteins or RNA with a well-established annotation. Sample preparation and microarray hybridization was carried out with the AffymetriGeneChip WT PLUS Reagent Kit at an Affymetrix Service Provider and Core Facility, “KFB - Center of Excellence for Fluorescent Bioanalytics” (Regensburg, Germany; www.kfb-regensburg.de) as described in the user Manual. In short: for each sample, double-stranded cDNA was generated from 200 ng of total RNA. 12 µg of subsequently synthesized cRNA was purified and reverse transcribed into sense-strand (ss) cDNA. Incorporation of unnatural dUTP residues also took place at this stage. Purified ss cDNA was fragmented using a combination of uracil DNA glycosylase (UDG) and apurinic/apyrimidinic endonuclease 1 (APE 1) followed by a terminal labeling with biotin. 3,8 µg of fragmented and labeled ss cDNA were hybridized to Affymetrix Human Gene 2.1 ST Array Plates. For hybridization, washing, staining and scanning an AffymetriGeneTitan system, controlled by the AffymetriGeneChip Command Console software v4.2, was used.

3.3.9 Microarray Quality Control

Different signal and quality metrics were calculated to assure data quality and to identify outlier samples. First, the signal strengths across all arrays were displayed in a histogram (**Figure 1**). Prior to data normalization, a Box Plot for Log Probe Cell Intensity (**Figure 2**) and a Box Plot for Relative Log Probe Cell Intensity (**Figure 3**) were created. This allowed a comparison of the distribution of intensities on each array with the mean value of the probe intensity of the whole group. After normalization and log₂-transformation, the logarithmic values of the signal strength of the expression were displayed in the form of a boxplot, both absolute (Log Expression Signal (**Figure 4**)) and relative (Relative Log Expression Signal (**Figure 5**)).

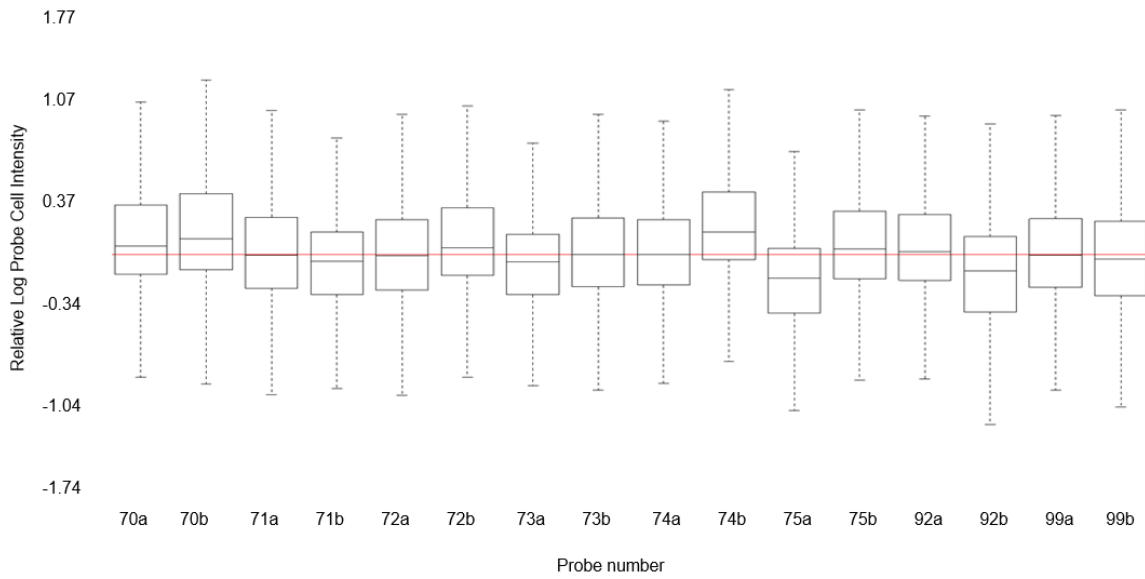


Figure 3: Relative log probe cell intensity

The relative log probe cell intensity summarizes the distribution of the ratio of signal for each probe set to the median probe set signal across all the selected arrays. Therefore, the plot compares the distribution of probe set signal values on each array to the median array for the group. Again, the data were homogeneous enough and no outliers could be identified.

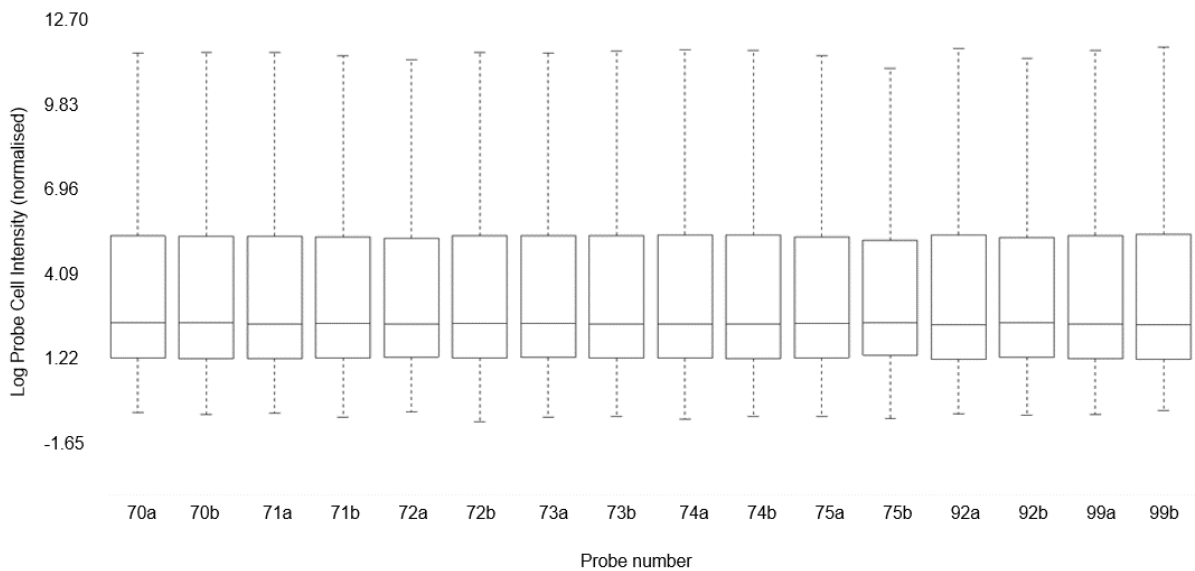


Figure 4: Log expression signal

This plot displays the results of log probe cell intensity (Fig. 2) after normalization. The normalized data were completely homogeneous and confirmed the reliability of the results obtained.

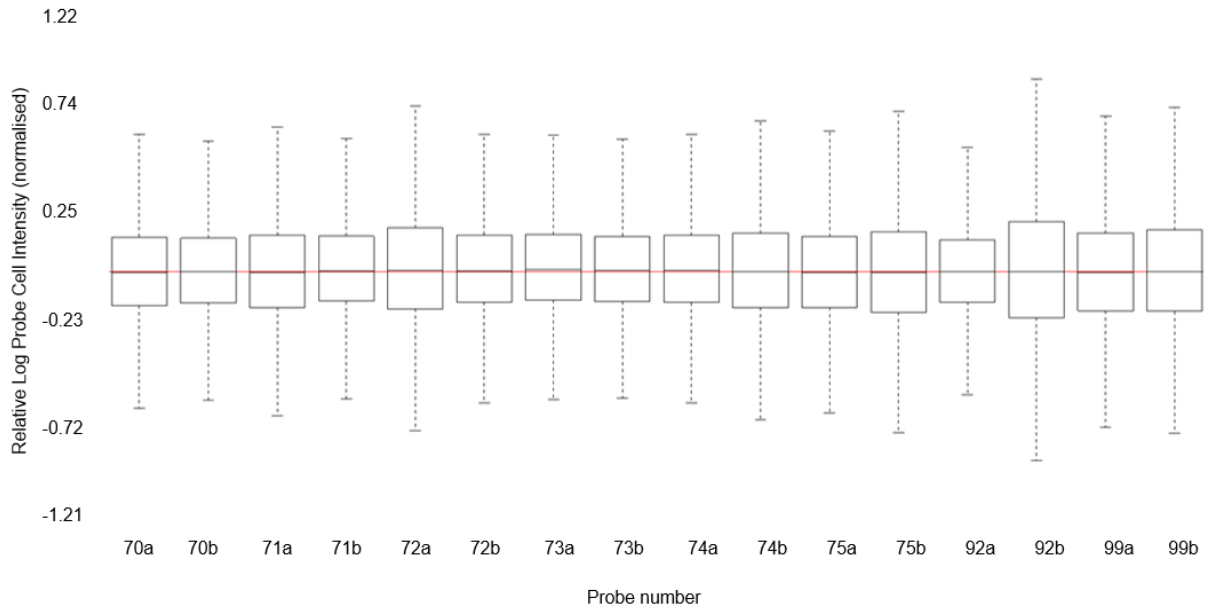


Figure 5: Relative log expression signal

This plot summarizes the ratio distribution of the signal for each probe set to the median probe set signal across all arrays. It allows the comparison of the distribution of probe set signal values on each array to the median array for the group, thus enabling the identification of outliers. Again, after normalization, the relative log expression signals were even more homogeneous.

Furthermore, to look at the relationship between the variables in our samples and to identify outliers, two standard statistical methods of linear correlation were used: Pearson's and Spearman Rank Correlation. The correlation values were displayed as heatmaps, in order to simplify the interpretation of the data (**Figure 6** and **Figure 7**). No outliers were identified with this method.

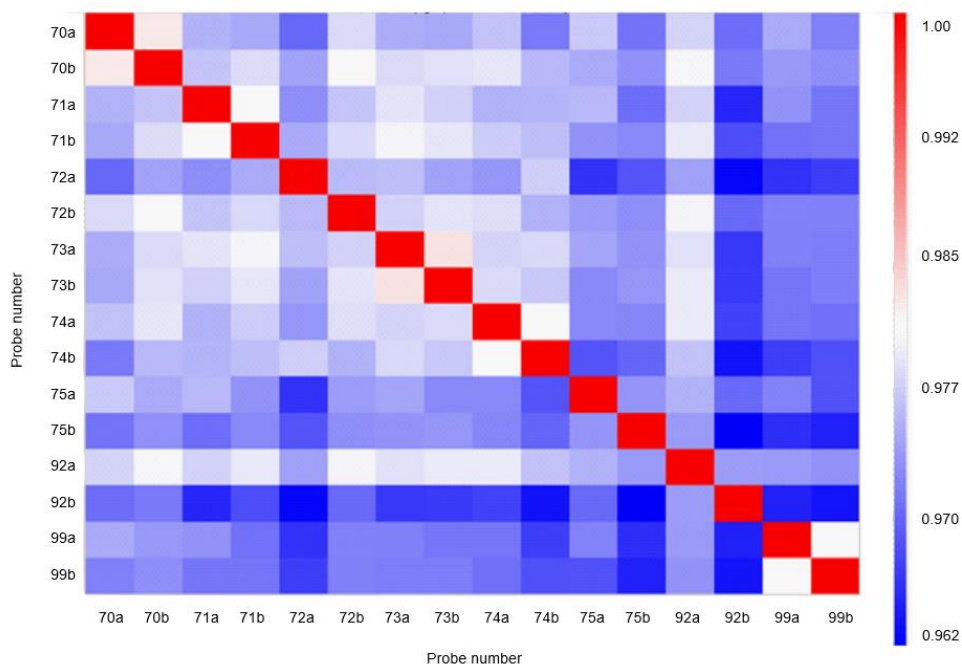


Figure 6: Pearson's correlation (signal)

The Pearson's correlation coefficient (r^2) value was used to evaluate signal concordance between two arrays. This heap map provides a pairwise comparison of signal values from all arrays. r^2 values have been converted into a pseudocolor scale. Darker red indicates higher concordance between the two signals, deeper blue means weaker concordance. No outliers could be identified.

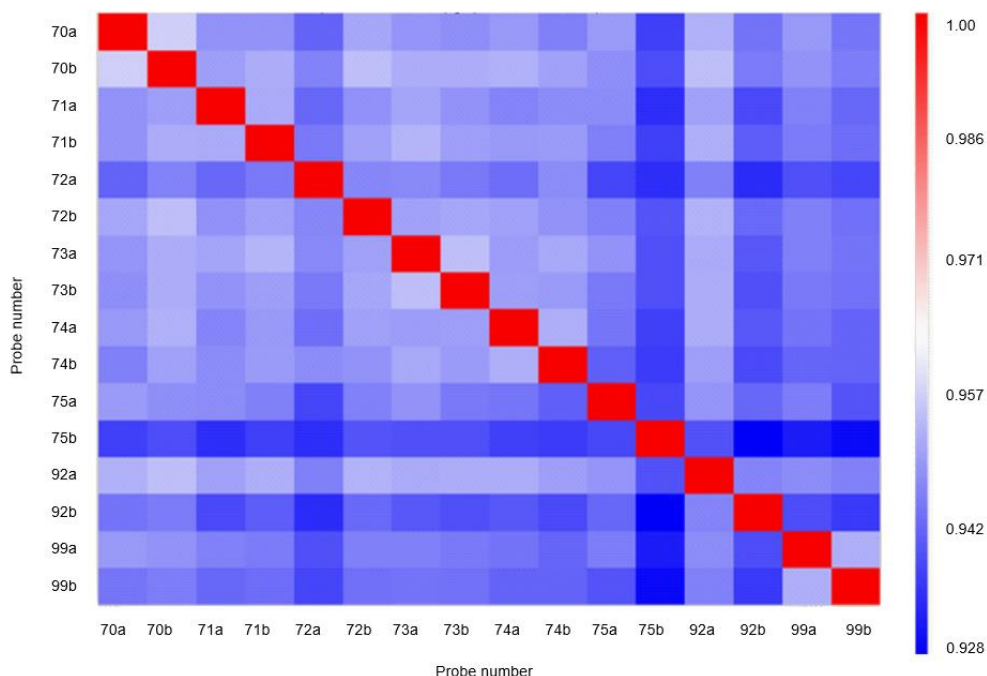


Figure 7: Spearman rank correlation (signal)

The Spearman's correlation is another method to evaluate signal concordance between two arrays. This heap map provides a pairwise comparison of signal values from all arrays, after the r^2 values have been converted into a pseudocolor scale. Darker red indicates higher concordance between the two signals, deeper blue means weaker concordance. No outliers could be identified.

Other metrics were calculated to assure data quality. The most important ones are listed here and in **Table 9** and **Table 10**.

Pm mean: The mean of the raw intensity for all probe sets on the array prior to any intensity transformation. This metric can be used to detect bright or dim arrays.

Bgrd mean: The mean of the raw intensity for the probes used to calculate background prior to any intensity transformations.

All probesets mad residual mean: The mean of the absolute deviation (MAD) of the residuals from the median imposed by RMA. The difference between the actual value and the predicted value is called the residual. One can use this metric to identify arrays that have a large number of probes that are behaving differently than predicted by the model. An unusually high value may be a sign of a problematic sample.

All probesets rle mean: The mean absolute relative log expression (RLE). The signal of each probe set is compared to the median signal value of this probe set in the study. The metric is the mean of these differences from all the probe sets. Unusually high values indicate that the signals on the array are different from others in the study, i.e., big values are bad. This metric is most useful for studies with similar sample types to detect outlier arrays. For a set of different tissues, for example, this metric is less useful.

Polya spike-AFFX-...: Each eukaryotic GeneChip probe array contains probe sets from several *B. subtilis* genes (lys, phe, thr, and dap) that are absent in eukaryotic samples. These exogenous Poly-A RNA controls are spiked into the RNA sample at staggered concentrations, carried through the sample preparation process, and evaluated like the internal control genes. Increasing signal values in the order of lys, phe, thr, dap, indicate that the entire target labeling process was successful.

While the Phe-Poly-A spike is a little lower in that the Lys-Poly-A spike in probes 72a, 73b and 99a, the consequent spikes show regular progression. Small variations are a common observation in such experiments. Most importantly the Pearson and Spearman rank correlation clearly demonstrated that no outliers occurred, and the entire process was successful for all probes.

Table 9: Quality control metrics 1

Probe	Pm mean	Bgrd mean	All probesets mad residual mean	All probesets rle mean
70a	155.140656	46.551620	0.473750	0.232106
70b	167.635880	48.638466	0.460750	0.215163
71a	144.445374	41.769939	0.485249	0.235982

71b	129.346237	42.630573	0.485151	0.219818
72a	137.584396	43.701363	0.513390	0.268264
72b	150.244781	44.657310	0.467746	0.220739
73a	131.385452	41.583717	0.466700	0.219056
73b	145.320129	42.438477	0.478096	0.218702
74a	142.617142	43.329399	0.475219	0.226132
74b	158.431885	47.384987	0.475677	0.249287
75a	118.250381	38.702301	0.489690	0.246375
75b	127.325378	44.568146	0.505307	0.273880
92a	149.966461	44.170410	0.457799	0.208877
92b	110.753960	44.606228	0.549525	0.313621
99a	143.950562	41.315315	0.482520	0.270620
99b	141.638412	41.163925	0.498369	0.278563

Abbreviations: *Pm*: Probe mean intensity; *Bgrd*: Background; *mad*: mean of the absolute deviation; *rle*: Relative log expression

Table 10: Quality control metrics 2

Probe	<i>Polya spike-AFFX-LysX-M</i>	<i>Polya spike-AFFX-PheX-M</i>	<i>Polya spike-AFFX-ThrX-M</i>	<i>Polya spike-AFFX-DapX-M</i>
70a	7.190930	7.538183	8.119799	10.079699
70b	7.094028	7.366222	7.724324	9.986629
71a	6.796246	7.054669	7.426122	9.831928
71b	7.228066	7.284276	7.874607	9.973407
72a	6.865479	6.745480	7.790881	9.884852
72b	7.073507	7.288373	7.646286	9.915456
73a	7.314280	7.389640	8.019044	9.997330
73b	7.068339	6.954660	7.894888	10.056053
74a	6.889834	7.126411	7.611820	9.936298
74b	6.775320	6.954896	7.520261	9.640957
75a	6.996794	7.371268	7.693502	10.129491
75b	7.435799	7.901404	7.965506	10.424582
92a	6.842246	6.876032	7.394284	9.674782
92b	7.521118	7.728622	8.210540	10.487738
99a	6.721220	6.647304	7.193521	9.733693
99b	7.946365	8.051426	8.522511	10.631655

3.3.10 Quantitative Real Time Polymerase Chain Reaction Validation

Validation of the results of the microarray data was performed for a selected number of genes by quantitative Real Time Polymerase Chain Reaction (qRT-PCR). After acquisition of the microarray expression data, we searched for genes with significant, preferably variable expression across different samples and a housekeeping gene as control. Another requirement was the availability of a suitable primer for each gene. Two genes were chosen with strong differential expression before and after vitamin D supplementation: allograft inflammatory factor 1 (*AIF1*) and C-type lectin domain family 7, member A (*CLEC7A*). One housekeeping gene was chosen to act as a control: ubiquitin conjugating enzyme E2D 2 (*UBE2D2*). For these three genes suitable primers were selected and synthesized (*Sigma-Aldrich, Darmstadt, Germany*) (**Table 11**). We then proceeded to reverse transcription, cDNA synthesis and RT-PCR.

Table 11: Oligonucleotide primers used for qRT-PCR

Gene Accession	Gene Symbol	Forward Primer	Reverse Primer
NM001623	<i>AIF1</i>	GCTATGAGCCAAACCAGGGA	CCAGTTTGGAGGGCAGATCC
NM022570	<i>CLEC7A</i>	GCTGGCAACTGGGCTCTAAT	AGGGCACACTACACAGTTGG
NM003339	<i>UBE2D2</i>	ATCACAGTGGTCTCCAGCAC	TCCCGAGCTATTCTGTTGTACTTTT

The cDNA synthesis was done with the SuperScript™ III Reverse Transcriptase kit, according to the accompanying protocol. Firstly, 0.5 µl of oligo(dT)₁₅ (50 µM), 1 µl of random primers, 1 µl of dNTP mix (10 mM) and 200 ng of RNA were added in a RNase-free microcentrifuge tube. The total volume depended on the concentration of the RNA of the according sample. The micro centrifuge tube was then filled with sterile, distilled water up to 14 µl volume. The mixture was heated up to 65 °C for 5 minutes and subsequently incubated for 2 minutes on ice. Following a brief centrifugation to collect the contents of the tube, another 4 µl 5x First-Strand Buffer™, 1 µl of 0.1 M DTT and 1 µl of SuperScript™ III RT (200 units/µl) were added to the mixture, followed by thorough mixing. Finally, the mixture was incubated at 55 °C for 45 minutes, followed by renewed heating to 70 °C to inactivate the reaction.

The reaction mix for the RT-PCR was performed with the LightCycler®FastStart DNA Master SYBR Green I according to the accompanying protocol. A 10 µM concentration solution was prepared for each primer. 2 µl of this primer solution were added to 2 µl LightCycler®FastStart DNA Master SYBR Green I, 0.4 µl of MgCl₂ (25 µM) and 13.6 µl of PCR grade water to a total volume of 18 µl in a 1.5 ml reaction tube on ice. The mixture was mixed gently through pipetting and subsequently placed in a 96 well plate. Finally, 2 µl of cDNA template were added for each

sample. Each well was sealed with an adhesive sealing film. We conducted two PCR for each of the different genes/samples and a negative control PCR.

Parameters for qRT-PCR are displayed in **Table 12** and **Table 13**:

Table 12: Parameters for PCR

Analysis mode	Cycles	Segment	Target temperature	Hold time	Acquisition mode
Pre-Incubation					
n/a	1		95 °C	10 min	none
Amplification					
Quantification	45	Denaturation	95 °C	10 s	none
		Annealing	s. Table 13	10 s	none
		Extension	72 °C	30 s	single
Melting Curve					
Melting Curves	1	Denaturation	95 °C	0 s	none
		Annealing	65 °C	15 s	none
		Extension	95 °C	0 s	continuous
Cooling					
n/a	1		40 °C	30 s	none

Abbreviations: n/a: not applicable.

Table 13: Annealing temperature of the different primers

Gene Primer	Annealing temperature during quantification
AIF1	66 °C
CLEC7A	66 °C
UBE2D2	66 °C

The individual annealing temperatures of the qRT-PCR are summarized in **Table 13**. The cycle threshold (Ct) values represent the mean of the two results for each gene/sample. Each result was normalized by subtracting the Ct value of the housekeeping gene from the corresponding Ct value of each gene, thus acquiring the Δ Ct value. Next, the $\Delta\Delta$ Ct (a-b) value after vitamin D substitution was calculated by subtracting the Δ Ct value after vitamin D substitution (Xb) from the Δ Ct value before vitamin D substitution (Xa) for each subject.

3.4 STATISTICAL ANALYSIS

3.4.1 Data Analysis Strategy

Our data analysis strategy was divided into four levels. Firstly, we looked for statistically significant differentially expressed genes (see 3.4.2 below). Secondly, we looked specifically at genes which are, according to current knowledge, involved in the induction of NK cell cytotoxicity. Our third analysis searched for upregulated or downregulated pathways which are part of the immune response in broader sense. Lastly, an unsupervised, explorative analysis searched for pathways which were statistically significant up- or downregulated after vitamin D3 supplementation without any further restrictions.

3.4.2 Comparisons

The primary comparison of this study is between the two vitamin D states:

a = deficiency

and

b = supplementation/substitution (these two terms are considered equivalent in this thesis).

Consequently, we defined two groups for the comparison:

- All test subjects in the vitamin D deficient state: “deficiency” (samples labeled with the suffix “a”)
- All test subjects after vitamin D substitution: “substitution” (samples labeled with the suffix “b”)

However, considering that sex may also play a role, four more groups were defined based on both vitamin D serum levels and sex:

1. Deficient female subjects: “female – deficiency”
2. Deficient male subjects: “male – deficiency”
3. Supplemented female subjects: “female – substitution”
4. Supplemented male subjects: “male – substitution”

Using these definitions following comparisons were performed:

Primary Comparison:

- Comparison I: “deficiency” versus “substitution”

Secondary Comparisons:

- Comparison II: “female” versus “male”
- Comparison III: “female – deficiency” versus “female – substitution”

- Comparison IV: “male – deficiency” versus “male – substitution”
- Comparison V: “female – deficiency” versus “male – deficiency”
- Comparison VI: “female – substitution” versus “male – substitution”

3.4.3 Differentially Expressed Genes

Probe set signals were background corrected, normalized and log₂-transformed using the Robust Multi-array Average (RMA) algorithm [46] with the AffymetriGeneChip Expression Console v1.4 Software. After exporting into Microsoft Excel comparison fold changes were calculated.

3.4.3.1 Comparison I:

The paired t-test statistic was used for the primary comparison between the (vitamin D) deficiency and (vitamin D) supplementation/substitution states. The software SPSS (*IBM SPSS statistics, version 23*) was used to perform a Kolmogorov-Smirnov test to check for normality in result distribution. The “R” software (*R Foundation for Statistical Computing, version 3.6.3*) with the “limma” package (*Bioconductor, version 3.42.2*) was used for gene expression analysis [121,130]. The RobiNA graphical interface (version 1.24) was used to access the R software [92,93]. The default settings were used. A p-value of < 0.01 was chosen for statistical significance. Multiple correction was performed with the Bonferroni method.

3.4.3.2 Comparisons II-VI:

For these comparisons, which include the four afore mentioned groups based on sex and vitamin D status another statistical method was required.

The analysis of variance (ANOVA) is a group of statistical methods that is used to determine if there statistically significant differences between the means of three or more groups of data. Thus, it can be used as an alternative to the t-test statistic for comparisons II-VI. Using the Transcriptome Analysis Console (TAC) Software (*Thermofisher Scientific, 4.0.2 Release*) with the integrated “limma” package (see above), two-sided analysis of variance (ANOVA), hierarchical clustering as well as principal component analysis (PCA) were performed.

PCA is the process of projecting a group of data in two- or three-dimensional space as vectors (principal components). The spatial relation of these vectors to each other provides an overview of the relation of the data sets to each other.

Lastly, clustering is the process of grouping similar entities together in an attempt to profile the attributes of different groups. It can be used to identify biological meaningful patterns of expression within the different groups, as has been demonstrated as early as 1998 [45].

For the before mentioned comparisons a $p < 0.01$ (ANOVA test) and an increase or decrease in fold change by factor > 1.5 were selected as criteria of significance. Correction for multiple testing was performed with the false discovery rate (FDR) method with a q-value < 0.05 considered as significant.

3.4.4 Pathway Analysis

For pathway analysis Gene Set Enrichment Analysis (GSEA) and the online software tool GeneTrail were used. We created two classes, the (vitamin D) deficient phenotype (suffix “a”) and the phenotype after vitamin D substitution/supplementation (suffix “b”). We used the default class metric, Signal2Noise, which is the difference of means scaled by the standard deviation, and the weighted ($p = 2$) enrichment statistic to generate a *ranked gene list*. For the second step, a *predefined gene set* is required, which includes biologically related genes (e.g. genes encoding products of the same pathway). GSEA determines then if the members of the predefined gene set are randomly distributed throughout the ranked gene list, or primarily found at the top or at the bottom of the list. Gene sets whose distribution lies closely to a particular phenotype (top or bottom of the list) are considered to be related to the specific phenotype. The extent of the correlation with a specific phenotype is measured with the *enrichment score*. A level of significance for the enrichment score was calculated additionally by using permutation of the gene sets (labels). This is the preferred method in studies with small number of samples for each phenotype. Only values < 0.05 were accepted as significance level (p) and False Discovery Rate (FDR), respectively.

We took a three-step approach to analyze our data. Firstly, we separated 7.705 genes known to be involved in the NK cell-mediated immune response according to the Gene Ontology database, irrespective of their individual expression. This dataset was used separately for specific analysis of the NK cell-cytotoxicity pathway to increase sensitivity. Secondly, the complete data set was used in an unsupervised, exploratory analysis to screen for other dysregulated pathways involved in the immune response and vitamin D homeostasis. *Predefined gene sets* representing specific pathways or genes involved in the same process can be found in online databases. One of the most comprehensive databases is the Molecular Signature Database [88]. This database includes a selection of gene sets involving core biological functions (“*Hallmark*” gene sets) and also features gene sets from other databases like the Biocarta, Gene ontology (GO), Kyoto Encyclopedia of Genes and Genomes (KEGG) and Reactome databases. From this broad library we selected 89 gene sets as *predefined gene sets* in our analysis. Both analyses were performed using the GSEA Software, Version 4.0.3, Broad Institute.

Finally, using the online software tool GeneTrail, we performed a screening for dysregulated pathways in the Hallmark, BioCarta, GO - Biological Process, GO - Cellular Component, GO -

Molecular Function, KEGG, Reactome and WikiPathways databases. Again, weighted GSEA was used. Because this was a non-hypothesis driven test, we reduced the p-value for significance to < 0.01 . The Benjamini-Hochberg method was used to adjust for multiple testing.

4 RESULTS

Initially, qRT-PCR was performed for result validation as explained in detail above (3.3.10, page 33). Thereafter, differential gene expression analysis was done using t-test statistic for the primary comparison and two-way ANOVA for the secondary comparisons (s. 3.4.2 and 3.4.3, page 35). Finally, we performed guided and unguided pathway analysis using the GSEA and GeneTrail software (s. 3.4.4, page 37).

4.1 QUANTITATIVE REAL TIME POLYMERASE CHAIN REACTION VALIDATION

qRT-PCR and fold change results obtained from the microarray are listed in **Table 14** and **Table 15** respectively. $\Delta\Delta Ct$ (a-b) values as per PCR are presented in **Table 16**.

Table 14: qRT-PCR results

Sample	UBC	AIF1			CLEC7		
	Ct	Ct	ΔCt	$\Delta\Delta Ct$ (a-b)	Ct	ΔCt	$\Delta\Delta Ct$ (a-b)
70a	22.61	28.13	5.52	-2.85	36.08	13.46	-2.86
70b	21.93	30.29	8.36		38.25	16.33	
71a	22.10	26.69	4.59	-6.67	35.24	13.14	-8.71
71b	23.16	34.42	11.27		45.01	21.85	
72a	22.51	34.77	12.25	6.98	43.15	20.64	6.70
72b	22.61	27.88	5.27		36.54	13.93	
73a	22.71	28.99	6.28	-0.71	37.62	14.91	0.55
73b	22.43	29.42	6.99		36.79	14.36	
74a	22.06	31.00	8.94	-4.01	36.02	13.96	-5.32
74b	22.55	35.50	12.95		41.83	19.28	
75a	22.36	25.28	2.93	-4.38	34.65	12.30	-7.64
75b	22.79	30.09	7.30		42.73	19.94	
92a	22.39	31.13	8.75	3.17	40.76	18.38	2.94
92b	24.01	29.59	5.58		39.44	15.43	
99a	22.04	26.03	4.00	-0.14	34.70	12.67	2.13
99b	23.22	27.36	4.14		33.76	10.54	

Abbreviations: Ct: Cycle threshold

Table 15: Fold change microarray signal values after vitamin D substitution

Gene	Subject							
	70	71	72	73	74	75	92	99
AIF1	-3.75	-7.01	6.54	-1.09	-1.54	-5.26	2.04	-2.25
CLEC7A	-7.75	-11.50	4.86	1.05	-1.24	-12.51	3.93	-3.13

Table 16: qRT-PCR $\Delta\Delta C_t$ (a-b) values after vitamin substitution

Gene	Subject							
	70	71	72	73	74	75	92	99
AIF1	-2.85	-6.67	6.98	-0.71	-4.01	-4.38	3.17	-0.14
CLEC7A	-2.86	-8.71	6.70	0.55	-5.32	-7.64	2.94	2.13

A graphical representation of the data depicted in **Table 15** and **Table 16** are shown in **Figure 8** and **Figure 9** respectively, shows that the PCR results in general correlate well with those obtained from the microarrays, thus confirming that the microarray assay results accurately represent the transcript levels expressed in the NK cells before and after vitamin D substitution.

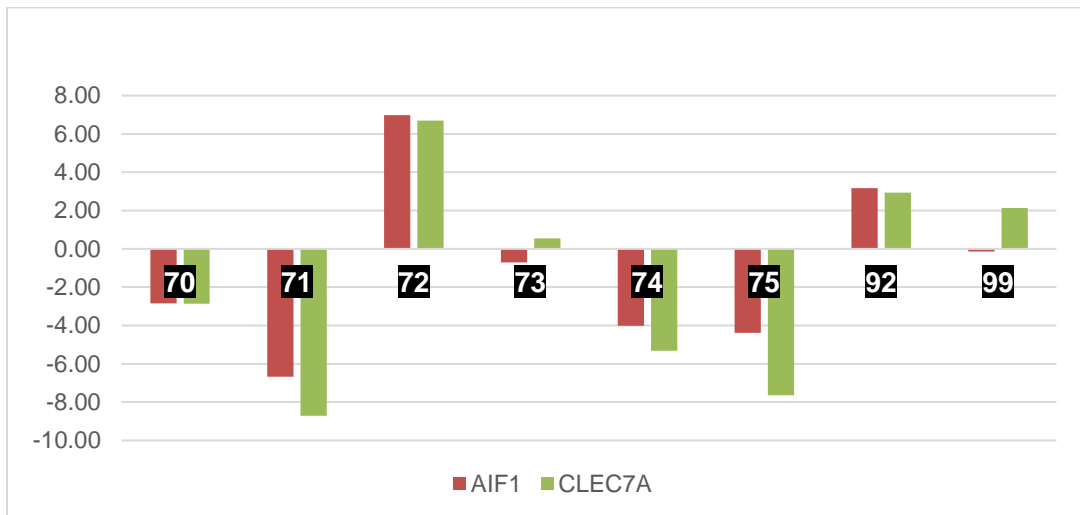


Figure 8: $\Delta\Delta C_t$ (a-b) values for the AIF1 and CLEC7A genes per qRT-PCR

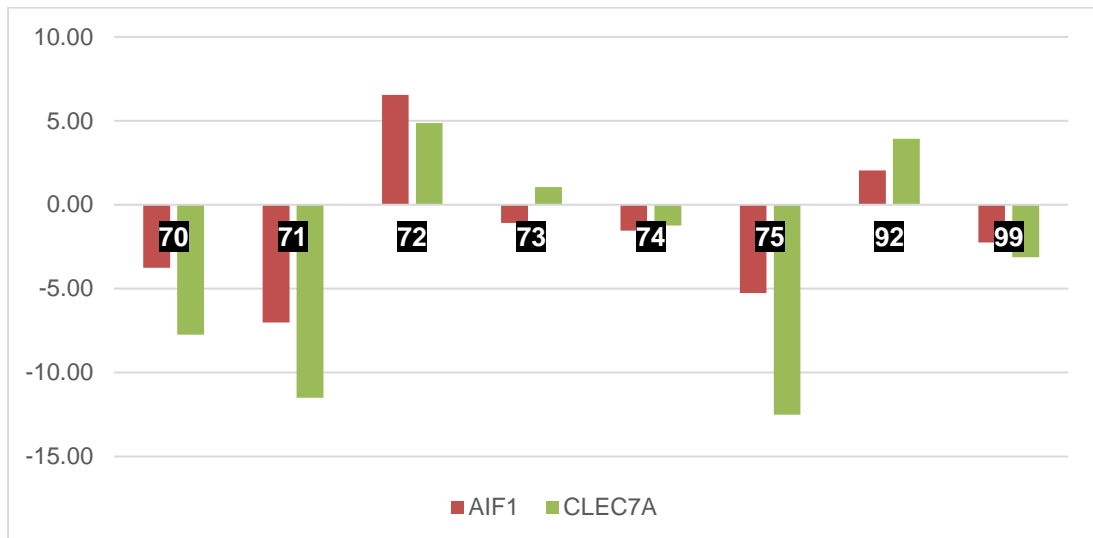


Figure 9: Fold change values for the AIF1 and CLEC7A genes per microarray

4.2 COMPARISON I: DEFICIENCY – SUBSTITUTION

4.2.1 Overview of Differentially Expressed Genes

The Kolmogorov-Smirnov test (**Figure 10** and **Figure 11**) confirmed the Gaussian distribution of our data. Thus, usage of parametric tests like t-test and ANOVA were feasible.

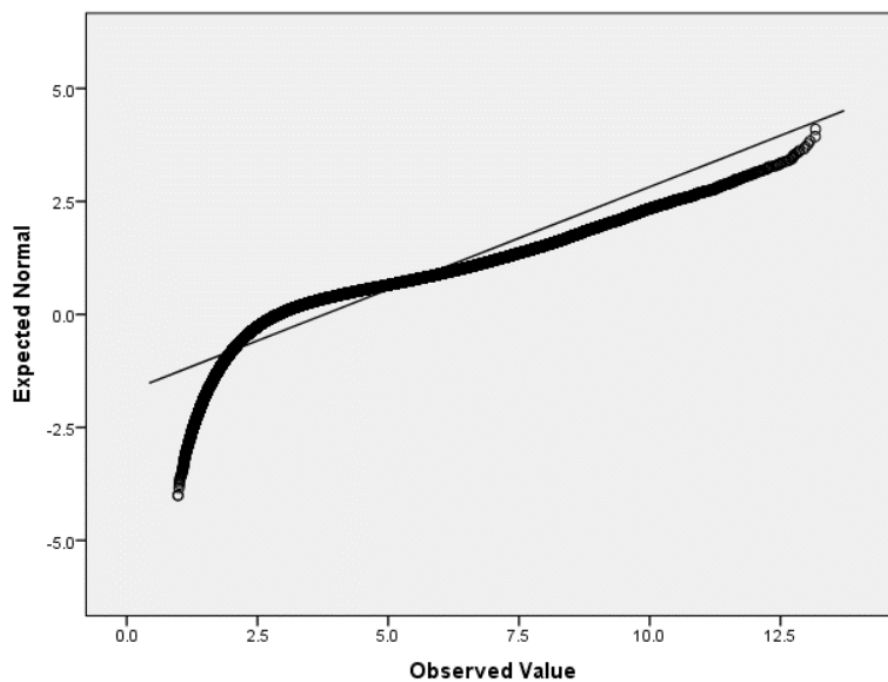


Figure 10. Normal Q-Q plot of average log₂ signal before supplementation

The distribution of our data before vitamin D supplementation approximates the expected Gaussian distribution ($p < 0.001$).

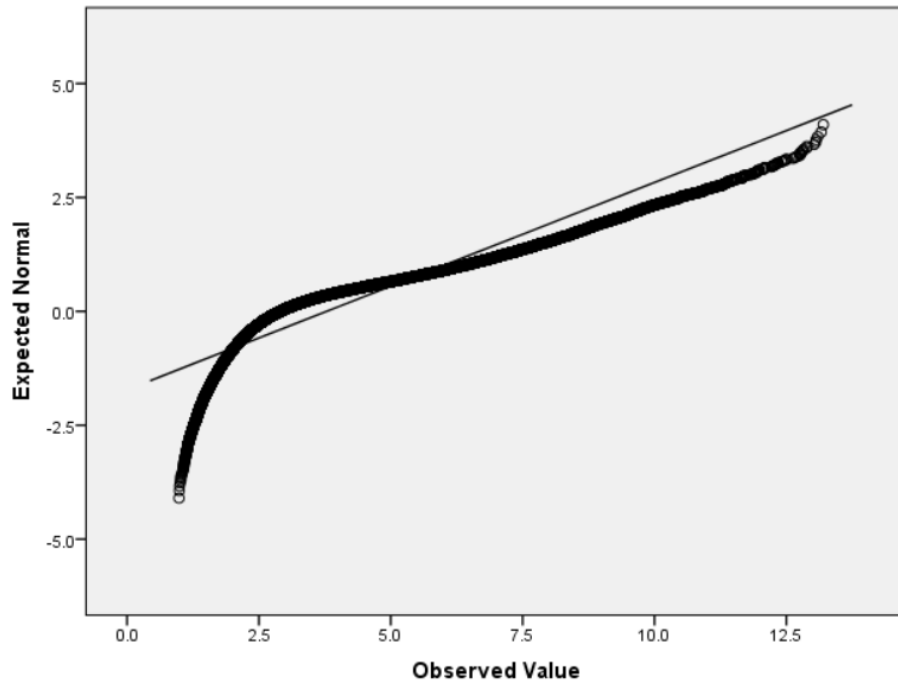


Figure 11. Normal Q-Q plot of average log₂ signal after supplementation

The distribution of our data after vitamin D supplementation approximates the expected Gaussian distribution ($p < 0.001$).

A total of 505 transcripts are significantly differently expressed before and after vitamin D supplementation for a p-value of < 0.01 (**Figure 12**). Hierarchical clustering enables a quick overview of the large amounts of data generated by such analyses. Furthermore, transcripts in the scatter plot (**Figure 13**) do not appear to deviate from the midline, again indicating the small effect of the intervention. The heatmap (**Figure 14**) displays that vitamin D supplementation has only a small effect on the NK-cell transcriptome.

Principal component Analysis (PCA) projects the summary of all transcripts as a vector for each individual into a 3D space. As can be seen, the samples do not seem to form clusters based on vitamin D levels. Thus, no clearly changed expression pattern can be observed that is clearly attributable to supplementation. There is, however, a clear spatial separation for sex (**Figure 15**).

However, the PCA shows for all but one subject (sample 73) a substantial influence of the application (same volunteers prior to and post stimulation have the same color). It is clear that vitamin D supplementation has an effect on the individual subject, but intrasubject variability is higher than the effect of vitamin D itself (**Figure 16**).

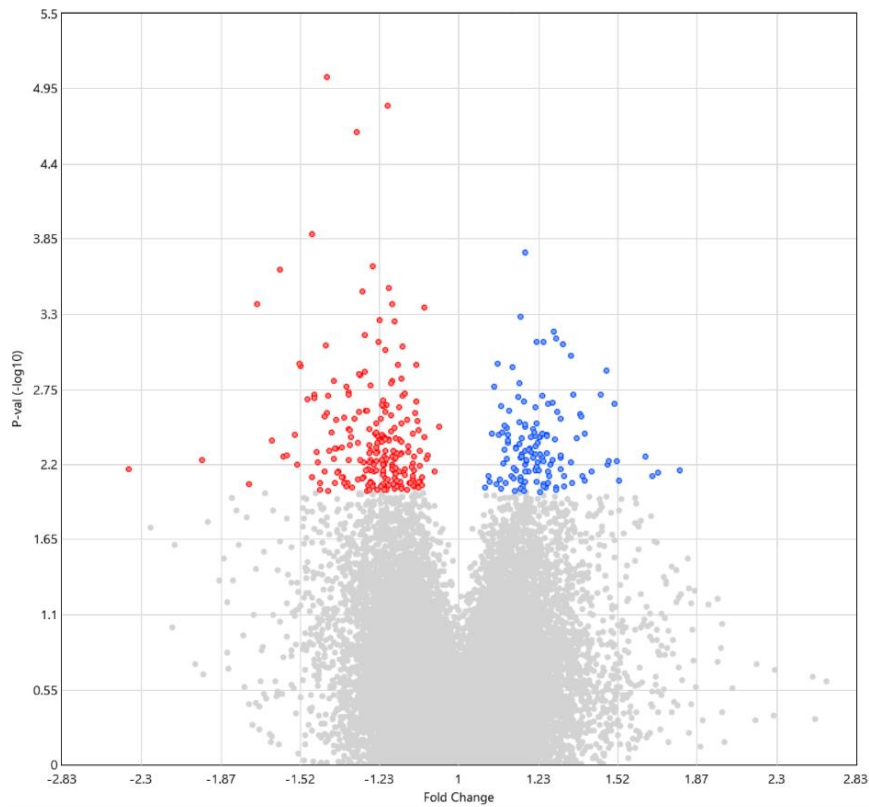


Figure 12: Volcano plot of log₂ p-values versus log₂ fold change

Each dot represents one single gene. Dots located on the left of the fold change value “1” represent upregulated genes, and those located on the right downregulated genes after supplementation of vitamin D3. The distance from the center of the graph (fold change value “1”) correlates with the magnitude of differential expression. In addition, the greater the distance from the x-axis, the lower is the p-value for statistical significance. Only transcripts with statistically significant differential expression (before multiple correction) for $p < 0.01$ are colored. Red signifies upregulated and blue downregulated genes. More genes are upregulated than downregulated.

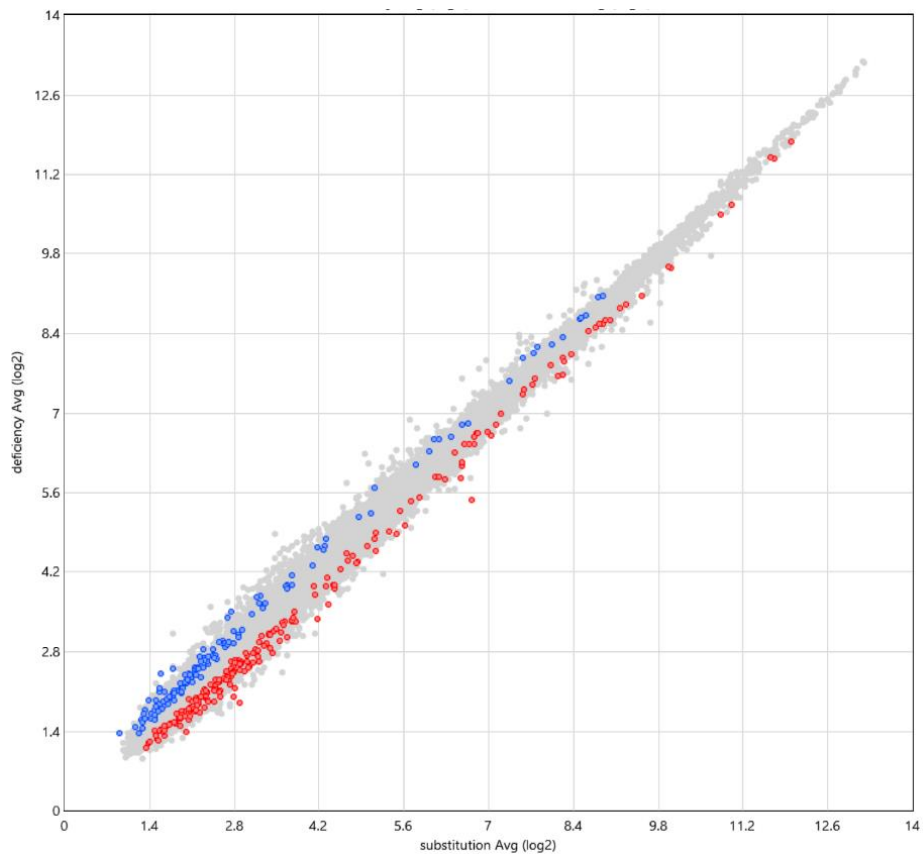


Figure 13: Scatter plot

The scatter plot demonstrates the distribution of the \log_2 -transformed expression values between the two vitamin D states. The more a dot deviates from the imaginary diagonal upwards along the y axis, the more the gene was downregulated after substitution with vitamin D and vice versa. A perfect diagonal would indicate that the supplementation had no effect on the transcriptome. Statistically significantly differently expressed transcripts are shown as colored dots. Red signifies higher and blue lower expression after substitution of vitamin D3. Some deviation from the midline diagonal is noted in both directions which implies that vitamin D had a slight effect on the NK cell transcriptome both in terms of upregulating some genes and in downregulating others. More upregulated genes than downregulated were noted.

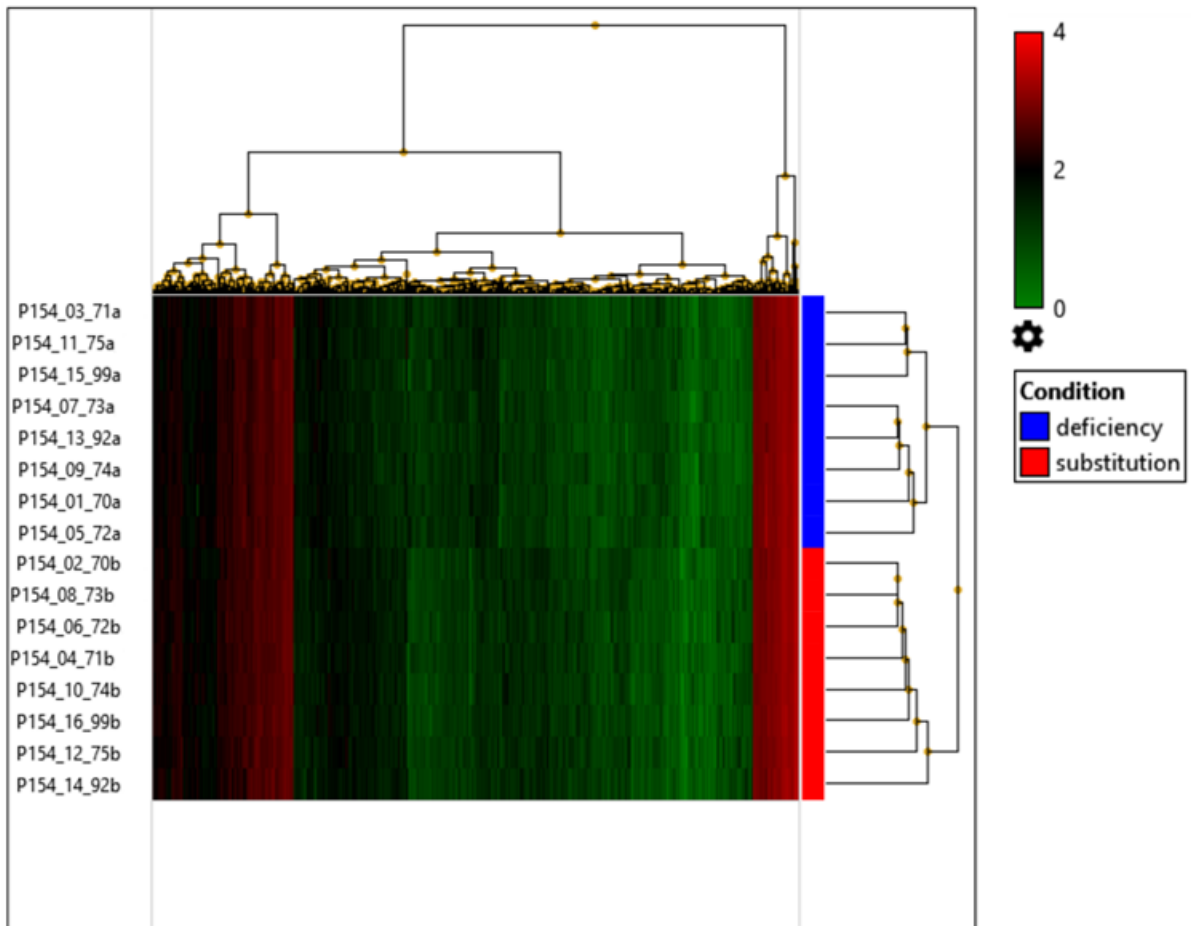


Figure 14: Hierarchical clustering

Hierarchical clustering based on the expression profile of transcripts that are up- or down-regulated based on $p < 0.05$ across the two different vitamin D levels. The color scale represents log₂-transformed expression of the single gene samples. Brighter green represents lower expression and brighter red represents higher expression. No gene clusters which clearly separate the two states could be identified.

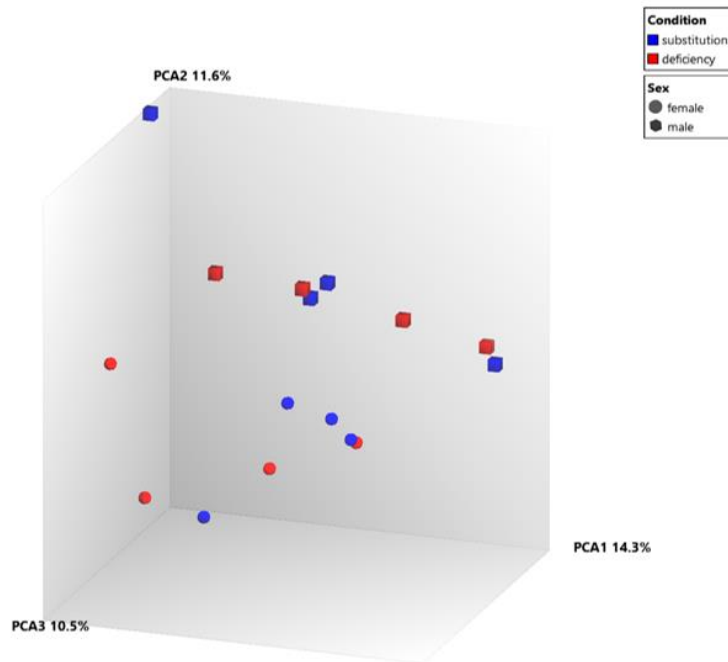


Figure 15: Principal component analysis – 1

Red indicates samples before and blue after vitamin D supplementation. Cubes indicate males and spheres indicate females. The individual samples do not seem to form clusters based on vitamin D levels. Thus, no clearly changed expression pattern could be observed which clearly is attributable to supplementation. However, a clear spatial separation for sex is noted (males concentrate in the upper part of the diagram, females in the lower part).

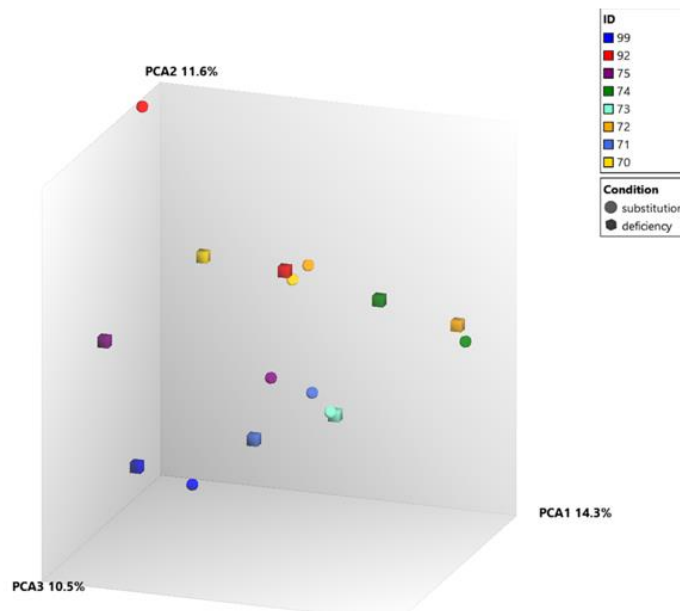


Figure 16: Principal component analysis – 2

Different colors represent the individual subjects, spheres indicate vitamin D deficiency and cubes indicate samples after substitution. Individual samples are well separated in the 3D space, especially samples 71, 73, 74, 75 and 99 in the bottom of the diagram. This highlights that individual transcriptome heterogeneity plays an important role in our experiment. A higher number of subjects would mitigate this effect.

4.2.2 Differentially Expressed Genes

Of the total 505 transcripts differentially expressed after vitamin D application with p-values of < 0.01 , only 256 have a well-established annotation to a specific coding or non-coding locus. No single gene remains significant after correction for multiple testing in the sex-independent analysis. This is a common problem of exome-wide analyses: the so-called “large P, small N” problem. It means that there are only a few data points “N” (samples, in our case 8 test subjects) but a large number of “P” (transcripts, in our case > 40.000) for each data point. Upregulated transcripts are listed in **Table 17**, whereas **Table 18** shows downregulated transcripts. **Table 19** displays genes related to the immune system or vitamin D signaling according to the GO Database.

Table 17: Upregulated transcripts after supplementation of vitamin D3 scoring $p < 0.01$

<i>Gene</i>	Description	<i>Gene</i>	Description
<i>CDH19</i>	cadherin 19, type 2	<i>LINC01144</i>	long intergenic non-protein coding RNA 1144
<i>CELSR3-AS1</i>	CELSR3 antisense RNA 1 (head to head)	<i>LINC01456</i>	long intergenic non-protein coding RNA 1456
<i>CHST15</i>	carbohydrate (N-acetylgalactosamine 4-sulfate 6-O) sulfotransferase 15	<i>LINC01624</i>	long intergenic non-protein coding RNA 1624
<i>COQ3</i>	coenzyme Q3 methyltransferase	<i>LRRC42</i>	leucine rich repeat containing 42
<i>CRELD2</i>	cysteine rich with EGF-like domains 2	<i>LRRC74A</i>	leucine rich repeat containing 74A
<i>CRSP8P</i>	mediator complex subunit 27 pseudogene	<i>MAP4K1</i>	mitogen-activated protein kinase kinase kinase kinase 1
<i>CTDNEP1</i>	CTD nuclear envelope phosphatase 1	<i>MED24</i>	mediator complex subunit 24
<i>CUEDC2</i>	CUE domain containing 2	<i>MIR1244-1</i>	microRNA 1244-1
<i>CYP21A1P</i>	cytochrome P450, family 21, subfamily A, polypeptide 1 pseudogene	<i>MIR548T</i>	microRNA 548t
<i>DDX39A</i>	DEAD (Asp-Glu-Ala-Asp) box polypeptide 39A	<i>MIR570</i>	microRNA 570
<i>DENND6B</i>	DENN/MADD domain containing 6B	<i>MT1B</i>	metallothionein 1B
<i>DMRTA1</i>	DMRT-like family A1	<i>MTRNR2L5</i>	MT-RNR2-like 5

DRD2	dopamine receptor D2	MYBL2	v-myb avian myeloblastosis viral oncogene homolog-like 2
EEF1A2	eukaryotic translation elongation factor 1 alpha 2	MYO7A	myosin VIIA
EIF5AL1	eukaryotic translation initiation factor 5A-like 1	NAV2-AS5	NAV2 antisense RNA 5
ELFN1	extracellular leucine-rich repeat and fibronectin type III domain containing 1	NRG4	neuregulin 4
EPB41L1	erythrocyte membrane protein band 4.1-like 1	OR52W1	olfactory receptor, family 52, subfamily W, member 1
EXOC6B	exocyst complex component 6B	P4HA2	prolyl 4-hydroxylase, alpha polypeptide II
F9	coagulation factor IX	PCBP4	poly(rC) binding protein 4
FAM189B	family with sequence similarity 189, member B	PERP	PERP, TP53 apoptosis effector
FAM217A	family with sequence similarity 217, member A	PI4KA	phosphatidylinositol 4-kinase, catalytic, alpha
FAM219A	family with sequence similarity 219, member A	PI4KAP1	phosphatidylinositol 4-kinase, catalytic, alpha pseudogene 1
FAM25C	family with sequence similarity 25, member C	PKD2L1	polycystic kidney disease 2-like 1
FAM53A	family with sequence similarity 53, member A	PLXDC1	plexin domain containing 1
FBL	fibrillarlin	POLR2L	polymerase (RNA) II (DNA directed) polypeptide L, 7.6kDa
FBLN7	fibulin 7	PPM1M	protein phosphatase, Mg ²⁺ /Mn ²⁺ dependent, 1M
FBXL6	F-box and leucine-rich repeat protein 6	PPP1R15B	protein phosphatase 1, regulatory subunit 15B
FN1	fibronectin 1	PRAMEF2	PRAME family member 2
GPR146	G protein-coupled receptor 146	PRPF31	pre-mRNA processing factor 31
HIST1H4F	histone cluster 1, H4f	PRR23D2	proline rich 23 domain containing 2
HLA-C	major histocompatibility complex, class I, C	PRRT3	proline-rich transmembrane protein 3

HPSE2	heparanase 2 (inactive)	PTPRCAP	protein tyrosine phosphatase, receptor type, C-associated protein
HULC	hepatocellular carcinoma up-regulated long non-coding RNA	PXMP2	peroxisomal membrane protein 2
IFITM5	interferon induced transmembrane protein 5	RARRES3	retinoic acid receptor responder (tazarotene induced) 3
IFNL3	interferon, lambda 3	RASA4B	RAS p21 protein activator 4B
IL17RE	interleukin 17 receptor E	RASL10B	RAS-like, family 10, member B
IL2RB	interleukin 2 receptor, beta	RETN	resistin
INO80E	INO80 complex subunit E	RHBDF1	rhomboid 5 homolog 1 (Drosophila)
ITGAM	integrin, alpha M (complement component 3 receptor 3 subunit)	RNU5D-1	RNA, U5D small nuclear 1
ITGAX	integrin alpha X	RPH3AL	rabphilin 3A-like (without C2 domains)
IVL	involucrin	RPL21P28	ribosomal protein L21 pseudogene 28
KDM8	lysine (K)-specific demethylase 8	RPL23AP87	ribosomal protein L23a pseudogene 87
KIF25	kinesin family member 25	RPS27	ribosomal protein S27
KRT17	keratin 17, type I	SEC11A	SEC11 homolog A, signal peptidase complex subunit
KRTAP22-2	keratin associated protein 22-2	SH3GLB2	SH3-domain GRB2-like endophilin B2
KRTAP5-1	keratin associated protein 5-1	SLPI	secretory leukocyte peptidase inhibitor
LIN7A	lin-7 homolog A (C. elegans)	SMARCB1	SWI/SNF related, matrix associated, actin dependent regulator of chromatin, subfamily b, member 1
LINC00619	long intergenic non-protein coding RNA 619	SNAR-I	small ILF3/NF90-associated RNA I
LINC00881	long intergenic non-protein coding RNA 881	SNORA35	small nucleolar RNA, H/ACA box 35

LINC01144	long intergenic non-protein coding RNA 1144	SNORD116-14	small nucleolar RNA, C/D box 116-14
LINC01456	long intergenic non-protein coding RNA 1456	SNORD20	small nucleolar RNA, C/D box 20
LINC01624	long intergenic non-protein coding RNA 1624	SNORD32B	small nucleolar RNA, C/D box 32B
LRRC42	leucine rich repeat containing 42	SOX13	SRY box 13
LRRC74A	leucine rich repeat containing 74A	SPATA20	spermatogenesis associated 20
MAP4K1	mitogen-activated protein kinase kinase kinase 1	SPINK1	serine peptidase inhibitor, Kazal type 1
MED24	mediator complex subunit 24	SSH3	slingshot protein phosphatase 3
MIR1244-1	microRNA 1244-1	STARD4-AS1	STARD4 antisense RNA 1
MIR548T	microRNA 548t	STARD9	StAR-related lipid transfer domain containing 9
MIR570	microRNA 570	TAAR3	trace amine associated receptor 3 (gene/pseudogene)
MT1B	metallothionein 1B	THOP1	thimet oligopeptidase 1
MTRNR2L5	MT-RNR2-like 5	TOX2	TOX high mobility group box family member 2
MYBL2	v-myb avian myeloblastosis viral oncogene homolog-like 2	TP53I13	tumor protein p53 inducible protein 13
MYO7A	myosin VIIA	TRAV8-4	T cell receptor alpha variable 8-4
IFITM5	interferon induced transmembrane protein 5	TRIM51HP	tripartite motif-containing 51H, pseudogene
IFNL3	interferon, lambda 3	TTY13	testis-specific transcript, Y-linked 13 (non-protein coding)
IL17RE	interleukin 17 receptor E	UCHL1	ubiquitin C-terminal hydrolase L1
IL2RB	interleukin 2 receptor, beta	UPK3B	uroplakin 3B
INO80E	INO80 complex subunit E	UROS	uroporphyrinogen III synthase

ITGAM	integrin, alpha M (complement component 3 receptor 3 subunit)	USH2A	Usher syndrome 2A (autosomal recessive, mild)
ITGAX	integrin alpha X	VAMP2	vesicle associated membrane protein 2
IVL	involucrin	VIP	vasoactive intestinal peptide
KDM8	lysine (K)-specific demethylase 8	WBSCR16	Williams-Beuren syndrome chromosome region 16
KIF25	kinesin family member 25	YKT6	YKT6 v-SNARE homolog (S. cerevisiae)
KRT17	keratin 17, type I	ZNF324	zinc finger protein 324
KRTAP22-2	keratin associated protein 22-2	ZNF692	zinc finger protein 692
KRTAP5-1	keratin associated protein 5-1	ZNF728	zinc finger protein 728
LIN7A	lin-7 homolog A (C. elegans)	ZNF733P	zinc finger protein 733, pseudogene
LINC00619	long intergenic non-protein coding RNA 619	ZNF788	zinc finger family member 788
LINC00881	long intergenic non-protein coding RNA 881		

Table 18: Downregulated transcripts after supplementation of vitamin D3 scoring $p < 0.01$

Gene	Description	Gene	Description
ADORA2B	adenosine A2b receptor	LRRC1	leucine rich repeat containing 1
AFF4	AF4/FMR2 family, member 4	LRRFIP2	leucine rich repeat (in FLII) interacting protein 2
ANAPC4	anaphase promoting complex subunit 4	MAF	v-maf avian musculoaponeurotic fibrosarcoma oncogene homolog
ANP32B	acidic nuclear phosphoprotein 32 family member B	MBTD1	mbt domain containing 1

ANXA8L1	annexin A8-like 1	METTL14	methyltransferase like 14
ASIP	agouti signaling protein	MGC16025	uncharacterized LOC85009
ATP11C	ATPase, class VI, type 11C	MIEF1	mitochondrial elongation factor 1
BBS5	Bardet-Biedl syndrome 5	MIR1-1	microRNA 1-1
BLOC1S6	biogenesis of lysosomal organelles complex-1, subunit 6, pallidin	MIR140	microRNA 140
C15orf57	chromosome 15 open reading frame 57	MIR3175	microRNA 3175
C16orf46	chromosome 16 open reading frame 46	MIR330	microRNA 330
CAMTA1	calmodulin binding transcription activator 1	MIR4496	microRNA 4496
CCDC81	coiled-coil domain containing 81	MIR933	microRNA 933
CCR10	chemokine (C-C motif) receptor 10	NFATC4	nuclear factor of activated T-cells, cytoplasmic, calcineurin-dependent 4
CCSAP	centriole, cilia and spindle-associated protein	NKAIN2	Na ⁺ /K ⁺ transporting ATPase interacting 2
CCT2	chaperonin containing TCP1, subunit 2 (beta)	OPCML	opioid binding protein/cell adhesion molecule-like
CDC14C	cell division cycle 14C	OR6C70	olfactory receptor, family 6, subfamily C, member 70
CDH13	cadherin 13	PADI4	peptidyl arginine deiminase, type IV
CDKL5	cyclin-dependent kinase-like 5	PGRMC2	progesterone receptor membrane component 2
CEP57L1	centrosomal protein 57kDa-like 1	PKN2	protein kinase N2
CHORDC1	cysteine and histidine rich domain containing 1	PLA2G4A	phospholipase A2, group IVA (cytosolic, calcium-dependent)
CLIP4	CAP-GLY domain containing linker protein family, member 4	PLEKHH2	pleckstrin homology domain containing, family H (with MyTH4 domain) member 2

CMSS1	cms1 ribosomal small subunit homolog (yeast)	PRKCH	protein kinase C, eta
CTRB1	chymotrypsinogen B1	PRR3	proline rich 3
CYTIP	cytohesin 1 interacting protein	PSMC6	proteasome 26S subunit, ATPase 6
DEFB124	defensin, beta 124	PTGER4	prostaglandin E receptor 4 (subtype EP4)
DENND5B-AS1	DENND5B antisense RNA 1	RAD51AP2	RAD51 associated protein 2
DHX15	DEAH (Asp-Glu-Ala-His) box helicase 15	RBM44	RNA binding motif protein 44
DICER1	dicer 1, ribonuclease type III	RGPD1	RANBP2-like and GRIP domain containing 1
DISP2	dispatched homolog 2 (Drosophila)	RHOB	ras homolog family member B
DNAJA4	DnaJ (Hsp40) homolog, subfamily A, member 4	RIOK3	RIO kinase 3
DOCK5	dedicator of cytokinesis 5	RPH3A	rabphilin 3A
DSCAM-IT1	DSCAM intronic transcript 1	RSPH10B	radial spoke head 10 homolog B (Chlamydomonas)
EFCAB10	EF-hand calcium binding domain 10	SAYSD1	SAYSVFN motif domain containing 1
EHHADH	enoyl-CoA, hydratase/3-hydroxyacyl CoA dehydrogenase	SCGB2B3P	secretoglobin, family 2B, member 3, pseudogene
EMC2	ER membrane protein complex subunit 2	SCUBE1	signal peptide, CUB domain, EGF-like 1
EXOG	endo/exonuclease (5-3), endonuclease G-like	SELK	selenoprotein K
FAM208B	family with sequence similarity 208, member B	SEN2	SUMO1/sentrin/SMT3 specific peptidase 2
FBXW9	F-box and WD repeat domain containing 9	SEN5	SUMO1/sentrin specific peptidase 5
FEM1C	fem-1 homolog c (C. elegans)	SERBP1	SERPINE1 mRNA binding protein 1
FETUB	fetuin B	SLMAP	sarcolemma associated protein

<i>FGD5P1</i>	FYVE, RhoGEF and PH domain containing 5 pseudogene 1	<i>SMCHD1</i>	structural maintenance of chromosomes flexible hinge domain containing 1
<i>GABPB1-AS1</i>	GABPB1 antisense RNA 1	<i>SMNDC1</i>	survival motor neuron domain containing 1
<i>GACAT2</i>	gastric cancer associated transcript 2 (non-protein coding)	<i>SNORD114-3</i>	small nucleolar RNA, C/D box 114-3
<i>GCOM1</i>	GRINL1A complex locus 1	<i>SPINT1</i>	serine peptidase inhibitor, Kunitz type 1
<i>GPATCH2L</i>	G-patch domain containing 2 like	<i>SRPK1</i>	SRSF protein kinase 1
<i>GS1-279B7.1</i>	microtubule-associated protein 1 light chain 3 beta pseudogene	<i>TAOK1</i>	TAO kinase 1
<i>HACD1</i>	3-hydroxyacyl-CoA dehydratase 1	<i>TPI1P3</i>	triosephosphate isomerase 1 pseudogene 3
<i>HOXD12</i>	homeobox D12	<i>TRBV5-4</i>	T cell receptor beta variable 5-4
<i>HYAL2</i>	hyaluronoglucosaminidase 2	<i>TSM</i>	Ts translation elongation factor, mitochondrial
<i>IMMP1L</i>	inner mitochondrial membrane peptidase subunit 1	<i>TTC39B</i>	tetratricopeptide repeat domain 39B
<i>IP6K2</i>	inositol hexakisphosphate kinase 2	<i>UGT2B17</i>	UDP glucuronosyltransferase 2 family, polypeptide B17
<i>IPO11</i>	importin 11	<i>UPRT</i>	uracil phosphoribosyltransferase (FUR1) homolog (S. cerevisiae)
<i>KCNE1</i>	potassium channel, voltage gated subfamily E regulatory beta subunit 1	<i>VWC2L-IT1</i>	VWC2L intronic transcript 1
<i>KIF15</i>	kinesin family member 15	<i>ZEB2</i>	zinc finger E-box binding homeobox 2
<i>KIF1B</i>	kinesin family member 1B	<i>ZNF709</i>	zinc finger protein 709
<i>KRTAP4-2</i>	keratin associated protein 4-2	<i>ZNF839</i>	zinc finger protein 839

Table 19: Selected genes associated with the immune system or vitamin D signaling

Gene Symbol	Gene Description	Fold Change	Paired p-value
TRAV8-4	T cell receptor alpha variable 8-4	-1.54	0.00761
MAP4K1	mitogen-activated protein kinase kinase kinase kinase 1	-1.34	0.00388
IFNL3	interferon, lambda 3	-1.30	0.00671
IL17RE	interleukin 17 receptor E	-1.24	0.00443
POLR2L	polymerase (RNA) II (DNA directed) polypeptide L, 7.6kDa	-1.23	0.00904
VIP	vasoactive intestinal peptide	-1.22	0.00146
C1orf147	chromosome 1 open reading frame 147	-1.21	0.00525
IFITM5	interferon induced transmembrane protein 5	-1.19	0.00350
SLPI	secretory leukocyte peptidase inhibitor	-1.19	0.00999
DRD2	dopamine receptor D2	-1.18	0.00661
ITGAM	integrin, alpha M (complement component 3 receptor 3 subunit)	-1.16	0.00232
IL2RB	interleukin 2 receptor, beta	-1.13	0.00802
VAMP2	vesicle associated membrane protein 2	-1.10	0.00815
MED24	mediator complex subunit 24	-1.09	0.00743
NRG4	neuregulin 4	-1.09	0.00871
HLA-C	major histocompatibility complex, class I, C	-1.08	0.00426
CCR10	chemokine (C-C motif) receptor 10	1.12	0.00455
PSMC6	proteasome 26S subunit, ATPase 6	1.13	0.00591
PTGER4	prostaglandin E receptor 4 (subtype EP4)	1.16	0.00388
SRPK1	SRSF protein kinase 1	1.18	0.00589
NFATC4	nuclear factor of activated T-cells, cytoplasmic, calcineurin-dependent 4	1.19	0.00520
BLOC1S6	biogenesis of lysosomal organelles complex-1, subunit 6, pallidin	1.22	0.00058
DEFB124	defensin, beta 124	1.23	0.00058
TRBV5-4	T cell receptor beta variable 5-4	1.30	0.00337
PADI4	peptidyl arginine deiminase, type IV	1.41	0.00820
PLA2G4A	phospholipase A2, group IVA (cytosolic, calcium-dependent)	1.67	0.00099

Selection of genes associated with the immune system or vitamin D signaling according to the GO Database with a significance level of $p < 0.01$. A negative fold change means increased expression, and a positive value decreased expression.

First, we could show that known vitamin D-dependent genes were differentially expressed for an uncorrected p value < 0.01. **MED24**, being upregulated, encodes one of the components of the so-called mediator complex, which is a transcriptional coactivator complex required for gene expression. The mediator complex is directly involved in VDR mediated gene expression [108]. Another gene associated with vitamin D, the **PLA2GA4** gene, is downregulated after supplementation. This encodes the phospholipase A2, group IVA (cytosolic, calcium-dependent) protein PLA2GA4, which belongs to a group of 4A phospholipases, whose expression is influenced by 1,25-(OH)₂D₃ in mast cells [141].

Second, the expression of genes with established roles in NK-cell regulation, which are affected from vitamin D supplementation. For instance, dopamin receptors have shown to modulate NK-cell cytotoxicity. Agonists of the dopamine receptor D2 (DRD2) particularly have been shown to suppress NK cells through the D3R/D4R-cAMP-PKA-CREB signaling pathway [167]. The **DRD2** gene is upregulated in our study.

In contrast, the **BLOC1S6** gene is downregulated. Its product, BLOC16S (biogenesis of lysosomal organelles complex-1, subunit 6, pallidin) is a component of the BLOC-1 complex which is necessary for lysosome function in NK cells. Mutations of the **BLOC1S6** gene lead to development of the Hermansky-Pudlak syndrome, which is characterized from abnormal function of lysosomes and lysosome-related organelles and consequently NK-cell dysfunction [11].

Studies have demonstrated that prostaglandin E2 receptor 4 (EP4), which is encoded by the **PTGER4** gene, suppresses NK-cell function [56]. It is therefore consistent with our findings that it is downregulated following vitamin D substitution. The **ITGAM** gene is upregulated following vitamin D substitution. It encodes Integrin α-M (CD11b), which is involved in several immune reaction processes such as phagocytosis, chemotaxis, cell-mediated cytotoxicity and cellular activation and is expressed in macrophages, monocytes, granulocytes and NK cells [132]. Finally, higher **HLA-C** (*human leukocyte antigen*) expression on NK cells has been clearly associated with decreased degranulation and in turn lower cytolytic activity. In contrast to what would be expected, NK cells in our study express higher HLA-C levels after vitamin D supplementation [86].

Furthermore, the influence of vitamin D serum levels can also be shown for some genes involved in cytokine regulation. **NFATC4** is downregulated after vitamin D supplementation. Its gene product, the nuclear factor of activated T-cells, cytoplasmic, calcineurin-dependent 4 protein, is a transcription modulator in lymphatic cells. Its overexpression suppresses IL-2 production in T cells and its downregulation is crucial for adequate cytokine-producing activity of T cells [68]. NFAT knockdown in mice leads to enhanced NK cell activity after exposure to target cells and activation with cytokines [126].

Lambda interferons (IFN- λ) belong to the type III interferon family and are a component of the innate immune defense to viruses, bacteria, and fungi. They have been shown to influence NK-cell responses to viral infection [22]. This mechanism is mediated through monocyte activation and production of IL-12 p40, which in turn leads to increased IFN- γ secretion from NK cells [75]. The ***IFNL3*** gene, responsible for IFN- λ 3 (also called IL-28B), was upregulated after supplementation with 1,25-(OH) $_2$ D $_3$.

Another cytokine axis involving IL-17, for which enhancement of NK-cell function has been postulated, is influenced by vitamin D treatment. ***IL17RE*** is upregulated in our experiment. It encodes the interleukin 17 receptor E, which is expressed on mRNA-level intracellularly but not on the surface [3].

More importantly, the beta subunit of the interleukin receptor 2 (***IL2RB*** gene) was upregulated in this study. IL-2 signaling through the IL-2 receptor is crucial for NK-cell function, as described in 2.1.1 (page 2). The specific role of IL-2 in NK-cell-mediated ADCC is elicited in 2.1.5 (page 8). Affinity of IL-2 to its receptor depends on the receptors chain composition. Low-affinity binding is associated with the alpha chain, intermediate-affinity binding with the beta chain, and high-affinity binding with a complex of the alpha and beta subunits. A gamma chain which associates with the beta chain has also been described [152].

Signal cascades also seem to be influenced by vitamin D substitution. After receptor activation of the NK cell, intracellular activation signals are mediated through the phosphorylation of the mitogen activated protein kinase (MAPK) pathway [57]. The MAPK family includes three kinase families, the extracellular signal-regulated kinases (ERK), the p38 kinases and the c-Jun N-terminal kinases (JNK) [127]. In our experiment, the gene ***MAP4K1*** is upregulated. This gene encodes the mitogen-activated protein kinase kinase kinase kinase 1, which is involved in the JNK pathway. While adequate NK-cell cytotoxicity requires all three kinase families, NK-cell-mediated ADCC specifically has been shown to be dependent of the p38 and ERK families [146]. Upstream activation of the MAPK signaling pathway depends partly on receptor kinases expressed on the cell surface. One of these is the ErbB4/Her4 receptor, which requires specific binding with the neuregulin 4 transmembrane protein for its activation [52]. ***NGR4***, the gene coding neuregulin 4, is found to be downregulated in our experiment.

Moreover, vitamin D supplementation affects genes which are generally involved in the immune response. The expression of two variable chains of the T-cell receptor: the alpha variable 8-4 (***TRAV8-4***) and the beta variable 5-4 (***TRBV5-4***) was found to be vitamin D dependent. ***TRAV8-4*** was upregulated, on the other hand ***TRBV5-4*** showed reduced expression in higher vitamin D serums levels. In NKT cells, which also express a T-cell receptor (see page 3, 2.1.1.3), the alpha chain has been shown to express an invariant rearrangement between V alpha 24 and J alpha Q [41]. However, a small group of NKT-like cells in mice

exists, which show alpha chain diversity including Va3-Ja9 or Va8. However, various experimental difficulties have so far prevented a more detailed characterization in humans [49]. More diversity has been demonstrated for the beta chain of the receptor, with five proven V beta gene families: V beta 2, 7, 8, 11, and 13 [119][49].

DNA-directed RNA polymerases I, II, and III subunit RPABC5, encoded by the **POLR2** gene, is involved in the recognition process of foreign RNA in the innate immune system [15]. It is upregulated in our experiment.

The vasoactive intestinal peptide (**VIP** gene), upregulated in our study, is a neuropeptide which is excreted in lymphatic as well as neural cells and has been shown to possess potent anti-inflammatory function by regulating the production of both anti- and pro-inflammatory mediators [40].

The gene product of the **IFITM5** gene, Interferon induced transmembrane protein 5, has been linked to viral response [87]. It is upregulated in the vitamin D supplemented state. Other transcripts like **C1orf147** (*chromosome 1 open reading frame 147*), which is upregulated too, has only been linked vaguely in expression studies with the immune system. The same applies for the **PSMC6** gene encoding the enzyme 26S proteasome AAA-ATPase subunit Rpt4, and the **SRPK1** gene encoding SRSF protein kinase 1, both downregulated in our experiment [9,27].

Lastly, some of the differentially expressed genes have no known roles in NK cells. The secretory leukocyte peptidase inhibitor, derived from the **SLPI** gene, is an enzyme that has antimicrobial properties in addition to its function as a protease inhibitor. It is upregulated after supplementation with vitamin D. However, its function in NK cells is not known [43]. The same holds true for **VAMP2**, coding the Vesicle-associated membrane protein 2, which has been shown to play a role in the fusion of membrane-enveloped vesicles and is also upregulated. The **CCR10** gene product, named C-C chemokine receptor type 10, which was downregulated, has also no function in NK cells [32],[80]. Another downregulated gene with no specific role on NK cells is **PADI4** [169]. It encodes the peptidyl arginine deiminase – type IV, which is involved in post-translational modification. Defensins are antimicrobial peptides expressed mainly by epithelial cells and neutrophils. The **DEFB124** gene encoding defensin beta 124, is downregulated in our study. Although NK cells have been shown to produce alpha defensins, we are aware of no data of beta defensin secretion from NK cells [30].

4.3 COMPARISONS BASED ON VITAMIN D STATUS UND SEX

As discussed above, using the TAC Software, we performed two-way ANOVA to compare the following four groups, as explained in 3.4.2, page 35: 1) deficient females, 2) deficient males, 3) supplemented females, and 4) supplemented males. The following criteria were used when testing for statistical significance: a p-value in the ANOVA test of < 0.01 and a decrease or increase in gene expression after vitamin D supplementation by a factor 1.5. Correction for multiple testing was performed with the false discovery rate (FDR) method for a q value < 0.05 .

A summary of comparisons II-IV is provided in **Figure 17**.

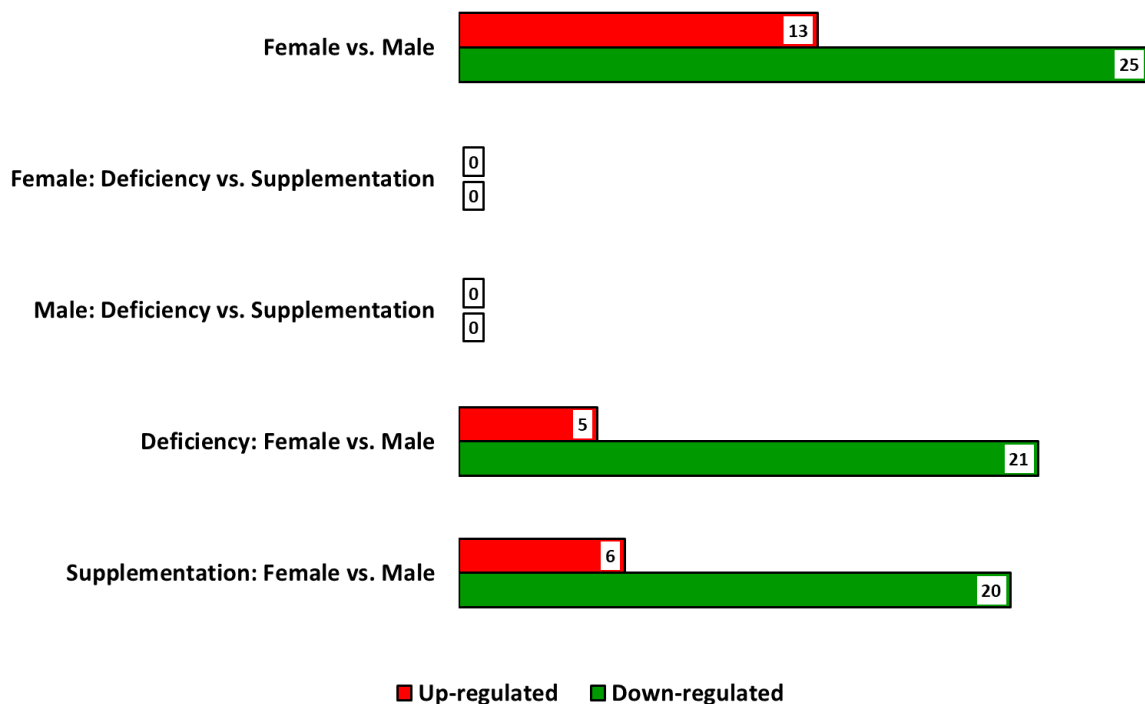


Figure 17: Summarized ANOVA results for comparisons II-VI

The diagram shows the number of genes statistically significant affected by vitamin D, which were either up-regulated (red) or down-regulated (green). Shown are the different comparisons that have been made (from top to bottom): Comparison II, III, IV, V, and IV

4.3.1 Comparison II: Male – Female

After correction for multiple testing, 38 transcripts showed a significantly altered expression between male and female subjects (**Figure 17**). 26/38 have well established annotations (**Table 20**).

Table 20: Comparison II – Significantly differentially expressed genes

Gene Symbol	Description	Chromosome	female avg. (log2)	male avg. (log2)	Fold Change	FDR p-value
TRPC3	transient receptor potential cation channel, subfamily C, member 3	chr4	3.31	2.35	1.94	0.0044
DDX43	DEAD (Asp-Glu-Ala-Asp) box polypeptide 43	chr6	2.78	4.6	-3.53	0.0162
ZFX	zinc finger protein, X-linked	chrX	6.07	5.36	1.63	0.0399
XIST	X inactive specific transcript (non-protein coding)	chrX	10.9	2.42	357.08	7.21E-12
TSIX	TSIX transcript, XIST antisense RNA	chrX	5.72	3.26	5.52	9.76E-08
JPX	JPX transcript, XIST activator (non-protein coding)	chrX	7.99	7.34	1.57	0.0014
EIF1AX	eukaryotic translation initiation factor 1A, X-linked	chrX	8.29	7.64	1.57	0.0129
CA5B	carbonic anhydrase VB, mitochondrial	chrX	6.79	5.78	2.01	0.0292
ZFY	zinc finger protein, Y-linked	chrY	2.42	5.37	-7.75	5.86E-06
USP9Y	ubiquitin specific peptidase 9, Y-linked	chrY	2.62	8.4	-54.87	2.89E-10
TXLNGY	taxilin gamma pseudogene, Y-linked	chrY	2.18	7.23	-33.09	6.05E-10
TXLNGY	taxilin gamma pseudogene, Y-linked	chrY	2.33	7.23	-29.9	1.36E-09
TTY15	testis-specific transcript, Y-linked 15 (non-protein coding)	chrY	2.54	8.28	-53.34	1.67E-10
TTY14	testis-specific transcript, Y-linked 14 (non-protein coding)	chrY	3.36	5.17	-3.53	1.15E-05
TTY14	testis-specific transcript, Y-linked 14 (non-protein coding)	chrY	1.76	2.89	-2.18	0.0005
TTY10	testis-specific transcript, Y-linked 10 (non-protein coding)	chrY	2.45	3.58	-2.2	0.0403

TMSB4Y	thymosin beta 4, Y-linked	chrY	2.77	4.49	-3.3	7.60E-05
RPS4Y1	ribosomal protein S4, Y-linked 1	chrY	2.64	4.93	-4.89	0.0032
PRKY	protein kinase, Y-linked, pseudogene	chrY	3.68	8.59	-29.99	1.79E-08
LINC00278	long intergenic non-protein coding RNA 278	chrY	3.23	6.65	-10.68	7.24E-07
KDM5D	lysine (K)-specific demethylase 5D	chrY	2.54	7.76	-37.32	2.47E-09
EIF1AY	eukaryotic translation initiation factor 1A, Y-linked	chrY	2.52	6.02	-11.3	0.0004
DDX3Y	DEAD (Asp-Glu-Ala-Asp) box helicase 3, Y-linked	chrY	2.11	8.22	-68.77	2.57E-10
CD24	CD24 molecule	chrY	2.2	4.93	-6.61	0.0004
BCORP1	BCL6 corepressor pseudogene 1	chrY	2.51	6.63	-17.43	8.14E-06
ANOS2P	anosmin 2, pseudogene	chrY	1.66	3.76	-4.31	0.0001

Differentially expressed genes between males and females (comparison II, $p < 0.05$) are listed here. A negative fold change signifies higher expression in the male and a positive fold change higher expression in the female. Genes not located on sex chromosomes are marked in bold.

Unsurprisingly, genes on the Y chromosome were overexpressed in males, whereas genes on the X chromosome were overexpressed in females. Interestingly, **DDX43** and **TRPC3**, although not located on either sex chromosome, are also found to be sex dependent. The DEAD-box protein DDX43, also called HAGE, is an RNA/DNA helicase that is required for the complete unwinding of the nucleic acid. The **DDX43** gene is located on chromosome 6 in humans and significant more copies of this gene can be found in males [142]. **TRPC3** is a gene located on chromosome 4 and encodes the calcium cation channel TRPC3 (transient receptor potential cation channel, subfamily C, member 3). This cation channel has been linked to lymphocyte and NK-cell response to haptens [50]. The **TRPC3** gene was more strongly expressed in women.

4.3.2 Comparison III: Differentially Expressed Genes – Female Subjects

The following criteria for statistical significance were used in the gender specific analysis: $p < 0.01$ and increase/decrease of fold change by a factor of 1.5. After correction for multiple testing, no genes remain significant. For hypothesis generation, unadjusted results are

presented in **Table 21**. Genes involved in the immune response, vitamin D response, or NK cell physiology are shown in bold.

Table 21: Comparison III – Differentially expressed genes in females

Gene Symbol	Description	Fold Change
<i>TRIM51</i>	tripartite motif-containing 51	-2.44
<i>MIR3180-5</i> ; <i>MIR3180-4</i>	microRNA 3180-5; microRNA 3180-4	-2.06
<i>ZNF733P</i>	zinc finger protein 733, pseudogene	-1.93
<i>TRBV7-6</i>	T cell receptor beta variable 7-6	-1.93
<i>WLS</i>	wntless Wnt ligand secretion mediator	-1.88
<i>KRTAP5-11</i>	keratin associated protein 5-11	-1.87
<i>SAMD5</i>	sterile alpha motif domain containing 5	-1.77
<i>MIR4330</i>	microRNA 4330	-1.68
<i>NBPF13P</i>	neuroblastoma breakpoint family, member 13, pseudogene	-1.66
<i>RGS8</i>	regulator of G-protein signaling 8	-1.63
<i>SYDE2</i>	synapse defective 1, Rho GTPase, homolog 2 (C. elegans)	-1.61
<i>IGKV5-2</i>	immunoglobulin kappa variable 5-2	-1.6
<i>SNORD116-20</i> ; <i>SNORD116@</i>	small nucleolar RNA, C/D box 116-20; small nucleolar RNA, C/D box 116 cluster	-1.59
<i>MIR187</i>	microRNA 187	-1.57
<i>ZNF649-AS1</i>	ZNF649 antisense RNA 1	-1.56
<i>OR5D14</i>	olfactory receptor, family 5, subfamily D, member 14	-1.53
<i>HULC</i>	hepatocellular carcinoma up-regulated long non-coding RNA	-1.52
<i>PART1</i>	prostate androgen-regulated transcript 1 (non-protein coding)	-1.51
<i>NPS</i>	neuropeptide S	-1.5
<i>PTPRO</i>	protein tyrosine phosphatase, receptor type, O	1.51
<i>PAK1</i>	p21 protein (Cdc42/Rac)-activated kinase 1	1.56
<i>LINC00853</i>	long intergenic non-protein coding RNA 853	1.56
<i>L1TD1</i>	LINE-1 type transposase domain containing 1	1.57
<i>KCNE1</i>	potassium channel, voltage gated subfamily E regulatory beta subunit 1	1.58
<i>CEP295NL</i>	CEP295 N-terminal like	1.6
<i>ARHGAP5</i>	Rho GTPase activating protein 5	1.6
<i>CNP</i>	2,3-cyclic nucleotide 3 phosphodiesterase	1.62
<i>SLC31A2</i>	solute carrier family 31 (copper transporter), member 2	1.63
<i>SIGLEC5</i>	sialic acid binding Ig-like lectin 5	1.64

<i>KDM1B</i>	lysine (K)-specific demethylase 1B	1.64
<i>USP12-AS2</i>	USP12 antisense RNA 2 (head to head)	1.67
<i>GCA</i>	grancalcin, EF-hand calcium binding protein	1.69
<i>MIR370</i>	microRNA 370	1.7
<i>DUSP3</i>	dual specificity phosphatase 3	1.7
<i>WFDC10B</i>	WAP four-disulfide core domain 10B	1.72
<i>SLC24A4</i>	solute carrier family 24 (sodium/potassium/calcium exchanger), member 4	1.73
<i>SLC37A2</i>	solute carrier family 37 (glucose-6-phosphate transporter), member 2	1.77
<i>CD99P1</i>	CD99 molecule pseudogene 1	1.79
<i>FGD6</i>	FYVE, RhoGEF and PH domain containing 6	1.82
<i>RPL23AP7</i>	ribosomal protein L23a pseudogene 7	1.83
<i>TLR5</i>	toll-like receptor 5	1.89
<i>CPM</i>	carboxypeptidase M	1.89
<i>MIR4309</i>	microRNA 4309	1.91
<i>C9orf72</i>	chromosome 9 open reading frame 72	1.93
<i>MS4A6A</i>	membrane-spanning 4-domains, subfamily A, member 6A	1.97
<i>FZD1</i>	frizzled class receptor 1	2.09
<i>SMPDL3A</i>	sphingomyelin phosphodiesterase, acid-like 3A	2.27
<i>IGSF6</i>	immunoglobulin superfamily, member 6	2.41
<i>CFP</i>	complement factor properdin	2.68
<i>PAPSS2</i>	3-phosphoadenosine 5-phosphosulfate synthase 2	2.89
<i>GAPT</i>	GRB2-binding adaptor protein, transmembrane	3.24
<i>MNDA</i>	myeloid cell nuclear differentiation antigen	3.74
<i>TLR8</i>	toll-like receptor 8	3.77
<i>RNU6-53P</i>	RNA, U6 small nuclear 53, pseudogene	4.24

Genes which were significantly differentially expressed ($p < 0.01$) and an increase/decrease of fold change at least by a factor of 1.5 are shown. A negative fold change signifies higher expression and, conversely, a positive fold change indicates a corresponding reduction in expression after vitamin D supplementation. Genes involved in the immune response, vitamin D response, or NK cell physiology are marked bold.

The role of T cell receptor chains in NKT cells are discussed in detail in 4.2.2, page 47. In females, ***TRBV7-6*** gene, encoding the beta T cell receptor beta variable chain 7-6, a component of the NK TCR, is overexpressed after vitamin D substitution.

Although immunoglobulins do not play a direct role in NK cells, antibody coating is crucial for ADCC. The upregulation of the **IGKV5-2** (*immunoglobulin kappa variable 5-2*) gene in women must be seen in this context [155].

The P21 (Cdc42/Rac)-activated kinase 1 (encoded by the **PAK1** gene) is involved in ERK signaling [64], whose importance in NK cell cytotoxicity in the MAPK-pathway is discussed in 4.2.2 (page 47). In females, a lower expression is seen after 1,25(OH)₂D₃ supplementation.

The Dual specificity protein phosphatase 3, encoded by the **DUSP3** gene, and further members of the DUSP-subfamily negatively regulate members of the MAP kinase superfamily [78] (see also chapter 4.2.2, page 47). Due to its decreased expression under vitamin D, the negative regulatory effect of DUSP3 on the MAP kinase pathway is in turn reduced, i.e. it leads to increased NK-cell activity. This is consistent with the results of our study on the influence of vitamin D on NK-cell-mediated ADCC.

The role of TLR in NK cells is described in chapter 2.1.4. (page 7). In females, the surface receptor TLR5 and the endosome receptor TLR8 are downregulated after supplementation of vitamin D.

Receptors of the Frizzled family (Fzd) are expressed on NKT cells (at least FZD1 and FZD9) and represent the membrane bound receptors of Wnt-signaling, which modulates IL-4 and IFN- γ production. IFN- γ excretion is halted and later sustained in a time- and b-catenin dependent manner [72]. The **FZD1** gene is downregulated in females. On the contrary, another gene product involved in the Wnt pathway is upregulated, the wntless Wnt ligand secretion mediator (encoded by the **WLS** gene). This protein is necessary for the secretion of Wnt proteins and their binding to FZD receptors [28,61,161].

Complement factor properdin, encoded by the **CPF** gene, is the only known positive regulator of the alternative complement pathway. Its role in NK cells is the binding to NKp46 and has been shown to be crucial to defense against *Neisseria meningitidis* infection [159]. It is downregulated in females in our experiment.

Lastly, the **GAPT** gene, encoding the GRB2-binding adaptor transmembrane protein, shown reduced expression after vitamin d supplementation. It has been linked to B cell proliferation and while it is expressed in NK cells, but its exact role is yet to be established [91].

4.3.3 Comparison IV: Differentially Expressed Genes – Male Subjects

With $p < 0.01$ and an increase/decrease of fold change by a factor of 1.5, a total of 28 transcripts with a well-established annotation were identified in male subjects after vitamin D supplementation. As in the previous analysis for the female subjects, after correction for multiple testing, no transcripts remain significant. In order to be able to formulate a hypothesis nevertheless, these 28 genes are summarized in **Table 22** for a better overview.

Table 22: Comparison IV – Differentially expressed genes in males

Gene Symbol	Description	Fold Change
<i>EIF5AL1</i>	eukaryotic translation initiation factor 5A-like 1	-2.28
<i>MIR548T</i>	microRNA 548t	-2.27
<i>MIR4476</i>	microRNA 4476	-2.17
<i>GGT1</i> ; <i>SNRPD3</i>	gamma-glutamyltransferase 1; small nuclear ribonucleoprotein D3 polypeptide	-2.16
<i>ARHGAP39</i>	Rho GTPase activating protein 39	-1.82
<i>FGF12-AS3</i>	FGF12 antisense RNA 3	-1.81
<i>TTY14</i>	testis-specific transcript, Y-linked 14 (non-protein coding)	-1.71
<i>MIR4279</i>	microRNA 4279	-1.68
<i>C9orf139</i>	chromosome 9 open reading frame 139	-1.68
<i>SLC52A1</i>	solute carrier family 52 (riboflavin transporter), member 1	-1.64
<i>SERPINA12</i>	serpin peptidase inhibitor, clade A (alpha-1 antiproteinase, antitrypsin), member 12	-1.64
<i>TUBA3D</i>	tubulin, alpha 3d	-1.62
<i>MIR125A</i>	microRNA 125a	-1.61
<i>SEMA6A</i>	sema domain, transmembrane domain (TM), and cytoplasmic domain, (semaphorin) 6A	-1.59
<i>LRRC3</i>	leucine rich repeat containing 3	-1.59
<i>EFCAB12</i>	EF-hand calcium binding domain 12	-1.59
<i>SNRPN</i>	small nuclear ribonucleoprotein polypeptide N	-1.55
<i>IFNL3</i>	interferon, lambda 3	-1.54
<i>BIRC7</i>	baculoviral IAP repeat containing 7	-1.52
<i>PLA2G4E-AS1</i>	PLA2G4E antisense RNA 1	-1.51
<i>USP51</i>	ubiquitin specific peptidase 51	1.51
<i>C5orf60</i>	chromosome 5 open reading frame 60	1.54
<i>ASAP1-IT2</i>	ASAP1 intronic transcript 2	1.64
<i>TPRX1</i>	tetra-peptide repeat homeobox 1	1.66
<i>MGAM2</i>	maltase-glucoamylase 2 (putative)	1.83
<i>ZSCAN5CP</i>	zinc finger and SCAN domain containing 5C, pseudogene	1.9
<i>MIR1827</i>	microRNA 1827	1.92
<i>IFNG</i>	interferon, gamma	2.12

Genes which were significantly differentially expressed ($p < 0.01$) and an increase/decrease of fold change at least by a factor of 1.5 are shown. A negative fold change signifies higher expression and, conversely, a positive fold change indicates a corresponding reduction in expression after vitamin D supplementation. Genes involved in the immune response, vitamin D response, or NK cell physiology are marked bold.

In males, the ***INFL3*** gene is shown to be upregulated after vitamin D supplementation. The role of its gene product was discussed in detail in chapter 4.2.2 on page 47.

Most interestingly, the ***IFNG*** gene, which encodes IFN- γ , is downregulated in men after substitution with vitamin D. IFN- γ plays an important role in viral clearance and viral infection control. It induces maturation and activation of DCs and macrophages and promotes T cell response. Specifically, it inhibits differentiation into IL-4- and IL-17-producing CD4+ T cells (Th2 and Th17) and induces differentiation into pro-inflammatory Th1 cells [112]. In target cells, IFN- γ induces upregulation of intercellular adhesion molecule 1 (ICAM-1) which promotes NK-target cell conjugation [154]. On the other hand, it can upregulate MHC-class I molecules, which, when expressed on cells targeted by NK cells, for instance tumors, function as an inhibitory KIR-ligand for NK-cell activation. Although IFN- γ plays a clear role in antiviral defense, it is due to this NK-cell inhibitory effect that its anti-tumor effects are less straightforward. In fact, in the presence of IFN- γ , NK cell-mediated tumor lysis may even be reduced. This is not only attributed to the afore mentioned overexpression of MHC-class I molecules on target cells, but also of other inhibitory ligand/receptor interactions like PD-L1, HLA-DR, CD95/FasR, and CD270/HVEM [6].

4.3.4 Comparison V: Female vs. Male in the Vitamin D Deficient State

Finally, males and females were compared in the vitamin D deficient state and after vitamin D supplementation. The Venn diagram below (**Figure 18**) provides an overview of the differentially expressed transcripts in the two groups and highlights those with unique differential expression depending on vitamin D serum levels.

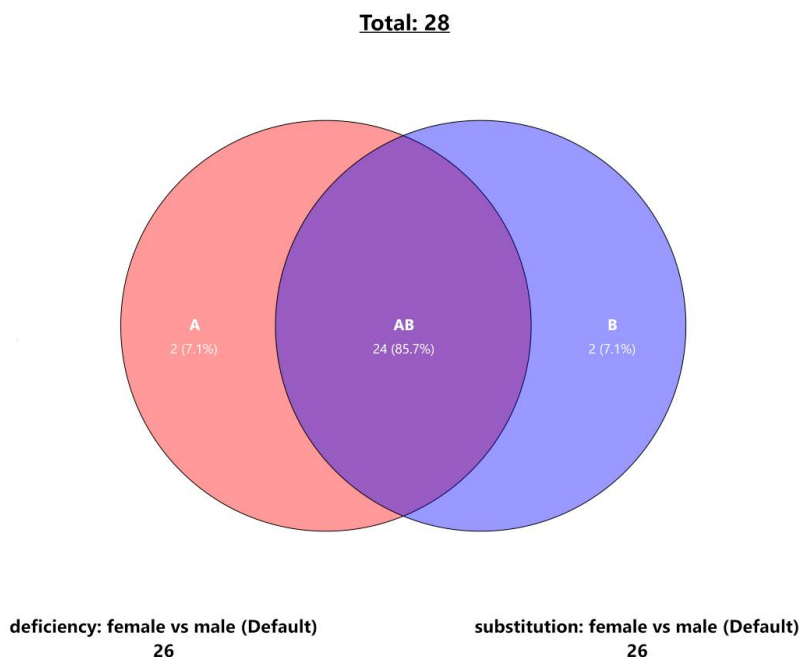


Figure 18: Venn diagram of comparisons II, V and VI

The Venn diagram shows the number of differentially expressed genes between males and females, in the vitamin D deficient state (orange) and after substitution (blue). The purple area represents the genes, which are expressed differently between females and males but are independent of vitamin D status.

26 transcripts were differentially expressed after correction for multiple testing between male- and female-derived NK cells in the deficient state (orange area in **Figure 18**). Coincidentally, after supplementation with vitamin D, the same number of transcripts was statistically significantly differentially expressed after adjustment for multiple testing between males and females ($n = 26$, blue area in **Figure 18**), but of those, only 24 were the same as in the deficient state (purple area in **Figure 18**) and two additional transcripts appeared. So, in total, 28 transcripts with sex- and vitamin D-dependent expression were identified. Of those, 24 (85.7%) are independent of vitamin D status. Two transcripts were shown to be sex-specifically differentially expressed only in the vitamin D deficient state and two different transcripts could be identified after vitamin D substitution.

Table 23 features the 18/26 genes (orange area in **Figure 18**) with known annotations which are differentially expressed by female and male NK cells in the deficient state. For one of the genes, **RPS4Y1**, overexpression in males compared to the female was higher in the vitamin D deficient state than after substitution. It is one of the two genes which encode the ribosomal protein S4. This is the only ribosomal protein known to be encoded by more than one gene, specifically ribosomal protein S4, Y-linked gene (**RPS4Y1**) and ribosomal protein S4, X-linked (**RPS4X**) [172]. A recent study has also demonstrated that expression of the Y-linked gene is vitamin D dependent, but in this study it was upregulated after supplementation [128]. The other differentially expressed transcript has no known annotation and is not shown in the table.

Table 23: Comparison V – Differentially expressed genes – Female vs. male in the vitamin D deficient state

Gene Symbol	Description	Chromosome	Fold Change	FDR p-value
XIST	X inactive specific transcript (non-protein coding)	X	350.73	4.60E-10
TSIX	TSIX transcript, XIST antisense RNA	X	6.11	4.35E-06
ZFY	zinc finger protein, Y-linked	Y	-6.57	0.0005
USP9Y	ubiquitin specific peptidase 9, Y-linked	Y	-44.55	2.88E-08
TXLNGY	taxilin gamma pseudogene, Y-linked	Y	-36.73	3.07E-08
TXLNGY	taxilin gamma pseudogene, Y-linked	Y	-32.29	7.46E-08
TTY15	testis-specific transcript, Y-linked 15 (non-protein coding)	Y	-58.68	7.90E-09
TTY14	testis-specific transcript, Y-linked 14 (non-protein coding)	Y	-3.79	0.0002
TMSB4Y	thymosin beta 4, Y-linked	Y	-4.66	0.0005
PRKY	protein kinase, Y-linked, pseudogene	Y	-31.87	9.36E-07
LINC00278	long intergenic non-protein coding RNA 278	Y	-12.66	2.41E-05
KDM5D	lysine (K)-specific demethylase 5D	Y	-39.08	1.33E-07
EIF1AY	eukaryotic translation initiation factor 1A, Y-linked	Y	-12.03	0.0056
DDX3Y	DEAD (Asp-Glu-Ala-Asp) box helicase 3, Y-linked	Y	-70.44	1.59E-08
CD24	CD24 molecule	Y	-6.32	0.0186
BCORP1	BCL6 corepressor pseudogene 1	Y	-16.46	0.0005
ANOS2P	anosmin 2, pseudogene	Y	-4.34	0.0069
RPS4Y1	ribosomal protein S4, Y-linked 1	Y	-5.29	0.0288

Differentially expressed genes between females and males in the vitamin D deficient state (comparison V, $p < 0.05$) are presented here. A negative fold change signifies higher expression in the male and a positive fold change higher expression in the female. Genes with no differential expression after vitamin D supplementation are marked in bold.

4.3.5 Comparison IV: Female vs. Male after Vitamin D Supplementation

19/26 genes with established annotations (blue area in **Figure 18**) which show differential expression after correction for multiple testing between the two sexes after supplementation are listed in **Table 24**. The differential expression of two of those genes is not only sex- but also vitamin D-dependent.

First, vitamin D substitution leads to increased expression of the **JPX** gene in females. Its gene product is a long noncoding RNA (lncRNA). It is located in the X-inactivation center and is involved in X chromosome inactivation in female mammals [144]. It is physiologically higher expressed in the female; however, restoration of vitamin D serum levels widens the RNA expression gap between the sexes.

After vitamin D substitution a second probe for **TTY14** (Testis-Specific Transcript, Y-Linked 14) was overexpressed in males. **TTY14** is another lncRNA class gene which is yet to be studied in detail. Its expression in tissues outside testis is unclear. Furthermore, no known associations with vitamin D or the immune system exist [38].

Table 24: Comparison VI – Differentially expressed genes – Female vs. male after vitamin D supplementation

Gene Symbol	Description	Chromosome	Fold Change	FDR p-value
<i>XIST</i>	X inactive specific transcript (non-protein coding)	X	374.13	4.47E-10
<i>TSIX</i>	TSIX transcript, XIST antisense RNA	X	5.11	7.09E-06
JPX	JPX transcript, XIST activator (non-protein coding)	X	1.81	0.0059
<i>ZFY</i>	zinc finger protein, Y-linked	Y	-7.93	0.0001
<i>USP9Y</i>	ubiquitin specific peptidase 9, Y-linked	Y	-61.73	1.32E-08
<i>TXLNGY</i>	taxilin gamma pseudogene, Y-linked	Y	-30.67	4.46E-08
<i>TXLNGY</i>	taxilin gamma pseudogene, Y-linked	Y	-28.99	9.13E-08
<i>TTY15</i>	testis-specific transcript, Y-linked 15 (non-protein coding)	Y	-48.4	1.32E-08
TTY14	testis-specific transcript, Y-linked 14 (non-protein coding)	Y	-3.06	0.0015
<i>TTY14</i>	testis-specific transcript, Y-linked 14 (non-protein coding)	Y	-2.82	0.0009
<i>TMSB4Y</i>	thymosin beta 4, Y-linked	Y	-2.91	0.0287
<i>PRKY</i>	protein kinase, Y-linked, pseudogene	Y	-28.55	1.17E-06

<i>LINC00278</i>	long intergenic non-protein coding RNA 278	Y	-9.76	6.45E-05
<i>KDM5D</i>	lysine (K)-specific demethylase 5D	Y	-34.26	1.50E-07
<i>EIF1AY</i>	eukaryotic translation initiation factor 1A, Y-linked	Y	-8.96	0.0419
<i>DDX3Y</i>	DEAD (Asp-Glu-Ala-Asp) box helicase 3, Y-linked	Y	-66.09	1.32E-08
<i>CD24</i>	CD24 molecule	Y	-6.32	0.0128
<i>BCORP1</i>	BCL6 corepressor pseudogene 1	Y	-18	0.0003
<i>ANOS2P</i>	anosmin 2, pseudogene	Y	-4.39	0.0028

Differentially expressed genes between females and males after vitamin D supplementation (comparison VI, $p < 0.05$) are presented here. A negative fold change signifies higher expression in the male and a positive fold change higher expression in the female. Genes with no differential expression in the vitamin D deficient state are marked in bold.

4.4 PATHWAY ANALYSIS

Pathway analysis was performed as described in 3.4.4, page 37. As mentioned afore, the first step in GSEA is to generate a ranked gene list. The top 50 upregulated and top 50 downregulated transcripts on the list according to the metric used (Signal-to-Noise) are presented in **Figure 19**. Based on this ranked gene list, a number of selected, predefined gene sets were tested for significance.

Results

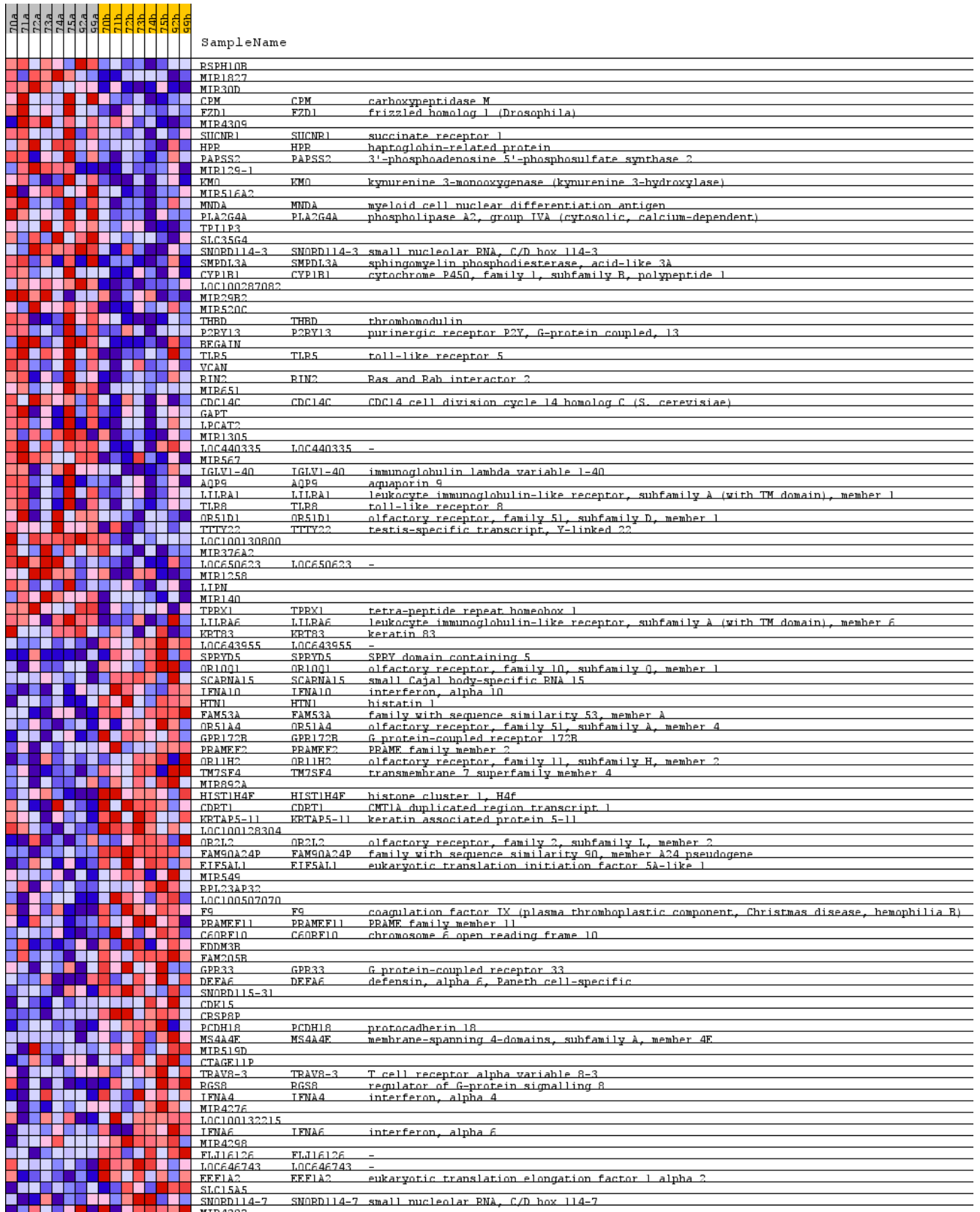


Figure 19: Heat map of the 50 most significant transcripts for each phenotype as per GSEA ranked list

The heatmap demonstrates the correlation between the ranked genes and the phenotypes (columns on the left: deficiency, columns on the right: substitution). The expression values are represented in a color scale, where the range of colors (red, pink, light blue, dark blue) shows the range of expression values (high, moderate, low, lowest). The metric used was the default Signal2Noise metric. Only the top 50 downregulated and top 50 upregulated transcripts are shown.

4.4.1 NK-Cell Cytotoxicity Pathway

The “*NK-cell cytotoxicity pathway*” was found to be significantly ($p = 0.016$) upregulated after vitamin D substitution (Table 25, Figure 20) within the prespecified gene subgroup. The genes, which shaped the enrichment score in the pathway, are listed in Table 26.

Table 25: NK cell cytotoxicity pathway – Metrics

Name	ES	NES	p-value	FDR q-value
KEGG NATURAL KILLER CELL MEDIATED CYTOTOXICITY	0.56	1.41	0.016	0.016

The definition and calculation method of the enrichment score is described in 3.4.4, page 37. The ES is normalized to adjust for variation on predefined gene set size. The FDR value is equal to the p-value in this case as no other gene set was included in this analysis. Abbreviations: ES: Enrichment Score, NES: Normalized Enrichment Score, FDR: false discovery rate, KEGG: Kyoto Encyclopedia of Genes and Genomes.

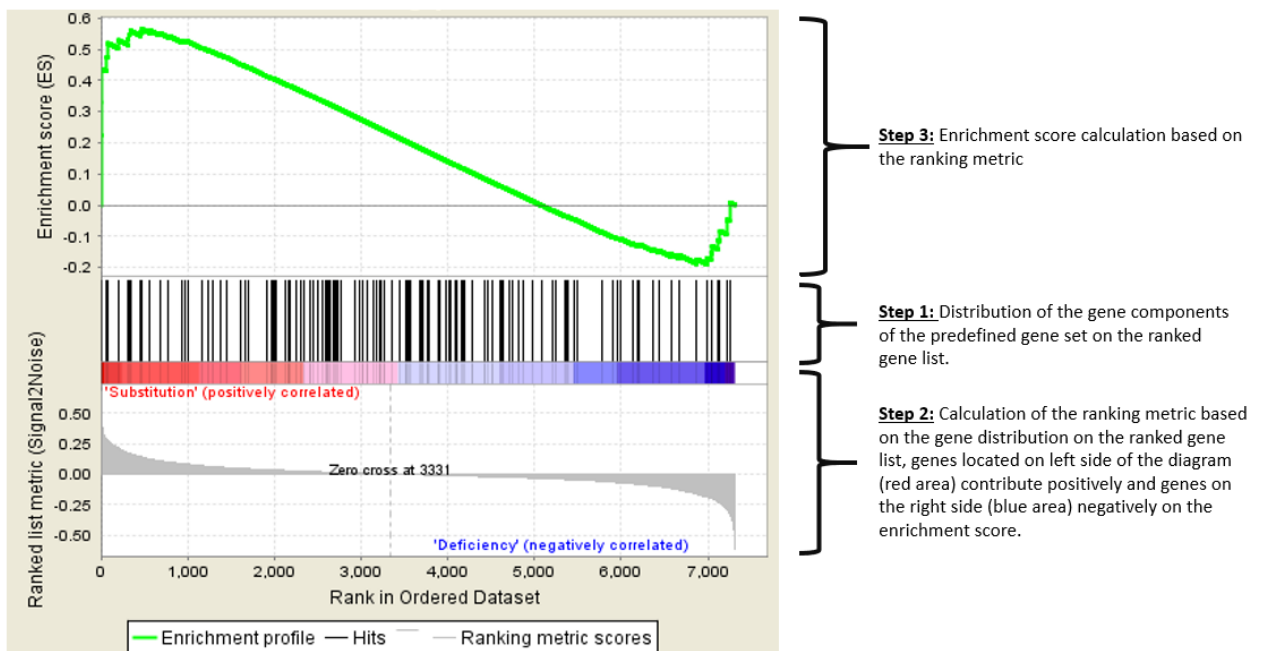


Figure 20: Enrichment Plot: “NK cell cytotoxicity” pathway

The upper part of the figure shows the running ES for the gene set as the analysis walks down the ranked list. A positive ES (the green line is mostly above 0.0) means overexpression. The middle part of the figure shows the placement of the individual genes of a certain set in the ranking of all genes. Each gene is represented by a line. The bottom part of the plot shows the value of the ranking metric, indicating the correlation of a gene to either one of the two phenotypes “substitution” or “deficiency”. It is positive (red) when the gene shows higher expression in the phenotype “substitution” and negative (blue) when expression is higher in the phenotype “deficiency”. The default GSEA metric signal-to-noise ratio was used.

Table 26: NK-cell cytotoxicity pathway - Genes contributing to the enrichment score

Gene symbol	Gene name	Rank in gene list	Rank Metric score	continuous ES
IFNA10	interferon, alpha 10	1	0.624	0.2226
IFNA6	interferon, alpha 6	5	0.436	0.3307
IFNA4	interferon, alpha 4	6	0.433	0.4379
IFNA2	interferon, alpha 2	66	0.287	0.4767
PPP3R2	protein phosphatase 3 (formerly 2B), regulatory subunit B, 19kDa, beta isoform (calcineurin B, type II)	76	0.280	0.5202
RAC3	ras-related C3 botulinum toxin substrate 3 (rho family, small GTP binding protein Rac3)	197	0.215	0.5298
RAET1L	retinoic acid early transcript 1L	310	0.172	0.5312
IFNA7	interferon, alpha 7	319	0.171	0.5469
NCR2	natural cytotoxicity triggering receptor 2	337	0.167	0.5605
IFNA13	interferon, alpha 13	460	0.143	0.5553
SHC2	SHC (Src homology 2 domain containing) transforming protein 2	474	0.140	0.5646

Abbreviations: ES: Enrichment Score

Type I interferons are a family of monomeric cytokines consisting of 14 IFN- α subtypes and one of IFN- β , IFN- ϵ , IFN- κ , and IFN- ω and are well identified as antimicrobial but also antitumoral substances. Most cell types in the human body can secrete type I IFNs in response to activation of TLRs and retinoic acid inducible gene-I-like RNA helicases. Signaling is mediated through interferon alpha receptor 1 (IFNRA1) or IFNAR2 and consequent activation of the signal transducers and activators of transcription (STAT) signaling complex and the IFN regulatory factor (IRF)-9 [104],[170].

Defects in type I IFN signaling in NK cells leads to reduced NK cell numbers and impaired NK cell-mediated cytotoxicity and in turn severely impaired tumor surveillance [104]. Also, NK cell-mediated viral clearance has been shown to depend on type I IFNs [170].

4.4.2 Immune System-Related Pathways – Upregulated

The second part of the analysis involved the entire gene expressions profile received from the microarray to look for dysregulated pathways involved in the immune system and vitamin D homeostasis. Using the criteria of FDR-value < 0.05, two pathways remained significantly upregulated: the “*regulation of type I interferon mediated signaling*” pathway (**Figure 21**) and the “*response to type I interferon*” pathway (**Figure 22**). **Table 27** lists the two pathways, which showed upregulation. To identify the genes that contribute to the upregulation of these pathways, leading edge analysis was performed (**Figure 23**). There are five interferon genes, *IFNA2*, *IFNA4*, *IFNA6*, *IFNA7* and *IFNA10* showing the highest differential expression within these pathways.

Table 27: Upregulated pathways involved in the immune response

Name of the Pathway	ES	NES	p-value	FDR q-value
GO – Regulation of type I interferon mediated signaling pathway	0.78	1.62	0.010	0.032
GO – Response to type I interferon pathway	0.68	1.56	0.009	0.048

Abbreviations: ES: Enrichment Score, NES: Normalized Enrichment Score, FDR: false discovery rate, GO: Gene Ontology

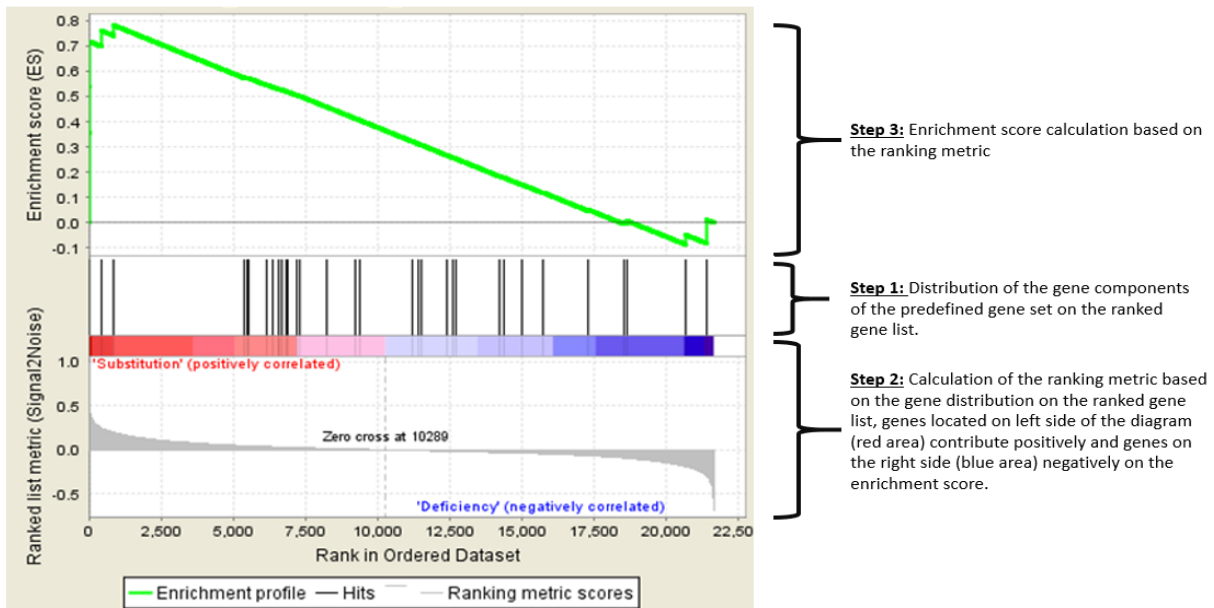


Figure 21: Enrichment plot: “Regulation of type I interferon mediated signaling” pathway

The upper part of the figure shows the running ES for the gene set as the analysis walks down the ranked list. A positive ES (the green line is mostly above 0.0) means overexpression. The middle part of the figure shows the placement of the individual genes of a certain set in the ranking of all genes. Each gene is represented by a line. The bottom part of the plot shows the value of the ranking metric, indicating the correlation of a gene to either one of the two phenotypes “substitution” or “deficiency”. It is positive (red) when the gene shows higher expression in the phenotype “substitution” and negative (blue) when expression is higher in the phenotype “deficiency”. The default GSEA metric signal-to-noise ratio was used.

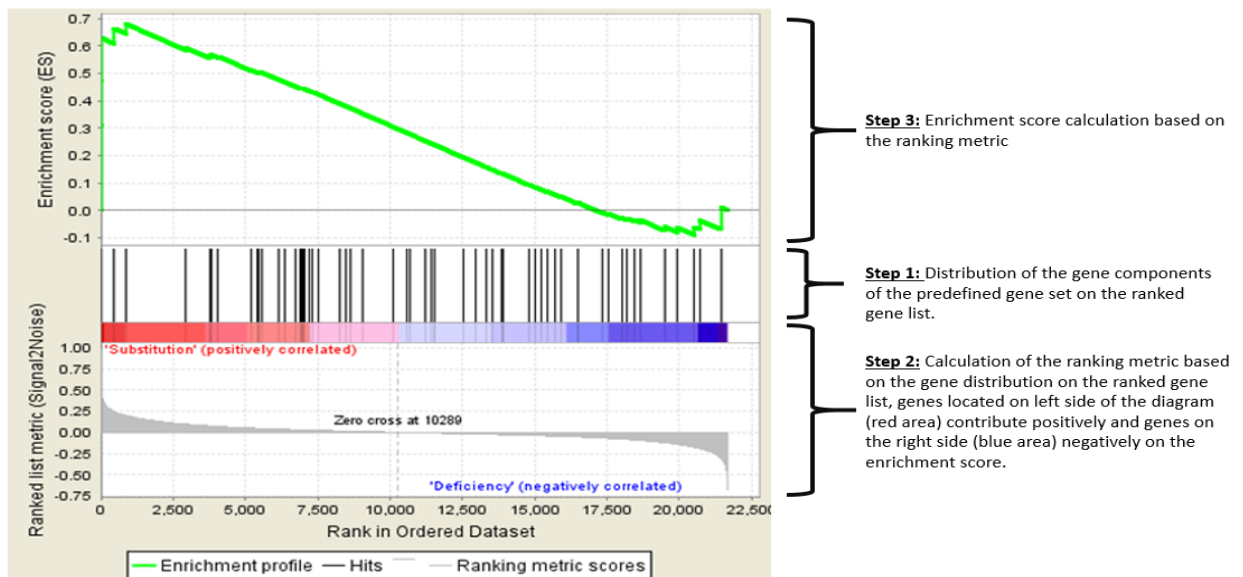


Figure 22: Enrichment plot: “Response to type I interferon” pathway

The upper part of the figure shows the running ES for the gene set as the analysis walks down the ranked list. A positive ES (the green line is mostly above 0.0) means overexpression. The middle part of the figure shows the placement of the individual genes of a certain set in the ranking of all genes. Each gene is represented by a line. The bottom part of the plot shows the value of the ranking metric, indicating the correlation of a gene to either one of the two phenotypes “substitution” or “deficiency”. It is positive (red) when the gene shows higher expression in the phenotype “substitution” and negative (blue) when expression is higher in the phenotype “deficiency”. The default GSEA metric signal-to-noise ratio was used.

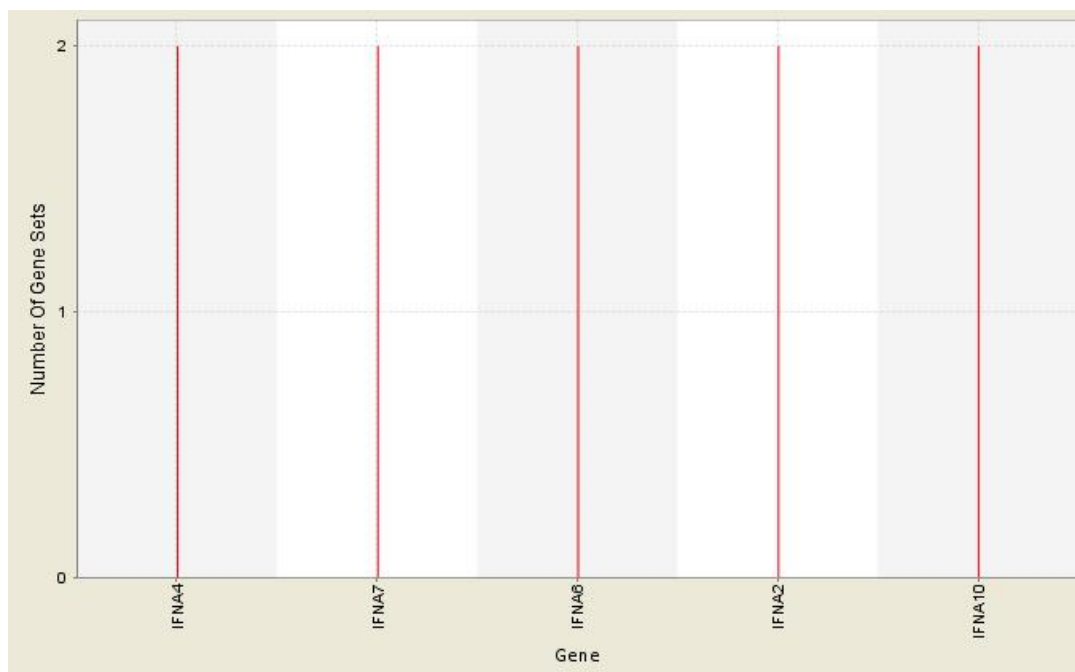


Figure 23: Leading edge analysis of the upregulated pathways involved in the immune response

Leading edge analysis can be used to highlight common genes in different pathways which show similar behavior (up- or downregulation) in gene expression analysis. Vertical bars indicate how often a gene appears in the gene sets under investigation. In this case, the maximum possible number of hits was 2, since two pathways were examined in this leading edge analysis. The figure shows that the genes of IFNA2, IFNA4, IFNA6, IFNA7, and IFNA10 are the common denominator of the two upregulated pathways “regulation of type I interferon mediated signaling” and “response to type I interferon”.

4.4.3 Immune System-Related Pathways – Downregulated

More pathways were found to be downregulated after vitamin D supplementation. These include: “FcεR1” (high-affinity IgE receptor) pathway, “activation of innate immune response” pathway, “complement” pathway, “interferon gamma response” pathway, pathway of “regulation of interferon beta production”, pathway of “positive regulation of interferon beta production”, pathway of “positive regulation of interferon alpha production”, “leukocyte chemotaxis” pathway, “IL6/JAK/STAT3 signaling” pathway, pathway of “activation of immune response” and finally “response to vitamin D” pathway (**Table 28**). Again, leading edge analysis was performed (**Figure 24**). Furthermore, the distribution of common genes between the downregulated pathways is presented in the heat map in **Figure 25**.

Table 28: Downregulated pathways involved in the immune response

Name of the Pathway	ES	NES	p-value	FDR q-value
Biocarta – FCεRI	0.90	1.88	< 0.001	< 0.001
GO – Activation of innate immune response	0.71	1.87	< 0.001	< 0.001
Hallmark – Complement	0.70	1.84	< 0.001	< 0.001
GO – Interferon Gamma response	0.68	1.78	< 0.001	< 0.001
GO – Regulation of interferon beta production	0.80	1.71	< 0.001	0.002
GO – Positive regulation of interferon beta production	0.86	1.70	< 0.001	0.002
GO – Leukocyte chemotaxis	0.67	1.64	< 0.001	0.013
GO – Positive regulation of interferon alpha production	0.89	1.59	0.002	0.032
Hallmark – IL6/JAK/STAT3 signaling	0.66	1.58	< 0.001	0.032
GO – Activation of immune response	0.57	1.57	< 0.001	0.032
GO – Response to vitamin D	0.77	1.57	0.012	0.031

Abbreviations: ES: Enrichment Score, NES: Normalized Enrichment Score, FDR: false discovery rate, GO: Gene Ontology

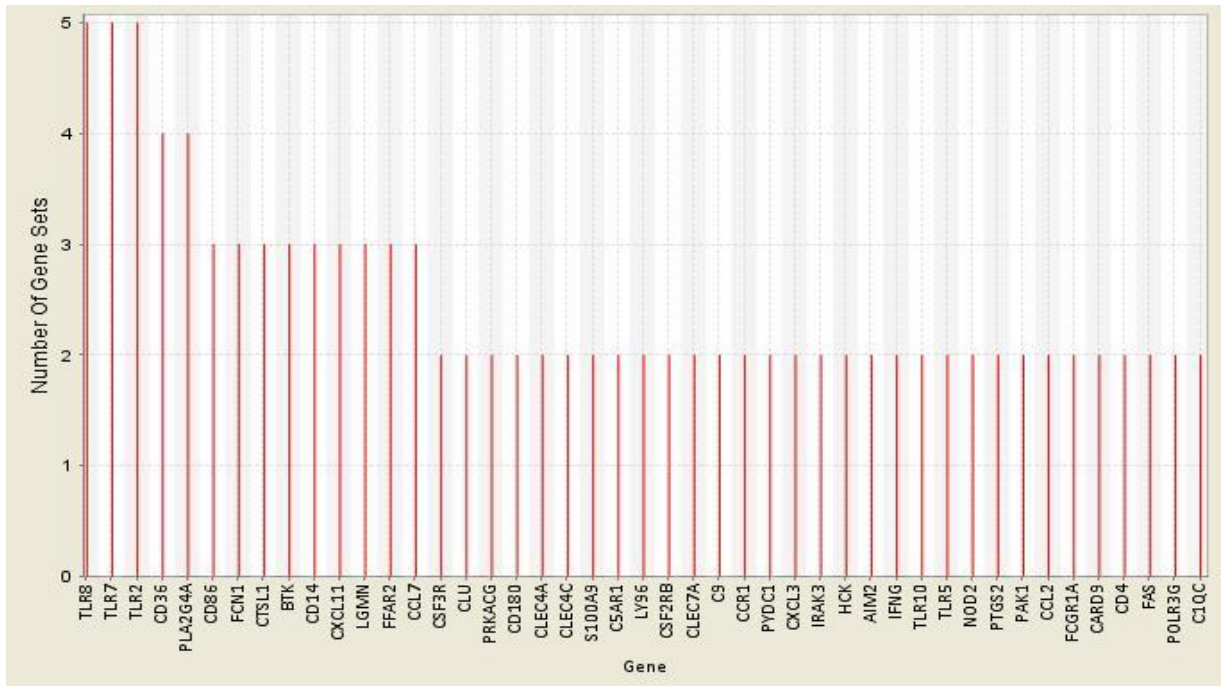


Figure 24: Leading edge analysis of the downregulated pathways involved in the immune response

Leading edge analysis can be used to highlight common genes in different pathways which show similar behavior (up- or downregulation) in gene expression analysis. Vertical bars indicate how often a gene appears in the gene sets under investigation. In this case, the maximum possible number of hits was 11, since eleven pathways were examined in this leading edge analysis. The figure shows the downregulated genes after vitamin D supplementation, which are represented in at least two of the investigated pathways.

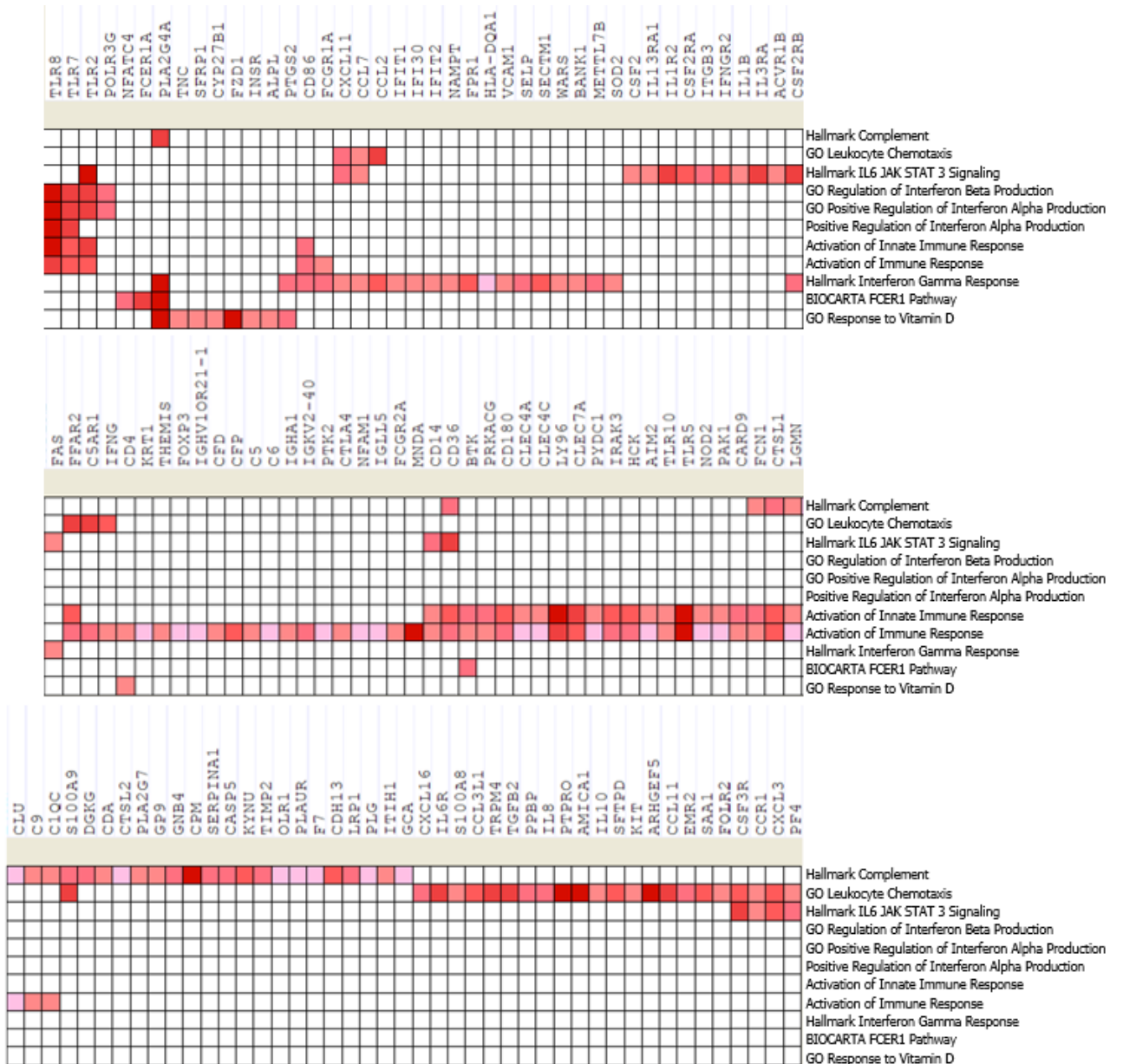


Figure 25: Common gene distribution among the downregulated pathways

This heat map shows the distribution of common genes among the downregulated pathways. Color intensity is analogous to the magnitude of reduced gene expression after vitamin D substitution, with rose demonstrating weaker and dark red stronger relative downregulation.

First, some selected downregulated pathways will be briefly described.

FcεRI (high-affinity IgE receptor) **pathway**: FcεRI is the major receptor for mast cell activation and its activation results in NF-kappa B activation and proinflammatory cytokine production [71]. A relationship to NK cells is not known.

Complement has been shown to promote complement-dependent cytotoxicity (CDC) which is a distinct and ADCC-independent mechanism of cytotoxicity. However, experimental models demonstrated that complement inhibition increases the availability of NK cells within neoplastic lesions and enhanced NK cell-dependent cytotoxic T-cell activity against tumor cells. It has

therefore been suggested, that the complement pathway could be a potent therapeutic target to improve NK-dependent antitumoral immune responses in cancer immunotherapy [62,63].

The ***IL-6/JAK/STAT3 signaling pathway***: has been shown to be aberrantly hyperactivated in patients with chronic inflammatory conditions and in those with hematopoietic malignancies or solid tumors. Furthermore, cell types in the tumor microenvironment including NK cells show STAT3 hyperactivation. It has been hypothesized, that therapeutic targeting of components of the IL-6/JAK/STAT3 can inhibit tumor cell growth and relieve immunosuppression in the tumor microenvironment. Specifically for NK cells, inhibition of IL-6-JAK/STAT3 signaling has been proven to increase the NK cell-mediated cytotoxicity against castration-resistant prostate cancer cells [65,160].

IFN- γ response: This pathway involves genes which are known to be up-regulated in response to IFN- γ stimulation. Its function is described in 4.3.3, page 64.

We could also demonstrate the downregulation of the **response to vitamin D (Figure 25)** pathway, as to be expected in the context of a vitamin D supplementation. Downregulated genes involved in this pathway included *PLA2G4A*, *TNC*, *SFRP1*, *CYP27B1*, *FZD1*, *INSR*, *ALPL*, *PTGS2* and *CD4*.

Finally, a close examination of **Figure 25** and **Figure 24** reveals a gene cluster which was found to be overrepresented in the significantly downregulated pathways. This cluster involves three ***toll-like receptor*** genes, *TLR2*, *TLR7* and *TLR8*. Furthermore, *TLR 5* and *TLR10* were also represented in the leading edge analysis, however less commonly represented in the pathways above. TLR genes expression of all subjects is shown in **Figure 26**. However, and as to be seen in **Figure 27**, in females TLR downregulation is more pronounced.

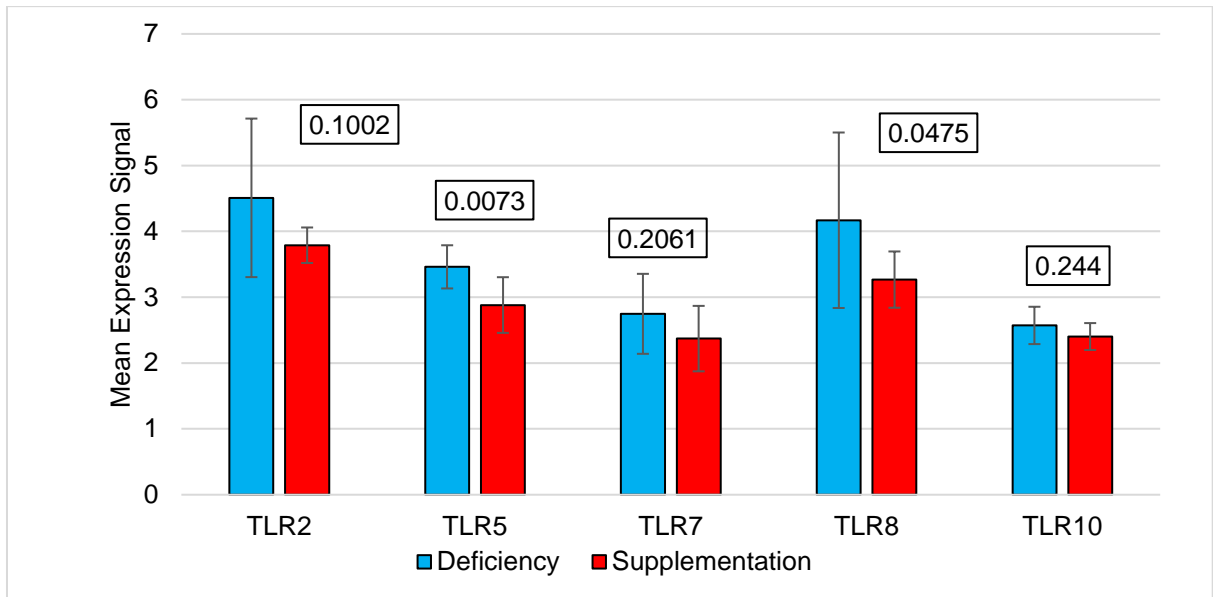


Figure 26: TLR gene expression in all subjects

Selected TLR gene expression before (blue columns) and after (red columns) vitamin D supplementation across all subjects. Standard deviation is shown as error bar. The unadjusted p-values according to two-way ANOVA are given above each pair of columns. Across all subjects, of the five TLR genes, TLR5 and TLR8 were downregulated (p-value < 0.05) after vitamin D supplementation.

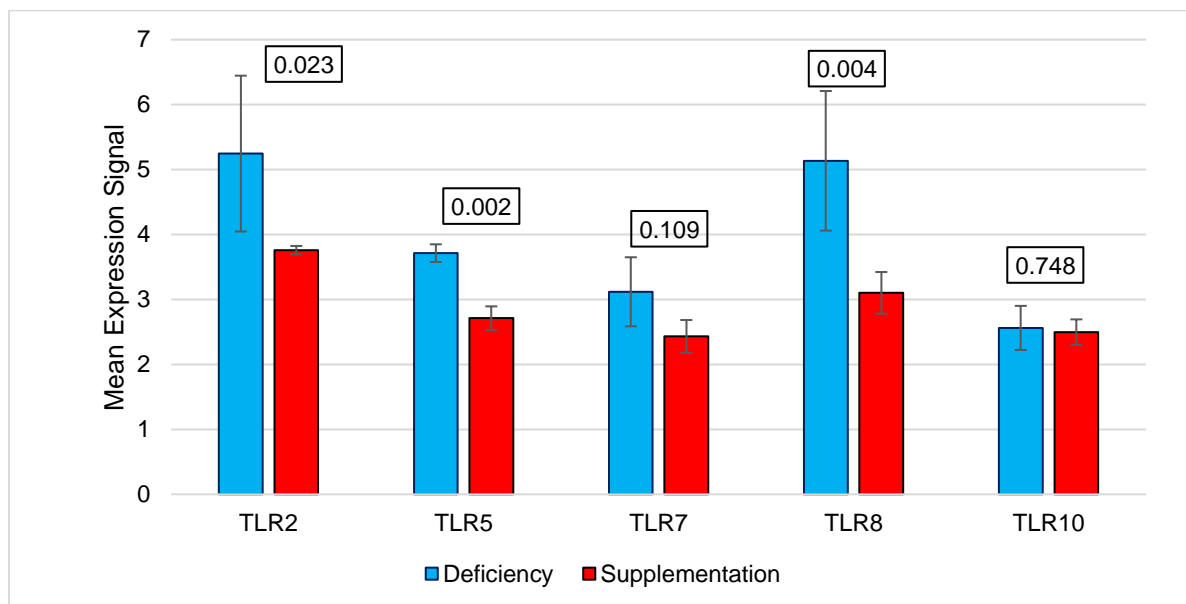


Figure 27: TLR gene expression in females

Selected TLR gene expression before (blue columns) and after (red columns) vitamin D supplementation in female subjects. Standard deviation is shown as error bar. The unadjusted p-values according to two-way ANOVA are given above each pair of columns. In addition to TLR5 and TLR8, TLR2 was also downregulated in female NK cells after vitamin D supplementation (p-value < 0.05).

4.4.4 Unsupervised Pathway Analysis

As a final step, an unsupervised pathway analysis was performed using the Genetrail web tool. The pathway databases analyzed were the ones on the default setting of the Genetrail algorithm. An adjusted p-value of < 0.01 was selected for significance, corrected according to the Bonferroni method. In total, six pathways were found to be enriched and five were depleted after in vivo supplementation of vitamin D. More detailed results are given in **Table 29** sorted by gene set database.

Table 29: Pathways influenced by vitamin D supplementation – Unsupervised analysis

Effect	Name	Adjusted p-value
<i>GO – Cellular Component</i>		
<i>downregulated</i>	ubiquitin ligase complex	7.10E-003
<i>GO – Biological Process</i>		
upregulated	detection of chemical stimulus involved in sensory perception of smell	1.03E-005
upregulated	sensory perception of smell	3.50E-005
upregulated	detection of chemical stimulus involved in sensory perception	4.12E-005
<i>downregulated</i>	biological phase	9.56E-003
<i>GO – Molecular Function</i>		
upregulated	olfactory receptor activity	3.01E-006
<i>downregulated</i>	ubiquitin like protein ligase activity	2.56E-003
<i>downregulated</i>	ubiquitin protein ligase activity	2.56E-003
<i>KEGG - Pathways</i>		
upregulated	olfactory transduction	07.50E-007
<i>Reactome - Pathways</i>		
upregulated	olfactory Signaling Pathway	6.29E-006
<i>downregulated</i>	generic Transcription Pathway	1.94E-005

This figure lists the pathways which were found to be upregulated (in bold) or downregulated in the unsupervised analysis. They are listed according to the reference database they were obtained from, which is reported in the gray lines (also see chapter 3.4.4 page 37).

A downregulation of ubiquitin ligase pathways was observed. Ubiquitination is a post-translational modification of proteins that involves the addition of ubiquitin to a target protein and is necessary for several cellular processes, like protein degradation by the proteasome, cell cycle progression, transcriptional regulation, DNA repair, and signal transduction. For ubiquitination three types of enzymes are required, E1 ubiquitin-activating enzymes, E2

ubiquitin-conjugating enzymes and E3 ubiquitin ligases [7]. **Table 30** lists the genes of the ubiquitin ligase complex family which were found to be significantly ($p < 0.05$) downregulated. Ubiquitin ligases mediate the inhibition of NK-cell activity [100]. Furthermore, the downregulation or knockout of ubiquitin ligases has been directly connected to enhanced NK cell antitumor activity in several studies [94,100].

Olfactory receptors are expressed in immune cells [97], but their role in NK cells remains unclear. Their participation in hapten recognition has been hypothesized but not confirmed [50]. The results of such unguided analysis must be interpreted with caution and with critical assessment of their biological relevance.

Table 30: Downregulated genes involved in the ubiquitin ligase complex

Gene Symbol	Description	Fold Change	p-value
FEM1C	fem-1 homolog c (C. elegans)	1.15	0.00928
ANAPC4	anaphase promoting complex subunit 4	1.11	0.00962
DCAF12L2	DDB1 and CUL4 associated factor 12-like 2	1.21	0.01035
MED17	mediator complex subunit 17	1.15	0.01044
DCAF16	DDB1 and CUL4 associated factor 16	1.10	0.01046
CACYBP	calcyclin binding protein	1.30	0.01730
PCGF5	polycomb group ring finger 5	1.16	0.01815
GLMN	glomulin, FKBP associated protein	1.12	0.01923
DCUN1D2	DCN1, defective in cullin neddylation 1, domain containing 2	1.15	0.02081
RCHY1	ring finger and CHY zinc finger domain containing 1, E3 ubiquitin protein ligase	1.21	0.02507
NCCRP1	non-specific cytotoxic cell receptor protein 1 homolog (zebrafish)	1.16	0.02847
RNF149	ring finger protein 149	1.13	0.03074
SUGT1P3	SGT1 homolog, MIS12 kinetochore complex assembly cochaperone pseudogene 3	1.34	0.03128
UBE2U	ubiquitin-conjugating enzyme E2U (putative)	1.13	0.03664
FBXO21	F-box protein 21	1.13	0.04002
MED14OS	MED14 opposite strand	1.14	0.04334
ATG3	autophagy related 3	1.12	0.04780
ARIH2	ariadne RBR E3 ubiquitin protein ligase 2	1.15	0.04844

5 DISCUSSION

The NK cells used in this study had demonstrated a significantly increased ADCC activity against the lymphoma cell line DAUDI in the presence of Rituximab under physiologically normal vitamin D serum concentrations or after supplementation of vitamin D *in vivo*, respectively [20,105]. Thus, the aim of this study was to investigate the molecular mechanisms of the influence of vitamin D on NK-cell activity. To this end, in this thesis mRNA expression profiles of NK cells were compared before and after supplementation of vitamin D *in vivo*.

5.1 ROLE OF PATHWAY ANALYSIS IN GENOMIC RESEARCH

In modern genome research DNA and cDNA microarrays and more recently next generation sequencing are part of daily practice. A widespread problem faced with gene expression profiling is the lack of statistical significance of individual genes after correcting for multiple testing. The level of differential expression may be discreet compared to the level of “false positive background” which always happens with such amounts of data. On the other hand, successfully identified differentially expressed genes, which not necessarily share biological functions, may cause a certain bias in interpreting the data under biological aspects. Furthermore, pure mathematical search for a single highly expressed gene may miss crucial subtle changes concerning a whole pathway, whose individual gene differential expression may not reach statistical significance after correcting for multiple testing. Considering biological or functional aspects it is clear, that changes concerning a complete pathway are much more interesting than just one single gene. Traditional methods to examine statistical significance would miss such a difference. Moreover, it has been shown that investigating individually expressed genes often leads to different results when different scientists were studying the same biological system.

To address this problem in the context of big data, several statistical methods have emerged. Some examples include Over Representation Analysis (OSA) [44], Gene Set Enrichment Analysis (GSEA) [138] and GO-Bayes, a gene ontology based overrepresentation Bayesian analysis.

GSEA is a method of statistical analysis which evaluates high-throughput microarray data at the level of gene sets. These gene sets are assembled based on already published, widely accepted data on pathways or co-expression shown in previous experiments. GSEA can be used to compare samples belonging to two classes, in our case the (vitamin D) deficient phenotype (suffix “a”) and the phenotype after vitamin D substitution (suffix “b”). Based on their differential expression as assessed by any suitable metric between the two different classes, at first a *ranked gene list* was generated. For the second step, a *predefined gene set* is required, which includes biologically related genes (e.g. genes encoding products of the same

pathway or belonging to the same GO category). GSEA determines then if the members of the predefined gene set are randomly distributed throughout the ranked gene list, or primarily found at the top or at the bottom of the list. Gene sets whose distribution lies closely to a particular phenotype (top or bottom of the list) are considered to be related to the specific phenotype. The extent of the correlation with a specific phenotype is measured with the *enrichment score*. A level of significance for the enrichment score was calculated additionally by using permutation techniques. Finally, the estimated significance level is adjusted for multiple testing.

There are several tools provided online to be used for pathway analysis. GeneTrail is a web-based application developed at the Saarland University, which allows the identification of enriched functional categories within protein or gene sets. Both OSA and GSEA are available in the algorithm, as well as a novel dynamic-programming algorithm that improves the p-value computation of GSEA methods [10].

Our results based solely on the comparison of single genes before and after supplementation were at first sight quite sobering, because, after correction of the expression data for multiple testing, no significant dysregulation of a single gene could be found. This result implies that a direct effect of supplementation in vitamin D deficient individuals on the NK-cell transcript is limited. However, the main reason for this result is certainly the small number of subjects included in the study of only eight people, leading inevitably to statistically extremely weak outcomes. Therefore, the problem of a "large P" combined with a "small N" had a strong impact as referred before (4.2.2, page 47). Thus, it can still be assumed that the expression differences, irrespective of the extent of their statistical significance have a certain relevance for the increase in NK-cell activity after vitamin D supplementation. With this in mind, a number of mechanisms seem relevant of discussion.

5.2 ALTERED CYTOKINE - mRNA PROFILE AFTER VITAMIN D SUPPLEMENTATION

The *IFG* gene, which encodes **IFN- γ** , was shown to be downregulated after vitamin D supplementation, with this effect being of particular magnitude in male subjects. IFN- γ modulates the immune response, in particular against intracellular bacteria, viruses and tumor cells. It is secreted by NK cells, NKT cells, cytotoxic CD8+ T cells and Th1 CD4+ T cells. Although its effect on cells on the immune system include stimulating Th1 differentiation, promoting leukocyte chemotaxis and enhancing macrophage functions [112]. IFN- γ also plays a central role in chemotaxis of NK cells in tumors and their accumulation at the site of infection or in the tumor [111,157], and intratumoral NK cell accumulation is positively associated with

improved survival in some cancer types, for example in colon cancer [37]. Additionally, IFN- γ leads to ICAM-1 upregulation on the target cell which facilitates NK cell binding to the target cell [154].

On the other hand, tumor cells overexpress inhibitory ligands like PD-L1, CD95 (FasR), and CD270 (HVEM) in the presence of IFN- γ , which may reduce T-cell responsiveness [6]. Moreover, increased IFN- γ levels also lead to stronger expression of MHC-I molecules on target cells. However, MHC-class I molecules are also inhibitory ligands for NK cells. Thus, when expressed on cells targeted by NK cells, for instance tumors, MHC-I molecules could lead to reduced NK cell-mediated killing. In fact, in vitro experiments have shown that in some tumors, the presence of IFN- γ leads to decreased NK cell-mediated tumor lysis. Specifically, leukemia and lymphoma cell lines appear to be protected from NK-cell activity in the presence of IFN- γ [6]. In this context, the downregulation IFN- γ is consistent with the finding of increased NK-cell-mediated ADCC in vitro against the lymphoma cell line DAUDI.

Another cytokine axis appears to be affected by vitamin D supplementation. IL-2 has been linked to NK-cell activation as early as 1981 [54]. The IL-2 receptor (IL-2R) is composed of three subunits α (CD25), β (CD122), and γ (CD132) [163]. The gene encoding the **β -chain of the IL-2 receptor** (CD122) was shown to be upregulated. Thus, vitamin D could be involved in priming NK cells for activation. At this point it must be emphasized, that the NK cells used in this study were not pretreated with IL-2. Lastly, another gene which has been shown to suppress IL-2 production in T cells, ***NFATC4***, was downregulated after vitamin D substitution. Thus, both the upregulation of CD122 and the weaker expression of *NFATC4* are consistent with an increased NK cell/ADCC activity after vitamin D administration.

Moreover, the receptor of another cytokine, the **IL-17 receptor** was also shown to be upregulated. IL-17 is linked to a rise in circulating NK cells and an increased expression of perforin and granzymes and cytolytic function [4]. As with the cytokines and their receptors mentioned above, the increased expression of IL-17R by vitamin D in the context of its described functions can also explain an increased NK-cell/ADCC activity.

The role of **type I** and **type III interferons** and their regulatory axes, however, are even more important. Several interferons of these gene families are upregulated in our experiment. In addition to various genes encoding IFN- α isoforms (*IFNA2*, *IFNA4*, *IFNA6*, *IFNA7*, and *IFNA10*) also *IFNL3* (encoding IFN- λ 3). Although the expression of these individual genes does not vary statistically significantly after supplementation, the cumulative expression differences of the respective gene families are significant. This also applies to the individual genes combined in pathways involved in different immune responses.

Type I interferons are cytokines which play a role in host defense against viruses but also in clearance of malignant cells. Type I interferons includes 14 IFN- α subtypes, IFN- β , IFN- κ , IFN-

ϵ , as well as IFN- ω . They can be produced by most human cells through PRR recognition such as TLRs. Downstream signaling is mediated by IFNAR inducing STAT1/2 and IRF9 activation. The latter form a complex called interferon-stimulated gene factor 3 or ISGF3 [104],[170]. In IFNAR-knockout mice, incapable of IFN- α signaling, lower NK-cell numbers were observed as well as reduced NK-cell-mediated cytotoxicity and consequently increased susceptibility to fibrosarcoma and lymphoma [104]. Beyond that IFN- α also stimulates DCs to produce IL-15 which promotes NK-cell development, proliferation, and function.

The type III interferon family includes four members: IFN- λ 1 (IL-29), IFN- λ 2 (IL-28A), IFN- λ 3 (IL-28B), and IFN- λ 4. Their signals are transmitted via the IFN-L receptor, which in turn activates ISGF3, similar to type I interferons. Thus, they not only influence NK-cell responses against viruses, but also play an important role in NK-cell-mediated tumor surveillance. IFN- λ enhances T- and NK-cell responses against tumors like melanoma, lung cancer, and breast cancer. *IFNLR1*^{-/-} NK cells have reduced tumor suppressing capacity in vivo [83]. Hence, an increased expression of IFN- α subtypes and IFN- λ 3 may again explain the increased rituximab-mediated NK-cell cytotoxicity after vitamin D substitution in deficient individuals.

5.3 ALTERED PATHWAYS AFTER VITAMIN D SUPPLEMENTATION

Downstream signaling upon IL-2R activation involves the **MAPK pathway** [33]. This pathway is important for mediation of intracellular activation signals in NK cells and encompasses three kinase families: ERK, p38, and JNK [127]. A gene encoding one of the components of the JNK family, **MAP4K1**, was found to be upregulated after taking vitamin D. This kinase family is required for NKG2D-mediated NK-cell activation [85]. However, the NK-cell-mediated ADCC is described as being specifically mediated by the P38 and ERK families [146], whose members not have been affected by vitamin D in our experiments. The vitamin D-induced increased expression of MAP4K1 from the JNK family may explain the increased natural NK-cell activity after supplementation. However, the equally increased ADCC activity of NK cells after vitamin D ingestion would be more consistent with an increased expression of members of the P38 or ERK families. However, it remains to be clarified whether MAP4K1/NKG2D-mediated NK-cell activation has a higher priority compared to ADCC signaling.

Even if for most humans in our geographical latitudes particularly over the winter and spring months a vitamin D undersupply or even a more or less complete deficiency is considered as normal, the question remains, how our immune system evolutionarily adapted itself to this chronic undersupply and/or to this deficiency. Apart from a significant increase in influenza infections, some of which are serious, and clinically hardly relevant flu infections of the respiratory tract, there are hardly any other seasonal infections worth mentioning during this

period. However, both the incidence of cancer and cancer associated mortality are increased during the winter. This observation has been associated with the seasonal variation of vitamin D levels [102].

The results of this study show for the first time an option how NK cells can compensate the **IFN pathways of type I and III**, which are weakened under vitamin D deficiency. The secretion of these cytokines, which are essential for NK-cell activity, is also regulated by **toll-like receptor-mediated signals** [53]. Thus, the stimulation of TLR5 induces the synthesis of IFN-I [166]. Increased expression of different TLRs (such as TLR2, TLR5, TLR7 and TLR8) in vitamin D undersupply or deficiency increases the signal flow via these receptors and thus can compensate for the "simultaneous" weaker expression of the IFN-I/III pathway. The MAPK pathway described above is also associated with TLR activation and cytokine production [118]. It is just as contracyclical of vitamin D as the TLR pathway. If vitamin D deficiency is compensated, in our study by in vivo supplementation with Dekristol™ or by increasing the body's own synthesis during summer, compensation of the synthesis of type I and III interferons is no longer necessary. The expression of the corresponding pathways of TLR and MAPK are reduced.

The downregulation of the **ubiquitin-ligase pathways** is of particular biological significance in the context of the changes observed so far. High quality data support the fact that genetic deletion or inhibition of the E3 ubiquitin-ligase casitas B-lineage lymphoma-b (Cbl-b) unleashes the antitumor potential of NK cells leading to control of tumor metastatic spread in mice [94]. Other E3 ligases have also been shown to inhibit NK-cell functions [42]. Kaposi's sarcoma-associated herpesviruses encoding E3 ubiquitin-ligases are able to evade NK-cell activity [143]. Others have suggested an interaction of KIRs and ubiquitin ligases in NK-cell inhibition [100]. Ubiquitin-ligases does not only play a role in inhibiting the NK cells in general, but also specifically in regulating the TLR/IFN axis. Ubiquitin ligases have been shown to inhibit TLR signaling of the nuclear factor (NF)-kB [29], and their knockdown led to higher levels of proinflammatory cytokines in an animal model via the TLR/IL-1R/TRAF6 pathway [168]. Production of IFN- α upon TLR stimulation is known to depend on the formation of a complex consisting of MyD88, IRF7, and TRAF6 as well as TRAF6-dependent ubiquitination [70]. Others inhibit type I IFN secretion through IRF3 and IRF7 ubiquitination [164] or through inhibition of retinoic acid-inducible gene I (*RIG-I*) and TRIM25 [58].

One connected pattern becomes apparent: the ubiquitin-ligase pathway, a negative regulator of type I interferon synthesis, becomes downregulated after supplementation with vitamin D leading to increased IFN- α production. The overexpression of TLRs in the vitamin D deficient state could be explained as a compensatory mechanism of the downstream suppression of the type I interferon production pathway caused by the excessive ubiquitin-ligase activity (**Figure 28**).

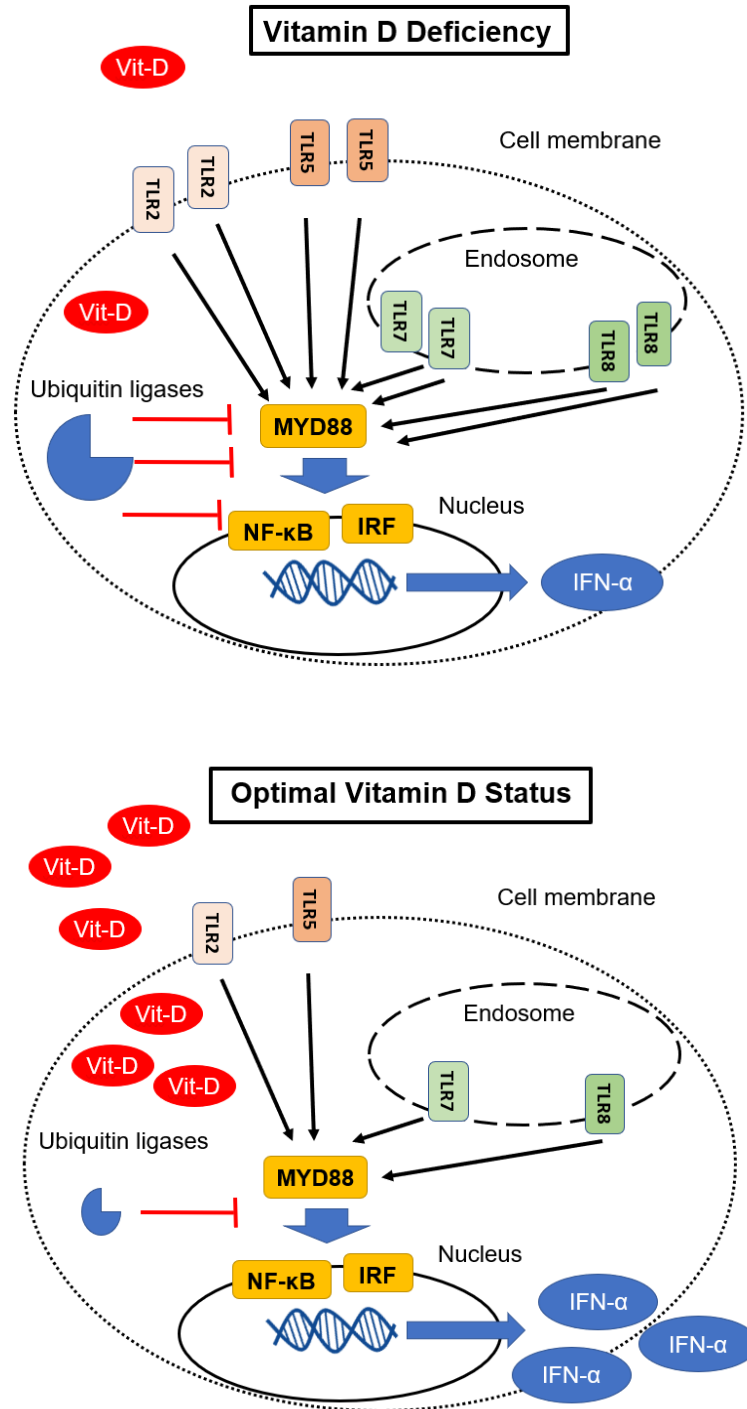


Figure 28: Proposed model of effect of vitamin D deficiency and supplementation on NK cells

In the state of vitamin D deficiency signaling pathways leading to IFN- α production are reduced due to an increased activity of the ubiquitin-ligase system. This leads to an overexpression of toll-like receptors. Once vitamin D levels are restored, the ubiquitin system is downregulated and therefore IFN- α production is restored. Compensatory toll-like receptor overexpression is no longer necessary and thus gene expression is reduced. (TLR: Toll-like receptor, IFN: interferon).

5.4 INDIRECT INFLUENCE OF VITAMIN D ON NK CELLS

Another approach to explain the changes observed in the NK-cell mRNA profile after vitamin D supplementation would be, if it is not the NK cells themselves which are direct targets of vitamin D, but another, “mediator” cell, like macrophages or DCs, which in turn directly influence the NK cells. The effect of $1,25(\text{OH})_2\text{D}_3$ on monocytes/macrophages is well established and described in detail in section 2.2.7 on page 12. This assumption is further supported by the fact that some of the genes/gene sets appearing to be dysregulated have no known role in NK cells, for example the $\text{Fc}\epsilon\text{RI}$ pathway, the *C1orf147* gene as well as other genes like *PSMC6*, *SRSF1*, *SLPI*, *VAMP2*, *CCR10*, and *PADI4*. Supportive of this notion, a comparison of our data set with known vitamin D-responsive genes in monocytes revealed several genes that are dysregulated in our experiment as well: The *COQ3*, *DENND6B*, *EPB41L1* and *ITGAM* genes [107].

Depending on the target cell, vitamin D also unfolds different immunomodulatory effects [12]. In vitro incubation with $1,25(\text{OH})_2\text{D}_3$ leads to reduced maturation of DCs and inhibits their capacity to express co-stimulatory molecules leading to reduced capacity of the DCs to activate T cells, as determined by decreased proliferation and IFN- γ secretion in mixed leukocyte cultures [115]. Other studies have also demonstrated lower TLR4 expression on the NK-cell surface as well as decreased TNF- α and IFN- γ production in NK cells after in vitro incubation with $1,25(\text{OH})_2\text{D}_3$. A direct effect of $1,25(\text{OH})_2\text{D}_3$ through NF- κB phosphorylation was postulated as mechanism behind these findings [110]. In addition, these expression changes induced by substitution in vitro are consistent with those in our study after in vivo supplementation. Thus, our findings of downregulation of pathways such as “activation of immune response”, “complement,” “interferon gamma response”, and “leukocyte chemotaxis” can also be interpreted in the context of the immunomodulatory/-suppressive function of vitamin D.

5.5 ROLE OF SEXUAL DIMORPHISM

The immune system of female and male mammals has been shown to have well defined differences, a phenomenon called sexual dimorphism. Females recover better from infections, sepsis and trauma than males [171]. This is due to the fact that they are able to mount more efficient immune response [99]. It is therefore not surprising that they also suffer more frequently from autoimmune diseases [16]. Furthermore, not only do men have a higher incidence of cancer, but the survival rate is lower in men than in women with the same cancer [36]. The female immune system is more effective than the male immune system and this is reflected in higher serum levels of IgM and IgG immunoglobulins and enhanced humoral and

cell-mediated immune responses [48]. A study comparing NK-cell activation in elderly men and women found higher ratios of immature CD56^{bright} to mature CD56^{dim} NK cells, increased IFN- γ response, and enhanced cytotoxic granule responses to K562 leukemia cells in elderly females [3]. Next to social, occupational, and behavioral factors, there are also well defined differences on molecular and cellular level which can explain sexual dimorphism.

First, sex hormones directly influence different effector cells. Estrogen exposure has been linked to increased IgG/IgM production in B lymphocytes and in other studies to increased IFN- γ and IL-2 production in T cells. Similarly, IL-6 secretion is stimulated in dendritic cells but halted in monocytes by estrogen. In NK cells, several studies have demonstrated a dose dependent effect of estrogens with high dose rates lead to suppression of NK-cell activity [109].

Another important aspect are chromosomal differences between both sexes. Thus, males possess a unique set of genes on the Y-chromosome. On the other hand, some genes on the second X-chromosome in females may escape inactivation which results in an increased expression of the respective gene(s) [116]. Two of these genes are *TLR7* and *TLR8*. Their higher expression in females has been explained by incomplete X inactivation [113]. As a result, higher IFN- α levels have been shown in female-derived PBMCs compared to males [18].

In our experiment, higher expression of the *JPX* gene could be demonstrated after vitamin D substitution in females. *JPX* (*Xist*) is a long non-coding RNA which is located on the X-inactivation center and is involved in X-chromosome inactivation in female mammals [141]. This could lead to inactivation of previously active areas on the second X-chromosome. As it was demonstrated before, *TLR7* mRNA levels were also lower in our experiments after supplementation of vitamin D in vivo. *TLR8*, which is also expressed on the X-chromosome was similarly downregulated after vitamin D substitution. This effect was more significant in female subjects. This demonstrates a clear pattern: Vitamin D supplementation restores epigenetic control over the X-inactivation center through increased *JPX* expression in females and leads to reduced *TLR7/8* expression. This would argue for a staggered influence of vitamin D on gene expression: Target genes whose expression is directly influenced by vitamin D and then downstream genes whose expression is indirectly regulated by the primary vitamin D targets. Sexual dimorphism cannot however account for the full extent of the changes observed in our experiment. *TLR2* and *TLR5* are located on chromosomes 4 and 1 respectively, and a mechanism which involves X-chromosome-dependent regulation could not be identified until now.

One other sex-specific gene with vitamin D dependency was highlighted in our experiment: *RPS4Y1*, located on the Y-chromosome. Its expression in males was reduced after vitamin D supplementation. It encodes along with *RPS4X* the ribosomal protein S4, which is the only

ribosomal protein to be encoded by two genes [172]. In contrast to our results, a recent randomized controlled double-blind clinical trial looking at the effect of vitamin D supplementation on buffy coat gene expression demonstrated overexpression for the Y-linked *RPS4Y1* gene after supplementation [128]. In addition to the overexpression of *RPS4Y1* after vitamin D treatment, Shirvani's study also found significantly altered expression in more than 1,000 additional whole genome genes with an increasing trend under continued supplementation. The reason for this, as a start, contradictory result, is quite certainly that in this study the *PBMC* of the test persons were examined. That means that apart from the NK cells, whose portion of the *PBMC* amounts to approx. 5 %, also monocytes and lymphocytes, e. g. T cells (CD4 and CD8) and B cells, were under the influence of Vitamin D. Thus, in the study by Shirvani et al. one or more of these non-NK populations were responsible not only for the overexpression of *RSP4Y1* but also for the principally higher genome wide vitamin D sensitivity. In this respect, the results of Shirvani et al. support the above described assumption that the influence of vitamin D on NK cells is (also) indirectly mediated via other cells that are under a more stringent influence of vitamin D, and that not all genes are affected to the same extent (chapter 5.4, page 89). Another difference between our study and that of Shirvani et al. is that Shirvani and colleagues used a protocol for vitamin D supplementation that was quite different in terms of dose and schedule. Thus, the average of about 30 ng/ml 25-OH(D) in serum was achieved by application of a low dose of cholecalciferol over several weeks. This resulted in a significantly longer response time for the vitamin D sensitive cells. To achieve mean normal serum levels of approximately 65 ng/ml 25-OH(D) within two weeks we administered up to 100,000 I. U. cholecalciferol over only 5-6 days with a further 4-5 days adaptation period (chapter 3.1.3, page 15). It is possible, that a longer lasting influence of appropriate vitamin D levels on NK cells would enhance the rather subtle effects we observed in our study.

5.6 VITAMIN D IN THE CONTEXT OF AUTOIMMUNITY AND CHRONIC INFLAMMATION

Next, the relation between vitamin D deficiency and autoimmunity / chronic inflammation has to be discussed in the context of our findings. Vitamin D deficiency has been linked in epidemiological studies with increased incidence of autoimmune diseases like diabetes mellitus type I, systemic lupus erythematosus (SLE), multiple sclerosis, inflammatory bowel disease, and rheumatoid arthritis [12]. Specifically in SLE the overactivation of the TLR/IFN- α/β axis has been given pathophysiological importance [13]. However, as in other trials, supplementation did not lead consistently to better disease control, although higher doses have been postulated to have better outcomes [59]. Chronic inflammation has been linked to

atherosclerosis, and TLR4 or MyD88 knockout protected mice from atherosclerosis [101]. This last quoted association between TLR4 knock out and a reduced incidence of atherosclerosis is consistent with the result of our study showing a significantly reduced TLR expression after vitamin D supplementation and the finding that chronic inflammation/autoimmunity is associated with vitamin D deficiency. Another, alternative hypothesis arises around the overexpression of TLR receptors in the vitamin D deficient state (which is per definition the “pathological” state): Their high expression contributes to a state of immune “overreaction” and predisposes to autoimmunity. This pathological “overexpression” is corrected after vitamin D serum concentration is restored to the physiological/normal level.

5.7 CRITICAL VIEW AND OUTLOOK

Our study also reveals some weak points that probably had an impact on the results. It has been repeatedly described before that a combination of a large number of investigated objects (in our case transcripts) in investigations of only a small cohort of test subjects, the so-called “large P/small N” situation, significantly strains the statistical significance of the results thus determined. However, it is difficult to recruit a larger number of volunteers from the immediate environment who are willing to participate in intervention studies. In addition, a vitamin D deficiency is limited to the few winter months only. As described in chapter 4.2.1, page 41, after supplementation only a very small number of the total 40,716 transcripts have an altered expression and, moreover, mostly concerning genes that are located in a suitable immunological context. Only after stringent correction for multiple testing, the p-values increased above 0.05. And the pathways mentioned above showed a significantly altered expression compared to the deficiency state, even after final stringent correction.

There is still another point that also must be discussed critically. Namely that we used resting NK cells for RNA extraction. It is well established that in vitro cytokine activation of NK cells has consequences on their phenotype, cytokine expression profile, and most importantly on their transcriptome [25]. It can therefore be assumed that some changes at the transcriptional level in the NK cells of our study after vitamin D treatment were too weak to be classified as significant. Other changes probably even remained entirely undetected. Possibly, the vitamin D-induced transcriptome alteration in NK cells would have been more significant after activation on their target cells before as well as after supplementation. The microarray used in this study provided broad transcriptome coverage. Thus, we refrained from additional testing for expression of receptors on the NK-cell surface or analysis of cytokine levels. We assumed that an increase/decrease in protein production is reflected in the transcribed mRNA levels. It is possible, that effects induced by RNA molecules with very small half-life, such as small interfering RNA (siRNA), would be missed by this approach. The observed changes in

ubiquitin-ligase complex mRNA expression allows us to assume changes in the post-translational modification after vitamin D supplementation, however our RNA-based approach does not allow further examination.

In genome wide expression studies which involve a large number of genes, a number of false positive results must always be expected. These may be reflected in some of the genes/pathways mentioned above (chapter 5.4, page 89) like the *FcεRI* pathway, which, under biological aspects, seem to fall out of context.

Despite of these limitations, this study showed at which points or via which pathways vitamin D can influence the activity of NK cells or safely does so. This results in possible starting points on which further investigations of this question should focus. For instance, it would be interesting to examine if the effect of increased NK cell-mediated ADCC after vitamin D supplementation is inhibited in the presence of IFN- α or IFN- λ antibodies. Furthermore, interference studies with siRNA targeting different TLRs or E3 ubiquitin-ligase genes could shed more light into the effect of vitamin D on NK-cell cytotoxicity.

5.8 CONCLUSION

To summarize, this study shows that vitamin D supplementation has an effect on the transcriptome of resting NK cells, but this effect was rather small. The results indicate the involvement of the TLR/IFN- α / λ axis and its regulation through the ubiquitin-ligase system. Furthermore, we demonstrate that differences in TLR expression are to some extent sex-specific and imply a role for vitamin D in *JPX*-mediated X chromosome deactivation. Immunomodulatory and immunosuppressive effects are also observed. It is also probable, that vitamin D does not exert its main effect on the NK cells directly, but the effect could be mediated through other regulatory cells such as DCs or macrophages.

6 REFERENCES

1. Adib-Conquy M, Scott-Algara D, Cavaillon JM, Souza-Fonseca-Guimaraes F (2014) TLR-mediated activation of NK cells and their role in bacterial/viral immune responses in mammals. *Immunol Cell Biol* 92:256–262
2. Ahlgrim M, Pfreundschuh M, Kreuz M, Regitz E, Preuss KD, Bittenbring J (2011) The impact of Fc- γ receptor polymorphisms in elderly patients with diffuse large B-cell lymphoma treated with CHOP with or without rituximab. *Blood* 118:4657–4662
3. Al-Attar A, Presnell SR, Peterson CA, Thomas DT, Lutz CT (2016) The effect of sex on immune cells in healthy aging: Elderly women have more robust natural killer lymphocytes than do elderly men. *Mech Ageing Dev* 156:25–33
4. Al Omar S, Flanagan BF, Almeahmadi M, Christmas SE (2013) The effects of IL-17 upon human natural killer cells. *Cytokine* 62:123–130
5. Anfossi N, André P, Guia S, Falk CS, Roetynck S, Stewart CA, Bresó V, Frassati C, Reviron D, Middleton D, Romagné F, Ugolini S, Vivier E (2006) Human NK cell education by inhibitory receptors for MHC class I. *Immunity* 25:331–42
6. Aquino-López A, Senyukov V V., Vlasic Z, Kleinerman ES, Lee DA (2017) Interferon gamma induces changes in Natural Killer (NK) cell ligand expression and alters NK cell-mediated lysis of pediatric cancer cell lines. *Front Immunol* 8:
7. Ardley HC, Robinson PA (2005) E3 ubiquitin ligases. *Essays Biochem* 41:15–30
8. Arnould L, Gelly M, Penault-Llorca F, Benoit L, Bonnetain F, Migeon C, Cabaret V, Fermeaux V, Bertheau P, Garnier J, Jeannin JF, Coudert B (2006) Trastuzumab-based treatment of HER2-positive breast cancer: An antibody-dependent cellular cytotoxicity mechanism? *Br J Cancer* 94:259–267
9. Ashburner M, Ball CA, Blake JA, Botstein D, Butler H, Cherry JM, Davis AP, Dolinski K, Dwight SS, Eppig JT, Harris MA, Hill DP, Issel-Tarver L, Kasarskis A, Lewis S, Matese JC, Richardson JE, Ringwald M, Rubin GM, Sherlock G (2000) Gene ontology: Tool for the unification of biology. *Nat Genet* 25:25–29
10. Backes C, Keller A, Kuentzer J, Kneissl B, Comtesse N, Elnakady YA, Müller R, Meese E, Lenhof H-P (2007) GeneTrail--advanced gene set enrichment analysis. *Nucleic Acids Res* 35:W186-92
11. Badolato R, Prandini A, Caracciolo S, Colombo F, Tabellini G, Giacomelli M, Cantarini ME, Pession A, Bell CJ, Dinwiddie DL, Miller NA, Hateley SL, Saunders CJ, Zhang L,

- Schroth GP, Plebani A, Parolini S, Kingsmore SF (2012) Exome sequencing reveals a pallidin mutation in a Hermansky-Pudlak-like primary immunodeficiency syndrome. *Blood* 119:3185–3187
12. Baeke F, Takiishi T, Korf H, Gysemans C, Mathieu C (2010) Vitamin D: Modulator of the immune system. *Curr Opin Pharmacol* 10:482–496
 13. Banchereau J, Pascual V (2006) Type I Interferon in Systemic Lupus Erythematosus and Other Autoimmune Diseases. *Immunity* 25:383–392
 14. Bartel Y, Bauer B, Steinle A (2013) Modulation of NK cell function by genetically coupled C-type lectin-like receptor/ligand pairs encoded in the human natural killer gene complex. *Front Immunol* 4:362
 15. Bauernfeind F, Ablasser A, Kim S, Bartok E, Hornung V (2010) RNA Biology An unexpected role for RNA in the recognition of DNA by the innate immune system.
 16. Beeson PB (1994) Age and sex associations of 40 autoimmune diseases. *Am J Med* 96:457–462
 17. Bendelac A, Savage PB, Teyton L (2007) The Biology of NKT Cells. *Annu Rev Immunol* 25:297–336
 18. Berghöfer B, Frommer T, Haley G, Fink L, Bein G, Hackstein H (2006) TLR7 Ligands Induce Higher IFN- α Production in Females. *J Immunol* 177:2088–2096
 19. Bischoff-Ferrari HA, Willett WC, Orav EJ, Oray EJ, Lips P, Meunier PJ, Lyons RA, Flicker L, Wark J, Jackson RD, Cauley JA, Meyer HE, Pfeifer M, Sanders KM, Stähelin HB, Theiler R, Dawson-Hughes B (2012) A pooled analysis of vitamin D dose requirements for fracture prevention. *N Engl J Med* 367:40–9
 20. Bittenbring JT, Neumann F, Altmann B, Achenbach M, Reichrath J, Ziepert M, Geisel J, Regitz E, Held G, Pfreundschuh M (2014) Vitamin D deficiency impairs rituximab-mediated cellular cytotoxicity and outcome of patients with diffuse large B-cell lymphoma treated with but not without rituximab. *J Clin Oncol* 32:3242–3248
 21. Braud VM, Allan DSJ, O'callaghan CA, Söderström K, D'andrea A, Ogg GS, Lazetic S, Young NT, Bell JI, Phillips JH (1998) HLA-E binds to natural killer cell receptors CD94/NKG2A, B and C. *Nature* 391:795
 22. Brias SG, Marsden M, Forbester J, Clement M, Brandt C, Harcourt K, Kane L, Chapman L, Clare S, Humphreys IR (2018) Interferon lambda is required for interferon gamma-expressing NK cell responses but does not afford antiviral protection during acute and persistent murine cytomegalovirus infection. *PLoS One* 13:e0197596

23. Brosseron F, Marcus K, May C (2015) Isolating peripheral lymphocytes by density gradient centrifugation and magnetic cell sorting. Humana Press Inc.
24. Bruns H, Büttner M, Fabri M, Mougiakakos D, Bittenbring JT, Hoffmann MH, Beier F, Pasemann S, Jitschin R, Hofmann AD, Neumann F, Daniel C, Maurberger A, Kempkes B, Amann K, Mackensen A, Gerbitz A (2015) Vitamin D-dependent induction of cathelicidin in human macrophages results in cytotoxicity against high-grade B cell lymphoma. *Sci Transl Med* 7:
25. Bryceson YT, March ME, Ljunggren HG, Long EO (2006) Synergy among receptors on resting NK cells for the activation of natural cytotoxicity and cytokine secretion. *Blood* 107:159–166
26. Caligiuri MA (2008) Human natural killer cells. *Blood* 112:461–469
27. Carbon S, Douglass E, Dunn N, Good B, Harris NL, Lewis SE, Mungall CJ, Basu S, Chisholm RL, Dodson RJ, Hartline E, Fey P, Thomas PD, Albou LP, Ebert D, Kesling MJ, Mi H, Muruganujan A, Huang X, Poudel S, Mushayahama T, Hu JC, LaBonte SA, Siegele DA, Antonazzo G, Attrill H, Brown NH, Fexova S, Garapati P, Jones TEM, Marygold SJ, Millburn GH, Rey AJ, Trovisco V, Dos Santos G, Emmert DB, Falls K, Zhou P, Goodman JL, Strelets VB, Thurmond J, Courtot M, Osumi DS, Parkinson H, Roncaglia P, Acencio ML, Kuiper M, Lreid A, Logie C, Lovering RC, Huntley RP, Denny P, Campbell NH, Kramarz B, Acquaah V, Ahmad SH, Chen H, Rawson JH, Chibucos MC, Giglio M, Nadendla S, Tauber R, Duesbury MJ, Del NT, Meldal BHM, Perfetto L, Porras P, Orchard S, Shrivastava A, Xie Z, Chang HY, Finn RD, Mitchell AL, Rawlings ND, Richardson L, Sangrador-Vegas A, Blake JA, Christie KR, Dolan ME, Drabkin HJ, Hill DP, Ni L, Sitnikov D, Harris MA, Oliver SG, Rutherford K, Wood V, Hayles J, Bahler J, Lock A, Bolton ER, De Pons J, Dwinell M, Hayman GT, Laulederkind SJF, Shimoyama M, Tutaj M, Wang SJ, D'Eustachio P, Matthews L, Balhoff JP, Aleksander SA, Binkley G, Dunn BL, Cherry JM, Engel SR, Gondwe F, Karra K, MacPherson KA, Miyasato SR, Nash RS, Ng PC, Sheppard TK, Shrivatsav Vp A, Simison M, Skrzypek MS, Weng S, Wong ED, Feuermann M, Gaudet P, Bakker E, Berardini TZ, Reiser L, Subramaniam S, Huala E, Arighi C, Auchincloss A, Axelsen K, Argoud GP, Bateman A, Bely B, Blatter MC, Boutet E, Breuza L, Bridge A, Britto R, Bye-A-Jee H, Casals-Casas C, Coudert E, Estreicher A, Famiglietti L, Garmiri P, Georghiou G, Gos A, Gruaz-Gumowski N, Hatton-Ellis E, Hinz U, Hulo C, Ignatchenko A, Jungo F, Keller G, Laiho K, Lemercier P, Lieberherr D, Lussi Y, Mac-Dougall A, Magrane M, Martin MJ, Masson P, Natale DA, Hyka NN, Pedruzzi I, Pichler K, Poux S, Rivoire C, Rodriguez-Lopez M, Sawford T, Speretta E, Shypitsyna A, Stutz A, Sundaram S, Tognolli M, Tyagi N, Warner K, Zaru R, Wu C, Chan J, Cho J, Gao S,

- Grove C, Harrison MC, Howe K, Lee R, Mendel J, Muller HM, Raciti D, Van Auken K, Berriman M, Stein L, Sternberg PW, Howe D, Toro S, Westerfield M (2019) The Gene Ontology Resource: 20 years and still GOing strong. *Nucleic Acids Res* 47:D330–D338
28. Carla Bänziger, Davide Soldini, Corina Schütt, Peder Zipperlen, George Hausmann KB (2006) Wntless, a conserved membrane protein dedicated to the secretion of Wnt proteins from signaling cells. *Cell* 125:509–522
29. Carmody RJ, Ruan Q, Palmer S, Hilliard B, Chen YH (2007) Negative regulation of toll-like receptor signaling by NF- κ B p50 ubiquitination blockade. *Science* (80-) 317:675–678
30. Chalifour A, Jeannin P, Gauchat JF, Blaecke A, Malissard M, N'Guyen T, Thieblemont N, Delneste Y (2004) Direct bacterial protein PAMP recognition by human NK cells involves TLRs and triggers α -defensin production. *Blood* 104:1778–1783
31. Chapuy MC, Preziosi P, Maamer M, Arnaud S, Galan P, Hercberg S, Meunier PJ (1997) Prevalence of vitamin D insufficiency in an adult normal population. *Osteoporos Int* 7:439–443
32. Chitirala P, Ravichandran K, Galgano D, Sleiman M, Krause E, Bryceson YT, Rettig J (2019) Cytotoxic Granule Exocytosis From Human Cytotoxic T Lymphocytes Is Mediated by VAMP7. *Front Immunol* 10:1855
33. Choudhry H, Helmi N, Abdulaal WH, Zeyadi M, Zamzami MA, Wu W, Mahmoud MM, Warsi MK, Rasool M, Jamal MS (2018) Prospects of IL-2 in Cancer Immunotherapy. *Biomed Res Int* 2018:
34. Chung W-H, Hung S-I, Yang J-Y, Su S-C, Huang S-P, Wei C-Y, Chin S-W, Chiou C-C, Chu S-C, Ho H-C, Yang C-H, Lu C-F, Wu J-Y, Liao Y-D, Chen Y-T (2008) Granulysin is a key mediator for disseminated keratinocyte death in Stevens-Johnson syndrome and toxic epidermal necrolysis. *Nat Med* 14:1343
35. Clayberger C, Krensky AM (2003) Granulysin. *Curr Opin Immunol* 15:560–565
36. Clocchiatti A, Cora E, Zhang Y, Dotto GP (2016) Sexual dimorphism in cancer. *Nat Rev Cancer* 16:330–339
37. Coca S, Perez-Piqueras J, Martinez D, Colmenarejo A, Saez MA, Vallejo C, Martos JA, Moreno M (1997) The prognostic significance of intratumoral natural killer cells in patients with colorectal carcinoma. *Cancer* 79:2320–2328
38. Colaco S, Modi D (2018) Genetics of the human Y chromosome and its association

- with male infertility. *Reprod Biol Endocrinol* 16:14
39. Cooper MA, Fehniger TA, Caligiuri MA (2001) The biology of human natural killer-cell subsets. *Trends Immunol* 22:633–640
 40. Delgado M, Abad C, Martinez C, Juarranz M, Arranz A, Gomariz R, Leceta J (2002) Vasoactive intestinal peptide in the immune system: potential therapeutic role in inflammatory and autoimmune diseases. *J Mol Med* 80:16–24
 41. Dellabona P, Padovan E, Casorati G, Brockhaus M, Lanzavecchia A (1994) An invariant $\alpha 24\text{-j}\alpha\text{Q}/\nu\beta 11$ t cell receptor is expressed in all individuals by clonally expanded CD4–8–t cells. *J Exp Med* 180:1171–1176
 42. Dou Y, Xing J, Kong G, Wang G, Lou X, Xiao X, Vivier E, Li XC, Zhang Z (2019) Identification of the E3 Ligase TRIM29 as a Critical Checkpoint Regulator of NK Cell Functions. *J Immunol* 203:873–880
 43. Doumas S, Kolokotronis A, Stefanopoulos P (2005) Anti-inflammatory and antimicrobial roles of secretory leukocyte protease inhibitor. *Infect Immun* 73:1271–1274
 44. Drăghici S, Khatry P, Martins RP, Ostermeier GC, Krawetz SA (2003) Global functional profiling of gene expression. *Genomics* 81:98–104
 45. Eisen MB, Spellman PT, Brown PO, Botstein D (1998) Cluster analysis and display of genome-wide expression patterns. *Proc Natl Acad Sci U S A* 95:14863–14868
 46. Feldman EJ, Lancet JE, Kolitz JE, Ritchie EK, Roboz GJ, List AF, Allen SL, Asatiani E, Mayer LD, Swenson C, Louie AC (2011) First-In-Man Study of CPX-351: A Liposomal Carrier Containing Cytarabine and Daunorubicin in a Fixed 5:1 Molar Ratio for the Treatment of Relapsed and Refractory Acute Myeloid Leukemia. *J Clin Oncol* 29:979–985
 47. Filipe-Santos O, Bustamante J, Chappier A, Vogt G, de Beaucoudrey L, Feinberg J, Jouanguy E, Boisson-Dupuis S, Fieschi C, Picard C (2006) Inborn errors of IL-12/23- and IFN- γ -mediated immunity: molecular, cellular, and clinical features. Elsevier
 48. Gal-Oz ST, Maier B, Yoshida H, Seddu K, Elbaz N, Czysz C, Zuk O, Stranger BE, Ner-Gaon H, Shay T (2019) ImmGen report: sexual dimorphism in the immune system transcriptome. *Nat Commun* 10:1–14
 49. Godfrey DI, MacDonald HR, Kronenberg M, Smyth MJ, Van Kaer L (2004) NKT cells: What's in a name? *Nat Rev Immunol* 4:231–237

50. Grandclément C, Pick H, Vogel H, Held W (2016) NK Cells Respond to Haptens by the Activation of Calcium Permeable Plasma Membrane Channels. *PLoS One* 11:e0151031
51. Hamerman JA, Ogasawara K, Lanier LL (2005) NK cells in innate immunity. *Curr Opin Immunol* 17:29–35
52. Harari D, Tzahar E, Romano J, Shelly M, Pierce JH, Andrews GC, Yarden Y (1999) Neuregulin-4: A novel growth factor that acts through the ErbB-4 receptor tyrosine kinase. *Oncogene* 18:2681–2689
53. Hemann EA, Gale M, Savan R (2017) Interferon lambda genetics and biology in regulation of viral control. *Front Immunol* 8:
54. Henney CS, Kuribayashi K, Kern DE, Gillis S (1981) Interleukin-2 augments natural killer cell activity. *Nature* 291:335–338
55. Holick MF (2007) Vitamin D deficiency. *N Engl J Med* 357:266–281
56. Holt D, Ma X, Kundu N, Fulton A (2011) Prostaglandin E 2 (PGE 2) suppresses natural killer cell function primarily through the PGE 2 receptor EP4. *Cancer Immunol Immunother* 60:1577–1586
57. Huth TK, Staines D, Marshall-Gradisnik S (2016) ERK1/2, MEK1/2 and p38 downstream signalling molecules impaired in CD56dimCD16+ and CD56brightCD16dim/- natural killer cells in Chronic Fatigue Syndrome/Myalgic Encephalomyelitis patients. *J Transl Med* 14:97
58. Inn KS, Gack MU, Tokunaga F, Shi M, Wong LY, Iwai K, Jung JU (2011) Linear Ubiquitin Assembly Complex Negatively Regulates RIG-I- and TRIM25-Mediated Type I Interferon Induction. *Mol Cell* 41:354–365
59. Iruretagoyena M, Hirigoyen D, Naves R, Burgos PI (2015) Immune response modulation by Vitamin D: Role in systemic lupus erythematosus. *Front Immunol* 6:513
60. Iwasaki A, Medzhitov R (2004) Toll-like receptor control of the adaptive immune responses. *Nat Immunol* 5:987–995
61. Janda CY, Waghray D, Levin AM, Thomas C, Garcia KC (2012) Structural basis of Wnt recognition by frizzled. *Science* (80-) 336:59–64
62. Janelle V, Langlois MP, Tarrab E, Lapierre P, Poliquin L, Lamarre A (2014) Transient complement inhibition promotes a tumor-specific immune response through the implication of natural killer cells. *Cancer Immunol Res* 2:200–206

63. Janelle V, Lamarre A (2014) Role of the complement system in NK cell-mediated antitumor T-cell responses. *Oncoimmunology* 3:
64. Jiang K, Zhong B, Gilvary DL, Corliss BC, Vivier E, Hong-Geller E, Wei S, Djeu JY (2002) Syk Regulation of Phosphoinositide 3-Kinase-Dependent NK Cell Function. *J Immunol* 168:3155–3164
65. Johnson DE, O’Keefe RA, Grandis JR (2018) Targeting the IL-6/JAK/STAT3 signalling axis in cancer. *Nat Rev Clin Oncol* 15:234–248
66. Kägi D, Ledermann B, Bürki K, Seiler P, Odermatt B, Olsen KJ, Podack ER, Zinkernagel RM, Hengartner H (1994) Cytotoxicity mediated by T cells and natural killer cells is greatly impaired in perforin-deficient mice. *Nature* 369:31
67. Kahwati LC, Weber RP, Pan H, Gourlay M, LeBlanc E, Coker-Schwimmer M, Viswanathan M (2018) Vitamin D, Calcium, or Combined Supplementation for the Primary Prevention of Fractures in Community-Dwelling Adults: Evidence Report and Systematic Review for the US Preventive Services Task Force. *JAMA* 319:1600–1612
68. Kaminuma O, Kitamura N, Nishito Y, Nemoto S, Tatsumi H, Mori A, Hiroi T (2018) Downregulation of NFAT3 Due to Lack of T-Box Transcription Factor TBX5 Is Crucial for Cytokine Expression in T Cells. *J Immunol* 200:92–100
69. Kaspar AA, Okada S, Kumar J, Poulain FR, Drouvalakis KA, Kelekar A, Hanson DA, Kluck RM, Hitoshi Y, Johnson DE, Froelich CJ, Thompson CB, Newmeyer DD, Anel A, Clayberger C, Krensky AM (2001) A Distinct Pathway of Cell-Mediated Apoptosis Initiated by Granulysin. *J Immunol* 167:350–356
70. Kawai T, Sato S, Ishii KJ, Coban C, Hemmi H, Yamamoto M, Terai K, Matsuda M, Inoue J, Uematsu S, Takeuchi O, Akira S (2004) Interferon- α induction through Toll-like receptors involves a direct interaction of IRF7 with MyD88 and TRAF6. *Nat Immunol* 5:1061
71. Klemm S, Ruland J (2006) Inflammatory signal transduction from the Fc ϵ RI to NF- κ B. *Immunobiology* 211:815–820
72. Kling JC, Jordan MA, Pitt LA, Meiners J, Thanh-Tran T, Tran LS, Nguyen TTK, Mittal D, Villani R, Steptoe RJ, Khosrotehrani K, Berzins SP, Baxter AG, Godfrey DI, Blumenthal A (2018) Temporal regulation of natural killer T cell interferon gamma responses by β -catenin-dependent and-independent wnt signaling. *Front Immunol* 9:483
73. Koch J, Steinle A, Watzl C, Mandelboim O (2013) Activating natural cytotoxicity

- receptors of natural killer cells in cancer and infection. *Trends Immunol* 34:182–191
74. Konjević G, Vuletić A, Martinović KM, Džodić R (2017) The Role of Activating and Inhibitory NK Cell Receptors in Antitumor Immune Response. InTechURL: <http://dx.doi.org/10.5772/intechopen.69729>
75. Krämer B, Sastre Turrión B, Glässner A, Wolter F, Kokordelis P, Eisenhardt M, Nischalke H, Strassburg C, Spengler U, Nattermann J (2014) TLR-activated monocytes express IFN-lambda receptor 1 and trigger IFN-gamma secretion of NK cells after stimulation with IFN-lambda. *Z Gastroenterol* 52:KG067
76. Kuijpers TW, Van Lier RA, Hamann D, de Boer M, Thung LY, Weening RS, Verhoeven AJ, Roos D (1997) Leukocyte adhesion deficiency type 1 (LAD-1)/variant. A novel immunodeficiency syndrome characterized by dysfunctional beta2 integrins. *J Clin Invest* 100:1725–1733
77. Kurai J, Chikumi H, Hashimoto K, Yamaguchi K, Yamasaki A, Sako T, Touge H, Makino H, Takata M, Miyata M, Nakamoto M, Burioka N, Shimizu E (2007) Antibody-dependent cellular cytotoxicity mediated by cetuximab against lung cancer cell lines. *Clin Cancer Res* 13:1552–1561
78. Lang R, Raffi FAM (2019) Dual-specificity phosphatases in immunity and infection: An update. *Int J Mol Sci* 20:
79. Lanier LL (1998) NK cell receptors. *Annu Rev Immunol* 16:359–393
80. Lanier TJ, Schall RD, Berahovich NL, Lai Z, Wei LL (2020) Chemokine Receptor Expression Evidence for NK Cell Subsets Based on.
81. Latinovic-Golic S, Walch M, Sundstrom H, Dumrese C, Groscurth P, Ziegler U (2007) Expression, processing and transcriptional regulation of granulysin in short-term activated human lymphocytes. *BMC Immunol* 8:9
82. Law RH, Lukoyanova N, Voskoboinik I, Caradoc-Davies TT, Baran K, Dunstone MA, D'Angelo ME, Orlova E V, Coulibaly F, Verschoor S, Browne KA, Ciccone A, Kuiper MJ, Bird PI, Trapani JA, Saibil HR, Whisstock JC (2010) The structural basis for membrane binding and pore formation by lymphocyte perforin. *Nature* 468:447–451
83. Lazear HM, Schoggins JW, Diamond MS (2019) Shared and Distinct Functions of Type I and Type III Interferons. *Immunity* 50:907–923
84. Lee N, Llano M, Carretero M, Akiko-Ishitani, Navarro F, López-Botet M, Geraghty DE (1998) HLA-E is a major ligand for the natural killer inhibitory receptor CD94/NKG2A. *Proc Natl Acad Sci U S A* 95:5199–5204

85. Li C, Ge B, Nicotra M, Stern JNH, Kopcow HD, Chen X, Strominger JL (2008) JNK MAP kinase activation is required for MTOC and granule polarization in NKG2D-mediated NK cell cytotoxicity. *Proc Natl Acad Sci U S A* 105:3017–3022
86. Li H, Ivarsson MA, Walker-Sperling VE, Subleski J, Johnson JK, Wright PW, Carrington M, Björkström NK, McVicar DW, Anderson SK (2018) Identification of an elaborate NK-specific system regulating HLA-C expression. *PLOS Genet* 14:e1007163
87. Liao Y, Goraya MU, Yuan X, Zhang B, Chiu SH, Chen JL (2019) Functional involvement of interferon-inducible transmembrane proteins in antiviral immunity. *Front Microbiol* 10:1097
88. Liberzon A, Birger C, Thorvaldsdóttir H, Ghandi M, Mesirov JP, Tamayo P (2015) The Molecular Signatures Database Hallmark Gene Set Collection. *Cell Syst* 1:417–425
89. Lips P (2006) Vitamin D physiology. *Prog Biophys Mol Biol* 92:4–8
90. Liu PT, Stenger S, Li H, Wenzel L, Tan BH, Krutzik SR, Ochoa MT, Schaubert J, Wu K, Meinken C, Kamen DL, Wagner M, Bals R, Steinmeyer A, Zügel U, Gallo RL, Eisenberg D, Hewison M, Hollis BW, Adams JS, Bloom BR, Modlin RL (2006) Toll-like receptor triggering of a vitamin D-mediated human antimicrobial response. *Science* (80-) 311:1770–1773
91. Liu Y, Zhang W (2008) Identification of a new transmembrane adaptor protein that constitutively binds Grb2 in B cells. *J Leukoc Biol* 84:842–51
92. Lohse M, Nunes-Nesi A, Kruger P, Nagel A, Hannemann J, Giorgi FM, Childs L, Osorio S, Walther D, Selbig J, Sreenivasulu N, Stitt M, Fernie AR, Usadel B (2010) Robin: An intuitive wizard application for R-based expression microarray quality assessment and analysis. *Plant Physiol* 153:642–651
93. Lohse M, Bolger AM, Nagel A, Fernie AR, Lunn JE, Stitt M, Usadel B (2012) RobiNA: a user-friendly, integrated software solution for RNA-Seq-based transcriptomics. *Nucleic Acids Res* 40:W622–W627
94. Lokody I (2014) Signalling: Loss of Cbl-b unleashes anti-metastatic natural killer cells. *Nat Rev Cancer* 14:218
95. Long EO (2007) Ready for prime time: NK cell priming by dendritic cells. *Immunity* 26:385–7
96. Maher SG, Romero-Weaver AL, Scarzello AJ, Gamero AM (2007) Interferon: cellular executioner or white knight? *Curr Med Chem* 14:1279–1289

97. Malki A, Fiedler J, Fricke K, Ballweg I, Pfaffl MW, Krautwurst D (2015) Class I odorant receptors, TAS1R and TAS2R taste receptors, are markers for subpopulations of circulating leukocytes. *J Leukoc Biol* 97:533–545
98. Mariani E, Ravaglia G, Forti P, Meneghetti A, Tarozzi A, Maioli F, Boschi F, Pratelli L, Pizzoferrato A, Piras F, Facchini A (1999) Vitamin D, thyroid hormones and muscle mass influence natural killer (NK) innate immunity in healthy nonagenarians and centenarians. *Clin Exp Immunol* 116:19–27
99. Markle JG, Fish EN (2014) Sex matters in immunity. *Trends Immunol* 35:97–104
100. Matalon O, Barda-Saad M (2016) Cbl ubiquitin ligases mediate the inhibition of natural killer cell activity. *Commun Integr Biol* 9:
101. Michelsen KS, Wong MH, Shah PK, Zhang W, Yano J, Doherty TM, Akira S, Rajavashisth TB, Arditi M (2004) Lack of toll-like receptor 4 or myeloid differentiation factor 88 reduces atherosclerosis and alters plaque phenotype in mice deficient in apolipoprotein E. *Proc Natl Acad Sci U S A* 101:10679–10684
102. Moan J, Lagunova Z, Bruland Ø, Juzeniene A (2010) Seasonal variations of cancer incidence and prognosis. *Dermatoendocrinol* 2:55–57
103. Müller C, Kägi D, Aebischer T, Odermatt B, Held W, Podack ER, Zinkernagel RM, Hengartner H (1989) Detection of perforin and granzyme A mRNA in infiltrating cells during infection of mice with lymphocytic choriomeningitis virus. *Eur J Immunol* 19:1253–1259
104. Müller L, Aigner P, Stoiber D (2017) Type I interferons and natural killer cell regulation in cancer. *Front Immunol* 8:
105. Neumann F, Acker F, Schormann C, Pfreundschuh M, Bittenbring JT (2018) Determination of optimum vitamin D3 levels for NK cell-mediated rituximab- and obinutuzumab-dependent cellular cytotoxicity. *Cancer Immunol Immunother* 67:1709–1718
106. Ng K, Nimeiri HS, McCleary NJ, Abrams TA, Yurgelun MB, Cleary JM, Rubinson DA, Schrag D, Miksad R, Bullock AJ, Allen J, Zuckerman D, Chan E, Chan JA, Wolpin BM, Constantine M, Weckstein DJ, Faggen MA, Thomas CA, Kournioti C, Yuan C, Ganser C, Wilkinson B, Mackintosh C, Zheng H, Hollis BW, Meyerhardt JA, Fuchs CS (2019) Effect of High-Dose vs Standard-Dose Vitamin D3 Supplementation on Progression-Free Survival Among Patients With Advanced or Metastatic Colorectal Cancer: The SUNSHINE Randomized Clinical Trial. *JAMA* 321:1370–1379

107. Nurminen V, Seuter S, Carlberg C (2019) Primary Vitamin D Target Genes of Human Monocytes. *Front Physiol* 10:194
108. Oda Y, Chalkley RJ, Burlingame AL, Bikle DD (2010) The transcriptional coactivator DRIP/mediator complex is involved in vitamin D receptor function and regulates keratinocyte proliferation and differentiation. *J Invest Dermatol* 130:2377–2388
109. Oertelt-Prigione S (2012) The influence of sex and gender on the immune response. *Autoimmun Rev* 11:A479–A485
110. Ota K, Dambaeva S, Kim MW-I, Han A-R, Fukui A, Gilman-Sachs A, Beaman K, Kwak-Kim J (2015) 1,25-Dihydroxy-vitamin D₃ regulates NK-cell cytotoxicity, cytokine secretion, and degranulation in women with recurrent pregnancy losses. *Eur J Immunol* 45:3188–3199
111. Pak-Wittel MA, Yang L, Sojka DK, Rivenbark JG, Yokoyama WM (2013) Interferon- γ mediates chemokine-dependent recruitment of natural killer cells during viral infection. *Proc Natl Acad Sci U S A* 110:E50–E59
112. Paolini R, Bernardini G, Molfetta R, Santoni A (2015) NK cells and interferons. *Cytokine Growth Factor Rev* 26:113–120
113. Park HJ, Choi JM (2017) Sex-specific regulation of immune responses by PPARs. *Exp Mol Med* 49:364
114. Pegram HJ, Andrews DM, Smyth MJ, Darcy PK, Kershaw MH (2011) Activating and inhibitory receptors of natural killer cells. *Immunol Cell Biol* 89:216–224
115. Penna G, Adorini L (2000) 1 α ,25-Dihydroxyvitamin D₃ Inhibits Differentiation, Maturation, Activation, and Survival of Dendritic Cells Leading to Impaired Alloreactive T Cell Activation. *J Immunol* 164:2405–2411
116. Pinheiro I, Heard E (2017) X chromosome inactivation: New players in the initiation of gene silencing. *F1000Research* 6:344
117. Pipkin ME, Rao A, Lichtenheld MG (2010) The transcriptional control of the perforin locus. *Immunol Rev* 235:55–72
118. Pisegna S, Pirozzi G, Piccoli M, Frati L, Santoni A, Palmieri G (2004) p38 MAPK activation controls the TLR3-mediated up-regulation of cytotoxicity and cytokine production in human NK cells. *Blood* 104:4157–4164
119. Porcelli S, Yockey CE, Brenner MB, Balk SP (1993) Analysis of T cell antigen receptor (TCR) expression by human peripheral blood CD4–8– $\alpha\beta$ T cells demonstrates

- preferential use of several V β genes and an invariant TCR α chain. *J Exp Med* 178:1–16
120. Quesada JM, Solana R, Martin A, Santamaria M, Serrano I, Martinez ME, Aljama P, Peña J (1989) The effect of calcitriol on natural killer cell activity in hemodialyzed patients. *J Steroid Biochem* 34:423–425
121. R Core Team (2020) R: A Language and Environment for Statistical Computing.
122. Rajagopalan S, Long EO (2005) Understanding how combinations of HLA and KIR genes influence disease. *J Exp Med* 201:1025–1029
123. Roda JM, Joshi T, Butchar JP, McAlees JW, Lehman A, Tridandapani S, Carson WE (2007) The activation of natural killer cell effector functions by cetuximab-coated, epidermal growth factor receptor - Positive tumor cells is enhanced by cytokines. *Clin Cancer Res* 13:6419–6428
124. Romagnani C, Juelke K, Falco M, Morandi B, D'Agostino A, Costa R, Ratto G, Forte G, Carrega P, Lui G (2007) CD56brightCD16– killer Ig-like receptor– NK cells display longer telomeres and acquire features of CD56dim NK cells upon activation. *J Immunol* 178:4947–4955
125. Rosen CJ (2011) Vitamin D insufficiency. *N Engl J Med* 364:248–254
126. Rothfelder K, Märklin M, Wild J, Dörfel D, Kanz L, Müller MR, Salih HR (2016) Involvement of NFAT Transcription Factors in NK Cell Reactivity. *Blood* 128:1344–1344
127. Roux PP, Blenis J (2004) ERK and p38 MAPK-Activated Protein Kinases: a Family of Protein Kinases with Diverse Biological Functions. *Microbiol Mol Biol Rev* 68:320–344
128. Shirvani A, Kalajian TA, Song A, Holick MF (2019) Disassociation of Vitamin D's Calcemic Activity and Non-calcemic Genomic Activity and Individual Responsiveness: A Randomized Controlled Double-Blind Clinical Trial. *Sci Rep* 9:1–12
129. Sivori S, Falco M, Della Chiesa M, Carlomagno S, Vitale M, Moretta L, Moretta A (2004) CpG and double-stranded RNA trigger human NK cells by Toll-like receptors: induction of cytokine release and cytotoxicity against tumors and dendritic cells. *Proc Natl Acad Sci U S A* 101:10116–10121
130. Smyth G, Hu Y, Ritchie M, Silver J, Wettenhall J, McCarthy D, Wu D, Shi W, Phipson B, Lun A, Thorne N, Oshlack A, de Graaf C, Chen Y, Langaas M, Ferkinstad E, Davy M, Pepin F, Choi D (2015) limma powers differential expression analyses for RNA-sequencing and microarray studies. *Nucleic Acids Res*

131. Smyth MJ, Cretney E, Kelly JM, Westwood JA, Street SEA, Yagita H, Takeda K, Dommelen SLH van, Degli-Esposti MA, Hayakawa Y (2005) Activation of NK cell cytotoxicity. *Mol Immunol* 42:501–510
132. Solovjov DA, Pluskota E, Plow EF (2005) Distinct roles for the α and β subunits in the functions of integrin α M β 2. *J Biol Chem* 280:1336–1345
133. Souza-Fonseca-Guimaraes F, Parlato M, Fitting C, Cavaillon J-M, Adib-Conquy M (2012) NK cell tolerance to TLR agonists mediated by regulatory T cells after polymicrobial sepsis. *J Immunol* 188:5850–5858
134. Souza-Fonseca-Guimaraes F, Parlato M, Philippart F, Misset B, Cavaillon J-M, Adib-Conquy M (2012) Toll-like receptors expression and interferon- γ production by NK cells in human sepsis. *Crit Care* 16:R206
135. Stolzenberg-Solomon RZ, Vieth R, Azad A, Pietinen P, Taylor PR, Virtamo J, Albanes D (2006) A prospective nested case-control study of vitamin D status and pancreatic cancer risk in male smokers. *Cancer Res* 66:10213–9
136. Stolzenberg-Solomon RZ, Jacobs EJ, Arslan AA, Qi D, Patel A V, Helzlsouer KJ, Weinstein SJ, McCullough ML, Purdue MP, Shu X-O, Snyder K, Virtamo J, Wilkins LR, Yu K, Zeleniuch-Jacquotte A, Zheng W, Albanes D, Cai Q, Harvey C, Hayes R, Clipp S, Horst RL, Irish L, Koenig K, Le Marchand L, Kolonel LN (2010) Circulating 25-hydroxyvitamin D and risk of pancreatic cancer: Cohort Consortium Vitamin D Pooling Project of Rarer Cancers. *Am J Epidemiol* 172:81–93
137. Strober W (2001) Trypan blue exclusion test of cell viability. *Curr Protoc Immunol* Appendix 3:A.3B.1-A.3B.2
138. Subramanian A, Tamayo P, Mootha VK, Mukherjee S, Ebert BL, Gillette MA, Paulovich A, Pomeroy SL, Golub TR, Lander ES, Mesirov JP (2005) Gene set enrichment analysis: A knowledge-based approach for interpreting genome-wide expression profiles. *Proc Natl Acad Sci* 102:15545 LP – 15550
139. Sutton VR, Trapani JA (2010) Proteases in lymphocyte killer function: Redundancy, polymorphism and questions remaining. *Biol Chem* 391:873–879
140. Svensson L, Howarth K, McDowall A, Patzak I, Evans R, Ussar S, Moser M, Metin A, Fried M, Tomlinson I (2009) Leukocyte adhesion deficiency-III is caused by mutations in KINDLIN3 affecting integrin activation. *Nat Med* 15:306
141. Szymczak-Pajor I, Kleniewska P, Wieczfinska J, Pawliczak R (2020) Wide-Range Effects of 1,25(OH)₂D₃ on Group 4A Phospholipases Is Related to Nuclear Factor κ -B

- and Phospholipase-A2 Activating Protein Activity in Mast Cells. *Int Arch Allergy Immunol* 181:56–70
142. Talwar T, Vidhyasagar V, Qing J, Guo M, Kariem A, Lu Y, Singh RS, Lukong KE, Wu Y, Sung P (2017) The DEAD-box protein DDX43 (HAGE) is a dual RNA-DNA helicase and has a K-homology domain required for full nucleic acid unwinding activity. *J Biol Chem* 292:10429–10443
143. Thomas M, Wills M, Lehner PJ (2008) Natural killer cell evasion by an E3 ubiquitin ligase from Kaposi's sarcoma-associated herpesvirus. URL: <http://www.ncbi.nlm.nih.gov/pubmed/18481981>
144. Tian D, Sun S, Lee JT (2010) The long noncoding RNA, Jpx, is a molecular switch for X chromosome inactivation. *Cell* 143:390–403
145. Trinchieri G (1989) Biology of Natural Killer Cells. *Adv Immunol* 47:187–376
146. Trotta R, Fettucciari K, Azzoni L, Abebe B, Puorro KA, Eisenlohr LC, Perussia B (2000) Differential Role of p38 and c-Jun N-Terminal Kinase 1 Mitogen-Activated Protein Kinases in NK Cell Cytotoxicity. *J Immunol* 165:1782–1789
147. Urashima M, Ohdaira H, Akutsu T, Okada S, Yoshida M, Kitajima M, Suzuki Y (2019) Effect of Vitamin D Supplementation on Relapse-Free Survival Among Patients With Digestive Tract Cancers: The AMATERASU Randomized Clinical Trial. *JAMA* 321:1361–1369
148. van Groningen L, Opdenoordt S, van Sorge A, Telting D, Giesen A, de Boer H (2010) Cholecalciferol loading dose guideline for vitamin D-deficient adults. *Eur J Endocrinol* 162:805–811
149. Vivier E, Nunès JA, Vély F (2004) Natural killer cell signaling pathways. *Science* (80-) 306:1517–1519
150. Vivier E, Tomasello E, Baratin M, Walzer T, Ugolini S (2008) Functions of natural killer cells. *Nat Immunol* 9:503
151. Voskoboinik I, Whisstock JC, Trapani JA (2015) Perforin and granzymes: function, dysfunction and human pathology. *Nat Rev Immunol* 15:388
152. Voss SD, Sondel PM, Robb RJ (1992) Characterization of the interleukin 2 receptors (H,2R) expressed on human natural killer cells activated in vivo by ID2: Association of the p64 ID2R γ chain with the ID2R β chain in functional intermediate-affinity ID2R. *J Exp Med* 176:531–541

153. Walzer T, Dalod M, Robbins SH, Zitvogel L, Vivier E (2005) Natural-killer cells and dendritic cells: "l'union fait la force." *Blood* 106:2252–2258
154. Wang R, Jaw JJ, Stutzman NC, Zou Z, Sun PD (2012) Natural killer cell-produced IFN- γ and TNF- α induce target cell cytotoxicity through up-regulation of ICAM-1. *J Leukoc Biol* 91:299–309
155. Wang W, Erbe AK, Hank JA, Morris ZS, Sondel PM (2015) NK cell-mediated antibody-dependent cellular cytotoxicity in cancer immunotherapy. *Front Immunol* 6:
156. Weiner GJ (2010) Rituximab: mechanism of action. *Semin Hematol* 47:115–123
157. Wendel M, Galani IE, Suri-Payer E, Cerwenka A (2008) Natural killer cell accumulation in tumors is dependent on IFN- γ and CXCR3 ligands. *Cancer Res* 68:8437–8445
158. Wicherts IS, van Schoor NM, Boeke AJP, Visser M, Deeg DJH, Smit J, Knol DL, Lips P (2007) Vitamin D status predicts physical performance and its decline in older persons. *J Clin Endocrinol Metab* 92:2058–65
159. Wu L, Kaer L Van (2011) Natural killer T cells in health and disease. *Front Biosci - Sch* 3 S:236–251
160. Xu LJ, Chen XD, Shen MJ, Yang DR, Fang L, Weng G, Tsai Y, Keng PC, Chen Y, Lee SO (2018) Inhibition of IL-6-JAK/Stat3 signaling in castration-resistant prostate cancer cells enhances the NK cell-mediated cytotoxicity via alteration of PD-L1/NKG2D ligand levels. *Mol Oncol* 12:269–286
161. Yu J, Chia J, Canning CA, Jones CM, Bard FA, Virshup DM (2014) WLS Retrograde transport to the endoplasmic reticulum during Wnt secretion. *Dev Cell* 29:277–291
162. Yu S, Cantorna MT (2008) The vitamin D receptor is required for iNKT cell development. *Proc Natl Acad Sci U S A* 105:5207–5212
163. Yu T-K, Caudell EG, Smid C, Grimm EA (2000) IL-2 Activation of NK Cells: Involvement of MKK1/2/ERK But Not p38 Kinase Pathway. *J Immunol* 164:6244–6251
164. Yu Y, Hayward GS (2010) The Ubiquitin E3 Ligase RAUL Negatively Regulates Type I Interferon through Ubiquitination of the Transcription Factors IRF7 and IRF3. *Immunity* 33:863–877
165. Yuan C, Sato K, Hollis BW, Zhang S, Niedzwiecki D, Ou FS, Wen Chang I, O'Neil BH, Innocenti F, Lenz HJ, Blanke CD, Goldberg RM, Venook AP, Mayer RJ, Fuchs CS, Meyerhardt JA, Ng K (2019) Plasma 25-hydroxyvitamin D levels and survival in

- patients with advanced or metastatic colorectal cancer: Findings from CALGB/SWOG 80405 (Alliance). *Clin Cancer Res* 25:7497–7505
166. Zanoni I, Granucci F, Broggi A (2017) Interferon (IFN)- λ takes the helm: Immunomodulatory roles of type III IFNs. *Front Immunol* 8:
167. Zhao W, Huang Y, Liu Z, Cao B-B, Peng Y-P, Qiu Y-H (2013) Dopamine Receptors Modulate Cytotoxicity of Natural Killer Cells via cAMP-PKA-CREB Signaling Pathway. *PLoS One* 8:e65860
168. Zhou FF, Zhang X, Van Dams H, Ten Dijk P, Huang H, Zhangs L (2012) Ubiquitin-specific protease 4 mitigates toll-like/interleukin-1 receptor signaling and regulates innate immune activation. *J Biol Chem* 287:11002–11010
169. Zhou Y, An LL, Chaerkady R, Mittereder N, Clarke L, Cohen TS, Chen B, Hess S, Sims GP, Mustelin T (2018) Evidence for a direct link between PAD4-mediated citrullination and the oxidative burst in human neutrophils. *Sci Rep* 8:1–13
170. Zhu J, Huang X, Yang Y (2008) A critical role for type I IFN-dependent NK cell activation in innate immune elimination of adenoviral vectors in vivo. *Mol Ther* 16:1300–1307
171. Zuk M (2009) The Sicker Sex. *PLoS Pathog* 5:e1000267
172. RPS4Y1 Gene - GeneCards. URL: <https://www.genecards.org/cgi-bin/carddisp.pl?gene=RPS4Y1>, date accessed: 18-07-2020

7 PUBLICATIONS

Parts of this work have been revealed in the following presentations/ publication(s):

- I. Christofyllakis K, Neumann F, Stilgenbauer S, Kaddu-Mulindwa D, Regitz E, Bewarder M, Keller A, Bittenbring JT
“Gene Set Enrichment Analysis Suggests That Increased Rituximab-Mediated NK Cell Cytotoxicity after Vitamin D Substitution Is Driven By Upregulation of Interferon Alpha (IFN- α) Isoforms”. Blood 132:3696
American Society of Hematology (ASH) 62nd Annual Meeting, San Diego USA, December 2018, Poster Presentation, Abstract ID: 3696
- II. Christofyllakis, K., Neumann F., Reichenbach F., Regitz E., Stilgenbauer S., Keller A., Kaddu-Mulindwa D., Bewarder M., Bittenbring J.T. (2019)
“Vitamin D Enhances Rituximab-mediated NK-cell Cytotoxicity via the Interferon- α Pathway”
Annual Meeting of the German, Austrian and Swiss Societies of Hematology and Medical Oncology, Berlin, Germany, October 2019, Oral Presentation, Abstract ID: V1065
- III. Christofyllakis, K., Neumann F., Regitz E., Stilgenbauer S., Keller A., Kaddu-Mulindwa D., Bewarder M., Bittenbring J.T.
“Impact of in vivo Vitamin D Supplementation in Genome-wide Expression of Natural Killer Cells in Vitamin D Deficient Individuals”
Manuscript submitted

8 ACKNOWLEDGEMENTS

My deepest gratitude goes to my supervisor PD Dr. rer. nat. Frank Neumann, for the constant support and invaluable guidance, and to Prof. Dr. med. Michael Pfreundschuh whose motivation and encouragement still drives me. I also sincerely thank Prof. Dr. med. Stephan Stilgenbauer for his motivating adherence to academic standards.

I am greatly indebted to Evi Regitz for her patience and support where I needed it most, this work would not be possible without her. My sincere gratitude goes also to Prof. Dr. Andreas Keller, whose advice was essential to completing this thesis.

This work would not be possible without the constant support of my wife Bediha, who patiently stood by my side. Finally, I want to express my deep gratitude to my mother Eirini and my father Charalambos for selflessly providing me the opportunities, upbringing and education that led me this far.

9 CURRICULUM VITAE

Aus datenschutzrechtlichen Gründen wird der Lebenslauf in der elektronischen Fassung der Dissertation nicht veröffentlicht.